Journal of Paleontology, Volume 98, Memoir 94, 2024, p. 1–59

0022-3360/24/1937-2337
doi: 10.1017/jpa.2023.81

JOURNAL OF PALEONTOLOGY
A PUBLICATION OF THE Paleontological SOCIETY

Ediacaran paleobiology and biostratigraphy of the Nama Group, Namibia, with emphasis on the erniettomorphs, tubular and trace fossils, and a new sponge, *Arimasia germsi* n. gen. n. sp.

Bruce Runnegar,[1]* James G. Gehling,[2] Sören Jensen,[3] and Matthew R. Saltzman[4]

[1]Department of Earth, Planetary, and Space Sciences and Molecular Biology Institute, University of California, Los Angeles, CA 90095-1567, USA <runnegar@ucla.edu>
[2]Palaeontology Division, South Australian Museum, Adelaide, South Australia 5000, Australia <gehling.jim@bigpond.com>
[3]Área de Paleontología, Facultad de Ciencias, Universidad de Extremadura, E-06006, Badajoz, Spain <soren@unex.es>
[4]School of Earth Sciences, Ohio State University, Columbus, OH 43210, USA <saltzman.11@osu.edu>

Non-technical Summary.—This work describes and illustrates Ediacaran (latest Precambrian) body and trace fossils collected in Namibia with the assistance of the Geological Survey of Namibia during 1993–1996. All of the fossils are impressions left in sandstones by the remains or activities of soft-bodied animals that have no obvious living counterparts. The challenge has been to understand the morphology of these organisms, describe their anatomy, and find places for them in the tree of life. The focus is on three erniettomorphs, *Ernietta*, *Pteridinium*, and *Swartpuntia*; a problematical organism named *Archaeichnium* that may be related to sea anemones; a new simple unmineralized sponge (*Arimasia*); and tubular fossils and trace fossils, all attributable to worms. We show how these fossils fit into the well-established stratigraphic context of the Nama sedimentary basin and briefly comment on their importance for the evolution of early animal life.

Abstract.—Ediacaran fossils, obtained in stratigraphic context in 1993, 1995, and 1996, with the assistance of A. Seilacher, IGCP project 320 scientists, and the Geological Survey of Namibia, are described for the first time. Most are from the Kliphoek and Buchholzbrunn members of the Dabis Formation and the Huns and Spitskop members of the Urusis Formation, Witputs subbasin, but a significant number, including *Pteridinium*, are from the Kliphoek Member, Zaris Formation, and the Neiderhagen Member, Nudaus Formation, north of the Osis arch, which separates the two subbasins. We extend the stratigraphic ranges and geographic distributions of several important taxa, including *Archaeichnium*, *Ernietta*, *Pteridinium*, and *Swartpuntia*, provide reassessments of the paleobiology of these and other organisms, and describe a new sponge—possibly an unmineralized archaeocyath—*Arimasia germsi* n. gen. n. sp. We also describe and illustrate various ichnofossils (including the oldest known traces from the Nama Group), narrow down the first appearance of *Treptichnus* in the Nama succession, and reinforce the idea that there was a prolific infauna of micrometazoans during the latest Ediacaran by naming and describing previously reported microburrows found on the surfaces of gutter casts as *Ariichnus vagus* n. igen. n. isp.

UUID: http://zoobank.org/8c267425-135a-4b0a-98b6-cf726515cbf2

Introduction

The superbly exposed latest Ediacaran to earliest Cambrian succession in southern Namibia has produced some of the most outstanding body and trace fossils of soft-bodied Precambrian animals since first explored early last century (Gürich, 1933; Richter, 1955; Haughton, 1960; Pflug, 1970a, b, 1972; Germs, 1972a, b, 1973; Glaessner, 1978, 1979a; Crimes and Germs, 1982; Hahn and Pflug, 1985a, 1988; Narbonne et al., 1997; Jensen et al., 2000; Grazhdankin and Seilacher, 2005; Jensen and Runnegar, 2005; Wilson et al., 2012; Vickers-Rich et al., 2013; Elliott et al., 2016; Ivantsov et al., 2016, 2019; Buatois et al., 2018; Darroch et al., 2021; Turk et al., 2022; Bowyer et al., 2023). We continue that tradition by describing and interpreting new material from the southern (Witputs) and northern (Zaris) subbasins that house the Nama succession and extend the known distribution of Ediacaran organisms both stratigraphically and geographically. We first describe the stratigraphic context for our samples (Figs. 1–5), then deal with their systematics (Figs. 6–26) and conclude with a discussion of the implications of our findings.

This study began with a generous invitation from Dolf Seilacher for JGG and BR to participate in a field discussion of

*Corresponding author.

Seilacher's vendobiont hypothesis at the now-famous Amphitheatre site on Aar farm and subsequently at H.D. Pflug's home in Lich, as chronicled by Mark McMenamin in *The Garden of Ediacara* (McMenamin, 1998). During that trip, we also tried to re-collect Germs and Richter's localities at Arimas, Chamis, Kliphoek, Kuibis, and Vrede, with limited but encouraging success. Subsequent work in 1995 and 1996, with the assistance and support of the Geological Survey of Namibia, produced much of the material described here. The work was and is aimed at documenting the Ediacaran biodiversity of Namibia. We illustrate, describe, and discuss the taxa studied but do not deal with some other well-known Namibian forms, such as *Rangea* Gürich, 1930 (Gürich, 1930a), which are well treated elsewhere. A few uncommon taxa are illustrated but not described.

Geological setting

Lithostratigraphy and geochronology.—The largely undeformed stratigraphy of the Nama Basin in southern Namibia was well described by Germs (1972a, 1974, 1983) and then put into a sequence stratigraphic framework by Saylor et al. (1995, 1998 2005), Smith (1999), and Saylor (2003). Briefly, the Nama Basin is divided into three subbasins by topographic highs that were present during sedimentation. Ediacaran fossils are found only in the two western subbasins, Zaris and Witputs, which are separated by the Osis arch (Fig. 1). Upper Nama Group sediments belonging to the Cambrian Fish River and largely Ediacaran Schwarzrand subgroups extend across the Osis arch; the older Ediacaran Kuibis Subgroup is thicker, more carbonate-rich, and apparently more complete in the north (Fig. 2). The only distinctive Kuibis unit that crosses the arch is the Kliphoek Member of the Dabis Formation, which projects as a tongue into the southern edge of the Zaris subbasin (Fig. 2; Germs, 1983, fig. 3; Germs and Gresse, 1991, fig. 3). Fortunately, the limestone overlying this tongue, which is clearly the Mooifontein Member of the Zaris Formation, preserves the older rising limb of a pronounced positive carbon isotope excursion (OMKYK, Figs. 2, 3; OME of Bowyer et al., 2022) that is well characterized from thick, carbonate-rich sections in the Zebra River area (Figs. 1–3; Grotzinger et al., 1995; Saylor et al., 1998; Smith, 1999; Wood et al., 2015) and is older than a prominent volcanic ash bed with a U–Pb age of 547.36 ± 0.23 Ma (Grotzinger et al., 1995; Bowring et al., 2007; Schmitz et al., 2020). As the peak of the Omkyk excursion can be followed southward in the Mooifontein Member (Fig. 3), its presence above fossiliferous horizons of the underlying Buchholzbrunn and Kilphoek members in the Witputs subbasin provides a minimum age of about 548 Ma for those assemblages (Fig. 2; Saylor et al., 1998).

A volcanic ash bed near Nooitgedacht (Fig. 1) at the "basal contact" of the siliciclastic Nudaus Formation, the oldest unit of the Schwarzrand Subgroup, has a U–Pb age of 545.27 ± 0.11 Ma (Nelson et al., 2022), thus implying an approximately 2 million-year hiatus between the Kuibis and Schwarzrand subgroups in the Witputs subbasin, where the Nudaus lies directly upon the Mooifontein (Fig. 2); carbonate and low-energy siliciclastic sedimentation seems to have continued through this hiatus in the north.

Another volcanic ash bed ~10 km southwest of Nooitgedacht in the Nasep Member of the heterogeneous Urusis Formation, which completes the Ediacaran section of the Schwarzrand Subgroup in the Witputs subbasin, has a U–Pb age of 542.65 ± 0.15 Ma (Fig. 2; Nelson et al., 2022). This constrains the fossiliferous intervals of the Schwarzrand Subgroup to between about 543 and 539 Ma in the Witputs subbasin, but the older Nudaus Formation is fossiliferous north of the Osis arch (UCLA 7320, Fig. 2; Darroch et al., 2016) and perhaps at Gründoorn, about 60 km from Karasburg (Figs. 1, 2; Haughton, 1960; Glaessner, 1978). The Nama section at Charliesput, ~95 km east of Karasburg, is almost entirely siliciclastic (Germs, 1972a, fig. 22; 1974, fig. 4). Glaessner (1978) followed Haughton (1960) in attributing the two slabs of sandstone that preserve the type specimens of *Archaeichnium haughtoni* Glaessner, 1963 to the Kuibis Formation equivalent, the Nababis Formation, but the stratigraphic range of *Archaeichnium* elsewhere suggests a younger, Schwarzrand equivalent provenance (Fig. 2).

The best-dated part of the Nama succession spans the Ediacaran–Cambrian boundary (Grotzinger et al., 1995; Linnemann et al., 2019; Nelson et al., 2022), and the relevant U–Pb ages for this work are summarized in Figures 2 and 5. The Precambrian–Cambrian boundary has traditionally been placed at a profound erosional surface at the base of the Nomtsas Formation (e.g., Germs, 1972a; Grotzinger et al., 1995; Wilson et al., 2012), but recently it has been suggested that the boundary should be lowered into the underlying Spitskop Member of the Urusis Formation (Fig. 2) because trace fossils of the *Treptichnus pedum* (Seilacher, 1955) type have been found within the Spitskop Member (Linnemann et al., 2019; Bowyer et al., 2022) and treptichnids lower down (Jensen et al., 2000; Darroch et al., 2021). The significance of these observations remains a matter for debate; here we follow the traditional view on the grounds that bone fide examples of *Treptichnus pedum* are found abundantly in the Nomtsas Formation (Fig. 25.3, 25.4; Wilson et al., 2012) whereas those present in the Spitskop Member (Fig. 25.1, 25.2; Germs, 1972b, pl. 2, fig. 1; Jensen et al., 2000; Darroch et al., 2021; Turk et al., 2022) are treptichnids but not *Treptichnus pedum*, a pattern seen elsewhere (Jensen, 2003), including Nevada (Tarhan et al., 2020). The persistence of characteristically Ediacaran fossils such as *Pteridinium* and *Swartpuntia* to near the top of the Spitskop Member is mirrored by the presence of *Ernietta* and other Ediacaran taxa immediately beneath the well-characterized Precambrian–Cambrian boundary in Nevada and Sonora, Mexico (Smith et al., 2016, 2022; Hodgin et al., 2021; Nelson et al., 2023). Thus, we regard all of the fossils discussed in this work, with the exception of *T. pedum* from the Nomtsas Formation, to be Ediacaran, not Cambrian, in age.

Biostratigraphy.—The regional distribution of the Ediacara fauna and associated calcareous fossils and trace fossils was first documented by Germs (1972a–c, 1973). He showed that Ediacaran fossils (*Rangea*, *Pteridinium*, *Ernietta*) are common in the triangular area bounded by Aus (16.25°E, 26.67°S), Helmeringhausen (16.82°E, 25.88°S), and Goageb (17.22°E, 26.75°S) at the siliciclastic to carbonate transition from the Kliphoek to Mooifontein members, since separated out as the Buchholzbrunn Member (Germs and Gresse, 1991; Germs, 1995)—which we use here (Figs. 2, 3)—or as the Aar Member (Hall et al., 2013). Germs also found one specimen

https://doi.org/10.1017/jpa.2023.81 Published online by Cambridge University Press

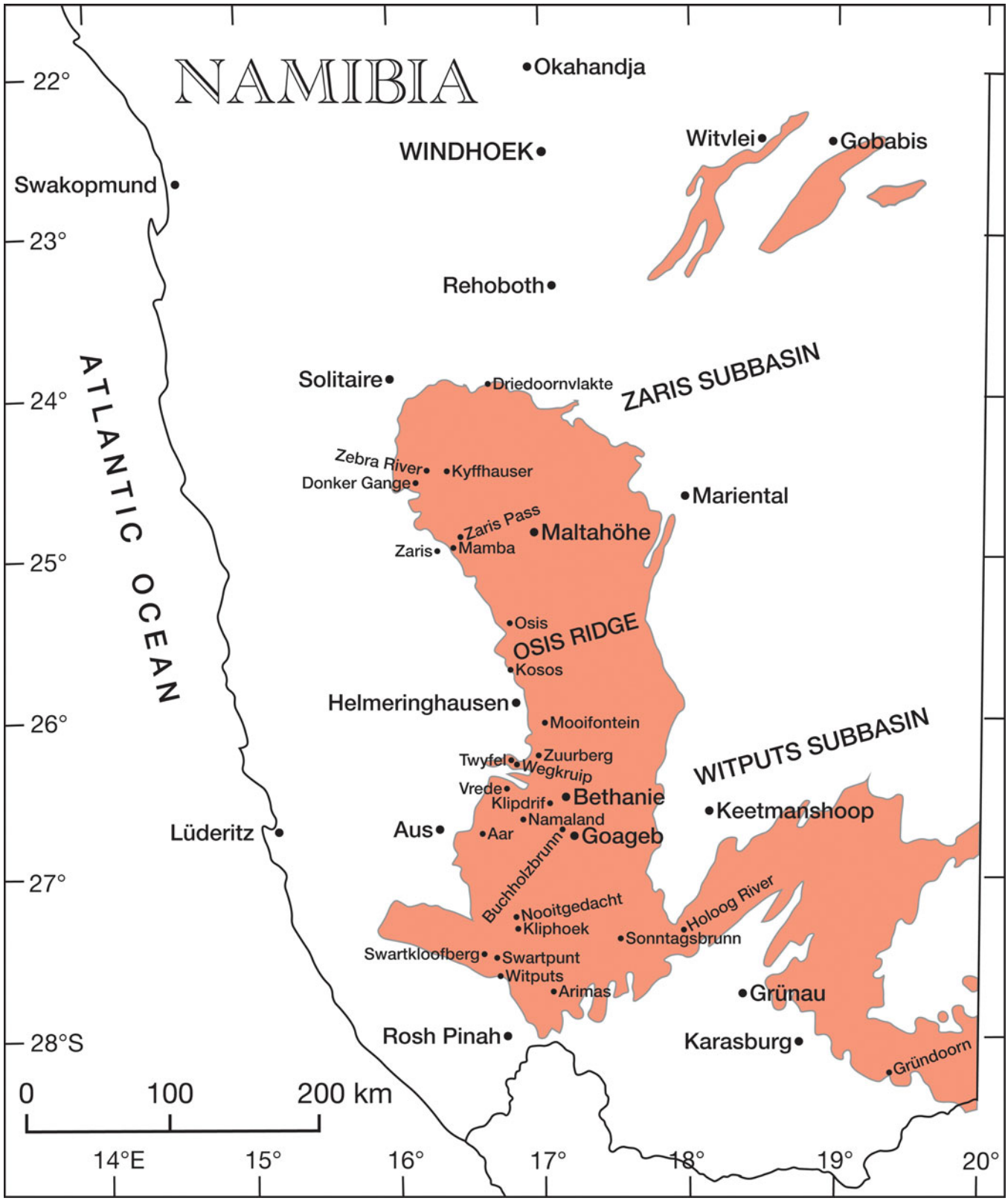

Figure 1. Nama Group outcrop (shaded area) and locality map of southern Namibia. Cities, towns, and major geological features are shown in larger lettering; farms and other local features are smaller.

of *Rangea* higher in the succession, just above the Mooifontein limestone in the Neiderhagen sandstone Member, Nudaus Formation, at Chamis (17.00°E, 26.05°S), but as the fossil was not in situ, its stratigraphic position may be questionable. A rather different assemblage, interbedded with carbonates, was found at a single site in the base of the Huns limestone,

https://doi.org/10.1017/jpa.2023.81 Published online by Cambridge University Press

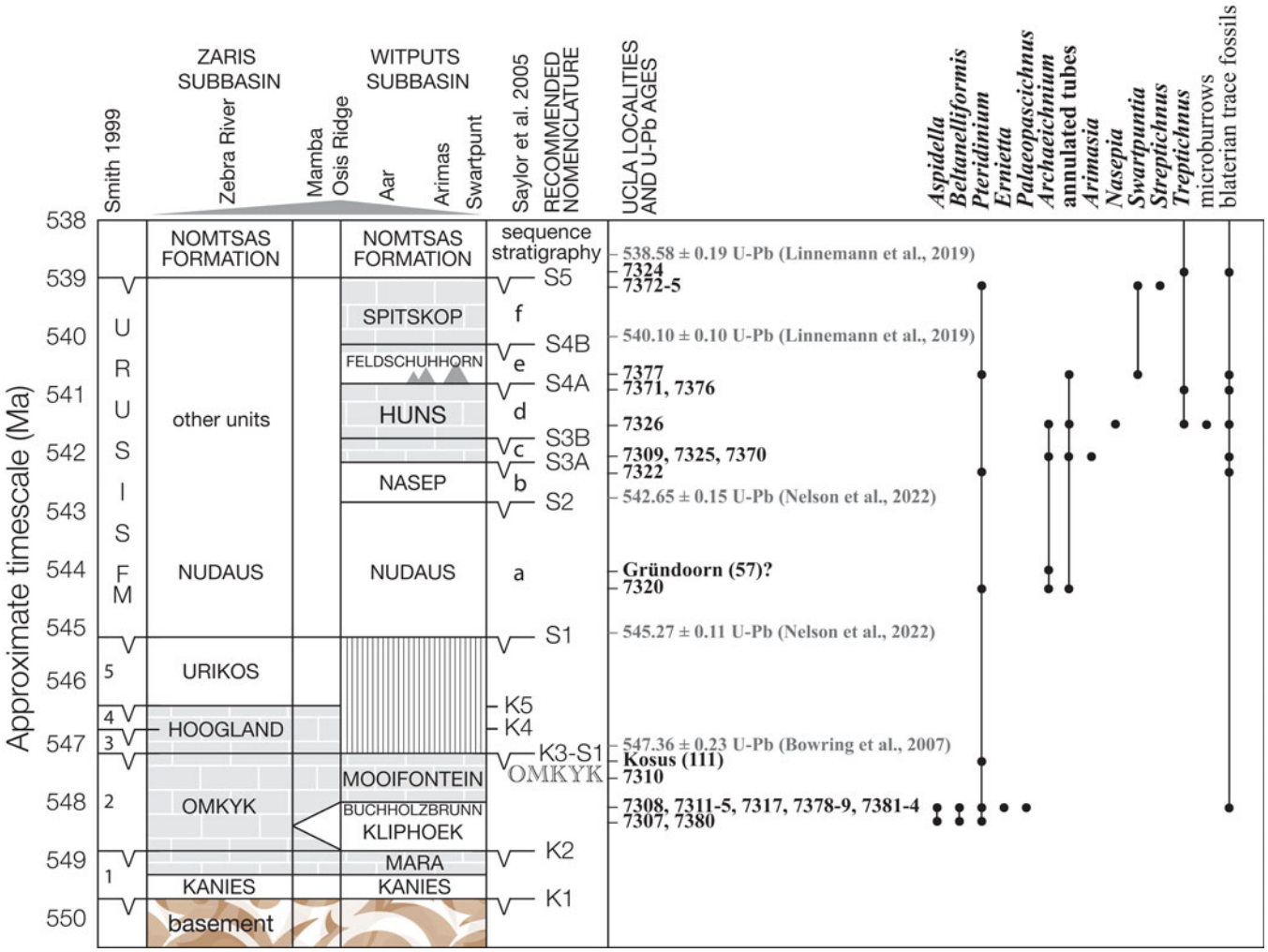

Figure 2. Lithostratigraphy of the Nama Group and stratigraphic ranges of taxa in this work. The lower parts of the successions of the Zaris and Witputs subbasins differ across the Osis ridge, and the ~2 million-year hiatus (vertical lines) proposed here for the Witputs subbasin is novel. Rock units shown are mainly members of the Kuibis (K) and Schwarzrand (S) subgroups rather than the formations as these are the most commonly used and mappable lithological subdivisions. The recommended nomenclature for the first-order sequence stratigraphy is developed from Saylor et al. (1995, 2005), Smith (1999), and Saylor (2003), and the terms apply to the sequences above each labeled boundary. The stratigraphic ranges shown are limited to genera and larger taxonomic groups to provide a clear overview of the distribution of key elements of the biota; specific details are provided in the systematic paleontology section. "OMKYK" shows the stratigraphic position of the Omkyk positive carbon isotope excursion (Bowyer et al., 2022) in both subbasins (Fig. 3), and the gray triangles within the Feldschuhhorn Member represent pinnacle reefs.

Urusis Formation, Schwarzrand Subgroup at Arimas (17.00°E, 27.70°S). Thus, there seemed to be two principal assemblages of Ediacaran organisms, an older one characterized by *Pteridinium* and *Ernietta* and a younger one that lacked both genera but yielded a variety of tubular and trace fossils, plus the new genus *Nasepia* (Germs, 1972a, c, 1973). This situation languished until Grotzinger et al. (1995) showed that *Pteridinium* and *Swartpuntia* (Narbonne et al., 1997) extended almost up to the disconformity that separates the Cambrian Nomtas Formation from older Schwarzrand units. There has been one recent report of an "indeterminate erniettomorph" in the Nomtsas Formation in South Africa (Nelson et al., 2022), but both the fossil and its stratigraphic level need further assessment.

In the carbonates, Germs (1972a, b) reported *Cloudina* from the Mara, Mooifontein, and Huns limestone members of the Wiputs subbasin, but all of the described material was from a bioherm, the Driedoornvlagte reef (Grotzinger et al., 2000, 2005; Adams et al., 2004; Wood et al., 2015), in the Zaris subbasin (Fig. 1). All occurrences of *Cloudina* in both subbasins were subsequently summarized by Grant (1990) and Yang et al. (2022). *Namacalathus* is found with *Cloudina* in the Driedoornvlagte reef (Germs, 1972c, pl. 1, fig. 4; Grotzinger et al., 2005; Penny et al., 2014; Wood et al., 2015) and in the Omkyk Member in the Zebra River section on Donker Gange (UCLA 7319; Grotzinger et al., 2000), but apparently without *Cloudina* in the pinnacle reefs of the Feldschuhhorn Member at Swartkloofberg, although both are present near ash 4 in the Dundas section on Swartpunt (Fig. 5; Wood et al., 2015, fig. 14).

Trace fossils have been important components of Nama Group biostratigraphy since the pioneering studies of Germs (1972a, c) and Crimes and Germs (1982). Their taxonomy has been reviewed and revised by Darroch et al. (2021), leading to the elimination of characteristically Phanerozoic genera such as *Zoophycos* and *Diplocraterion*. What was left are putative cnidarian resting or dwelling traces (*Conichnus*, *Bergauria*) and possible

https://doi.org/10.1017/jpa.2023.81 Published online by Cambridge University Press

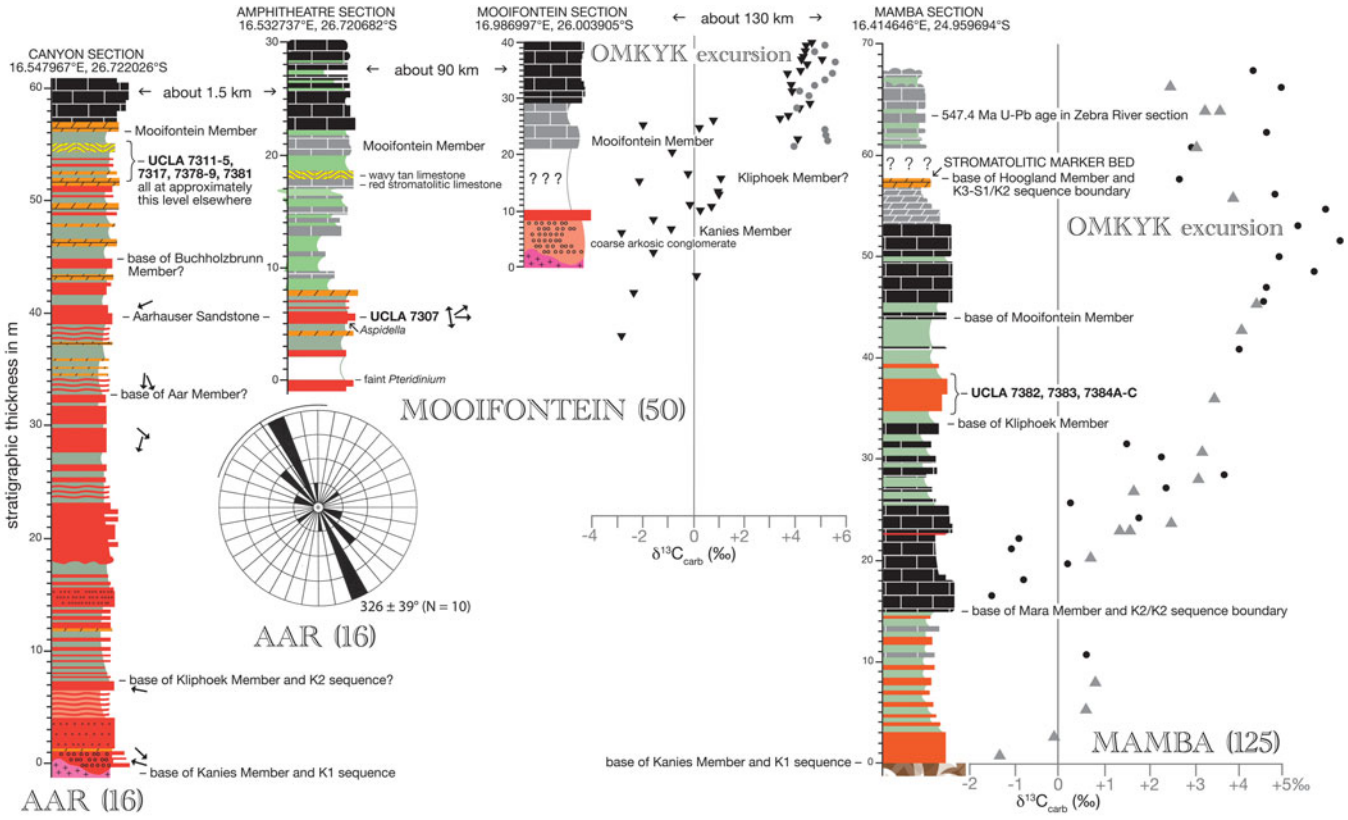

Figure 3. Measured stratigraphic sections from a north–south transect across the Osis ridge at farms Aar, Mooifontein, and Mamba (Fig. 1); rock types are siliciclastics (red/dark gray), carbonates (brick-wall patterns), and siltstones (green/light gray). The canyon section (Aar) incudes almost all of the Dabis Formation from granitic basement to the top of the Mooifontein limestone member; the Amphitheatre section, which transects the famous *Pteridinium* locality on Aar (UCLA 7307), is the source of the carbon isotope values shown by triangles (Supplemental dataset 1); the thinner and unfossiliferous Mooifontein section, closer to the Osis ridge, provided the carbon isotope values shown as gray filled circles (Supplemental dataset 1). The Mamba section, on the north side of the Osis ridge, has a siliciclastic tongue of Kliphoek Member between the Mara and Mooifontein limestone members (Fig. 2; Germs, 1983, fig. 3).); carbon isotope values from this section (black filled circles, Supplemental dataset 1) and those from the far thicker section along the Zebra River (gray triangles; Saylor et al., 1998) are correlated by normalizing the thicknesses between the basal unconformities and a distinctive stromatolitic marker bed, visible in both sections. Fossiliferous horizons sampled in this study are shown by their UCLA numbers. The single- and double-headed arrows are current directions, and the rose diagram illustrates the orientation of 10 transported specimens of *Pteridinium simplex* measured at UCLA 7307 (all measurements corrected for –19° magnetic declination). Lithologic symbols: brick wall patterns = limestones, dark (black) and light (gray); rhomboidal brick patterns = dolomites; red = sandstones and arenites; recessive units, gray or green = mainly siltstones.

narrow, horizontal burrows (*Helminthopsis*) in the Kuibis Subgroup and more diverse ichnofossil assemblages in the Schwarzrand Subgroup (Darroch et al., 2021, fig. 18b). The only sizable, Cambrian-like traces are *Streptichnus nabonnei* Jensen and Runnegar, 2005 from the uppermost Spitskop Member (UCLA 7375, Fig. 5) and *Parapsammichnites pretzeliformis* Buatois et al., 2018 from lower in the Spitskop in the Fish River area; the rest are narrow, subhorizontal burrows or levée-lined trenches (*Archaeonassa*, *Gordia*, *Helminthoidichnites*, *Helminthopsis*) that are similar to co-occurring tubular body fossils and, when inadequately preserved, may be confused with them. Although *Streptichnus* is "Cambrian-like" and has been invoked to lower the eon boundary into the Spitskop Member (Linnemann et al., 2019), its only other known occurrence is in the Ediacaran of China (Xiao et al., 2021; Mitchell et al., 2022).

The taxon of greatest interest, first found by Germs (1972a, b), is an ichnospecies that Jensen et al. (2000) referred to *Treptichnus*, but not *T. pedum* (Fig. 25.1, 25.2; Darroch et al., 2021, fig. 13). Our work reinforces this picture (Fig. 2), but we present clear examples of horizontal burrows (*Gordia* sp.) in the Kiphoek Member (Fig. 24.11, 24.13, 24.14), provide evidence for bioturbation down to depths of several centimeters in the Nasep and Huns members, and show that *Archaeichnium haughtoni* (Figs. 20, 21) is a body fossil rather than a trace fossil (Glaessner, 1963; Turk et al., 2022). We also suggest that structures (Fig. 12) that Darroch et al. (2021) called "guitar strings" are the tool and mold marks of current-transported erniettomorphs—probably *Pteridinium*—rather than sponge wall fragments.

Chemostratigraphy.—Carbonate hand samples, spaced 1 m apart where possible, were collected by MRS and BR from limestone sections measured by them and/or JGG from the Mooifontein Member on Aar, Mamba, Mooifontein, and Twyfel farms; from the Omkyk Member at Swartmodder on Omkyk; from the Urikos, Neiderhagen, and Vingerbreek members on Saurus; and from the Huns Member on Arimas and Swartkloofberg; but samples from only some of those sections were processed because of funding constraints. All isotopic data are tabulated in Supplemental dataset 1 and plotted against stratigraphic heights in Figure 2. Our results confirm previous and subsequent studies (Kaufman et al., 1991; Saylor et al., 1998; Smith, 1999; Wood et al., 2015).

https://doi.org/10.1017/jpa.2023.81 Published online by Cambridge University Press

Overall, the record is monotonous apart from the Omkyk excursion, which stands out from background but is not well expressed elsewhere except, perhaps, South China (Bowyer et al., 2022). Whether or not the negative values from the Mara and other lower Kuibis members, which Bowyer et al. (2022) term the "basal Nama excursion" (BANE), represent a post-Shuram, pre-basal Cambrian excursion (BACE) negative event of intercratonic significance is uncertain, given the paucity of other occurrences (Chai et al, 2021; Yang et al., 2021). Conversely, the position of the BACE, which is missing from the Nama succession, remains unresolved. Previously, it was thought to have been eliminated by the basal Nomtsas disconformity, but recent U–Pb ages suggest other possibilities (Linnemann et al., 2019; Hodgin et al., 2021; Bowyer et al., 2022; Topper et al., 2022; Nelson et al., 2023). In summary, the positive Omkyk excursion and the lower Kuibis negative intervals are the only features of the carbon isotope record of the Nama Group that are potentially useful for more than regional correlation.

Stratigraphic information.—See Figures 2–5, Appendix, and the discussion under Materials and methods.

Locality information.—We used the UCLA locality numbering system (e.g., UCLA 7307) for sites, occasionally at the same place in stratigraphic order, and numbered each piece of rock collected accordingly. Important fossils were then given decimal numbers corresponding to localities (e.g., 7307.1, 7307.2, etc.). Parts of an individual fossil were given the same decimal number, and different fossils on the same slab are identified by letters (e.g., 7307.3A, 7307.3B, etc.). These UCLA numbers for individual fossils were replaced by National Earth Sciences Museum numbers (GSN F) after the collection was repatriated to Namibia, but the UCLA locality numbers (e.g., UCLA 7307) still pertain. Locality details are described in the Appendix. Because this work was carried out before GPS became widely available, particularly in the Southern Hemisphere, the geographic positions of localities were plotted on photocopies of the relevant 1:50,000 scale topographic maps of South West Africa issued by the Surveyor General, Department of Justice, Government of Namibia. These map records were used recently to find the exact locations of the sites on Google Maps and to obtain their decimal longitudes and latitudes (Appendix); Google Maps uses the WGS84 standard.

Names of higher taxa.—There is an emerging consensus that the majority of Ediacaran soft-bodied organisms are metazoans, but their phylum and class level assignments remain uncertain. To provide a framework for discussion, we assign taxa to some extinct higher taxa (e.g., class Archaeocyatha) and indicate under remarks and discussion where such plesions probably join the tree of life (e.g., stem Demospongiae).

Materials and methods

Most of the material used for this study was obtained during fieldwork carried out in Namibia in 1993, 1995, and 1996 with the assistance and cooperation of A. Seilacher, University of Tübingen (August 1993) and the participants in an International Union of Geological Sciences–International Geoscience Programme-funded field workshop on the Terminal Proterozoic System (May 1995) and the support and advice of the Geological Survey of Namibia (May 1995 and August–September 1996). In addition, we had access to the Pflug collection, housed in Germany before it was returned to Namibia (August 1993), to the Richter collection (Richter, 1955) in the Senckenberg Museum of Natural History, Frankfurt (July 1993), to the Haughton types and some of the Germs collection (Haughton, 1960; Germs, 1972a, 1973) in the Iziko South African Museum, Cape Town (August 1993), and to a large number of plaster casts of specimens of *Pteridinium* held by the State Museum of South West Africa, Windhoek. Those casts were made at UCLA in 1966 by LouElla Rankin Saul, then a Museum Scientist and curator of the paleontological collections (Groves and Squires, 2023), from material that was borrowed and returned about that time by Preston Cloud (Cloud and Nelson, 1966).

Stratigraphic sections were measured using a Jacob staff, and stratigraphic thicknesses were checked, where possible, with a Thommen Altitronic Traveller altimeter on the assumption that the dips are negligible in the sections measured. The accuracy but not precision of the altimeter was checked at the trigonometric station at the top of Dundas Hill on Swartpunt farm on 23 August 1996, when the altimeter recorded an elevation of 1,124 m versus the surveyed height of 1,169 m. There are, however, some discrepancies between our measurements and those of others who have studied the same sections. To illustrate these discrepancies, we tabulated the measured heights of these and other features, such as bed boundaries and distinctive rock types identified by us, Saylor (1996), and Turk et al. (2022) in the Arimas section (Fig. 4).

In the case of the Dundas section on Swartpunt farm (Figs. 1, 5), the fossiliferous interval includes a deformed slump or fault block that varies in thickness along strike and is, at least, slightly allochthonous, although its internal stratigraphy is thought to be intact (Saylor, 1996; Saylor and Grotzinger, 1996; Narbonne et al., 1997; Darroch et al., 2015; Linnemann et al., 2019). Differences between our measurements and those of other authors may therefore be partly attributable to the fact that we measured a thinner section of the slumped sequence. However, we also place the upper four of five dated volcanic ash beds at lower elevations in the profile than did Saylor (1996) and Linnemann et al. (2019), despite the fact that our thickness measurements agree with those of the other authors overall. As correct superpositional order is more important than absolute thicknesses, except for relocating sampled horizons, these discrepancies in measured thickness are not considered significant.

Preparation of the fossils has been minimal. Field photographs and images of specimens taken during the 1990s were made with a Minolta X700 35 mm FSLR camera equipped with Minolta MC Macro Rokkor-QF 50 mm lens using Kodak Ektachrome Professional film. Color slides and negatives were digitized using an Epson Perfection V700 Photo scanner. Digital images, taken more recently, were made with a Nikon D3100 DSLR camera equipped with Nikon AF-S Micro Nikkor 40 mm lens. Preparation of the figures was carried out with Adobe Photoshop, Adobe Illustrator, Aldus Super3D, and Synergy KaleidaGraph.

Carbonate hand samples for isotopic analysis were collected at 1 m intervals, where possible. Carbonate powders were

https://doi.org/10.1017/jpa.2023.81 Published online by Cambridge University Press

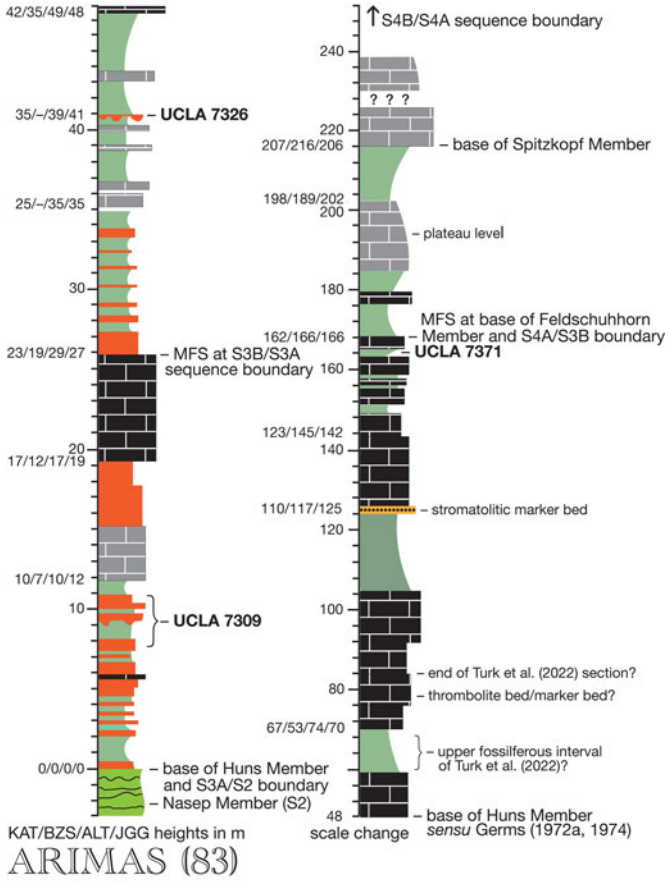

Figure 4. Measured stratigraphic section, Arimas; rock types are siliciclastics (red/dark gray), carbonates (brick-wall patterns), and siltstones (green/light gray). This section was also measured by Saylor (1996, section 20, p. 296–304) and Turk et al. (2022, fig. 4), so normalized estimates of common distinctive horizons (KAT, Turk et al., 2022; BZS, Saylor, 1996; and ALT, altimeter) are listed for comparison with JGG's Jacob staff measurements. Fossiliferous levels sampled in this study are shown by their UCLA numbers. The S3B/S3A sequence boundary at the top of the second limestone is a marine flooding surface (MFS) that is correlated with prominent karst horizons at Witputs and Swartkloofberg (Saylor, 1996, p. 269, 339; Saylor, 2003). Lithologic symbols: brick wall patterns = limestones, dark (black) and light (gray); rhomboidal brick patterns = dolomites; red = sandstones and arenites; recessive units, gray or green = mainly siltstones.

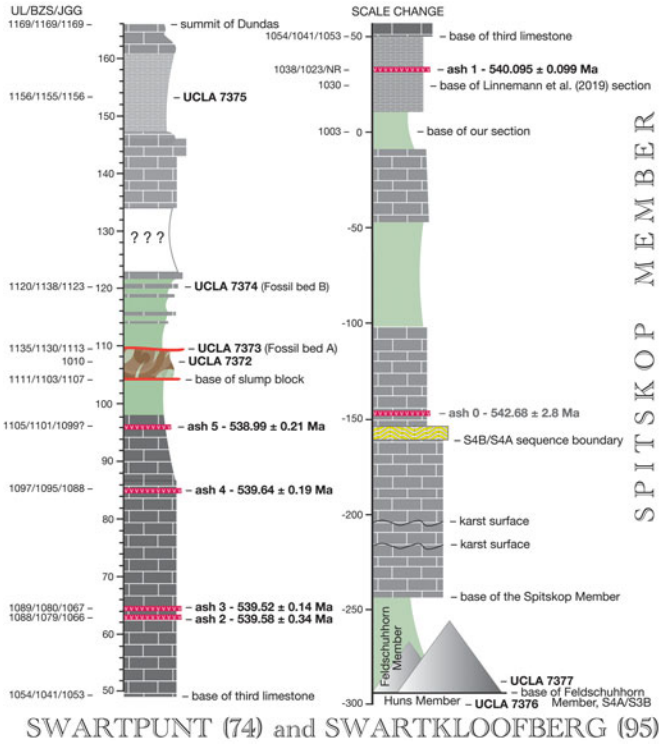

Figure 5. Measured stratigraphic sections, Dundas, Swartpunt, and Swartkloofberg farms; rock types are siliciclastics (red/dark gray), carbonates (brick-wall patterns), siltstones (green/light gray), and volcanic ash beds (red/gray with white v pattern); the cones represent pinnacle reefs that grew upward from the S4A/S3B sequence surface and were buried by the Feldschuhhorn Member (Saylor and Grotzinger, 1996; Grotzinger et al., 2000). The uppermost 50 m of this section (left) has also been measured by Saylor (1996, section 14, p. 291–293) and Linnemann et al. (2019, fig. 3), so estimates of the elevations of significant horizons, normalized in each case from the surveyed summit of Dundas (1,169 m; 2716B Rekvlakte 1:50 000 topographic map, 1979), are also shown (UL, Linnemann et al., 2019; BZS, Saylor, 1996) for comparison with JGG's Jacob staff measurements. Most of the right column is taken from Saylor (1996, section 14, p. 288–293) and Saylor and Grotzinger (1996, fig. 4C), again shown as if measured downward from the summit of Dundas. Fossiliferous horizons sampled in this study are listed by their UCLA numbers; "Fossil Bed A" and "Fossil Bed B," named by Narbonne et al. (1997), are shown at our measured stratigraphic positions; the U–Pb ages are from Schmitz (2012) and Linnemann et al. (2019), but the plotted levels of ashes 2–5 are from our own observations. *Pteridinium* and *Swartpuntia* have also been reported from near the top of our unexposed interval by Saylor (1996) and Darroch et al. (2015). Lithologic symbols: brick wall patterns = limestones, dark (black) and light (gray); rhomboidal brick patterns = dolomites; red = sandstones and arenites; recessive units, gray or green = mainly siltstones; wavy pattern = stromatolitic horizon; v pattern = ash beds.

obtained, so far as was practical, from micritic sections of sawn and smoothed slabs, avoiding fractures and secondary cements. No attempt was made to vet the samples for diagenesis using chemical or optical methods on the grounds that diagenetically altered samples are relatively easy to distinguish using oxygen isotope measurements in densely sampled sections. All isotope measurements were made at Harvard University (Mooifontein section) or the University of California, Santa Cruz, using standard methods (e.g., Kaufman et al., 1991; Zachos et al., 1997).

Repositories and institutional abbreviations.—Types, figured, and other specimens examined in this study are (or were) deposited in the following institutions: National Earth Sciences Museum, Ministry of Mines and Energy (GSN), Windhoek, Namibia; State Museum of South West Africa (SMSWA), Windhoek, Namibia; Iziko South African Museum (ISAM), Cape Town, South Africa; Senckenberg Museum of Natural History (SMNH), Frankfurt, Germany; Yale Peabody Museum (YPM), New Haven, Connecticut, USA; North Carolina State Museum of Natural Sciences (NCSM), Raleigh, North Carolina, USA; Department of Geology, University of North Carolina (UNC), Chapel Hill, North Carolina, USA; Los Angeles County Museum of Natural History (LACMNH), Los Angeles, California, USA; Department of Earth, Planetary, and Space Sciences, University of California, Los Angeles (UCLA), Los Angeles, California, USA. Some specimens remain in the field, as noted in the figure explanations.

Systematic paleontology

Kingdom Animalia Linnaeus, 1758
Phylum Porifera Grant, 1836
Class Archaeocyatha? Bornemann, 1884

https://doi.org/10.1017/jpa.2023.81 Published online by Cambridge University Press

Order Monocyathida? Okulitch, 1935
Genus *Arimasia* new genus

Type species.—*Arimasia germsi* n. gen. n. sp. from the Huns Member of the Urusis Formation, Schwarzrand Subgroup, Arimas farm, Namibia.

Diagnosis.—As for the type species by montypy.

Etymology.—Named for Arimas farm, the type locality.

Remarks.—Nothing similar to *Arimasia* has been described from the Neoproterozoic or, so far as we are aware, from the Phanerozoic. It seems to be a one-walled, solitary, and sessile animal, preserved as a composite mold of both inner and outer surfaces, perhaps resembling an unmineralized version of a monocyathid archaeocyath or a vauxiid sponge.

Arimasia germsi new species
Figure 6

Holotype.—GSN F 1960H from the Huns Member of the Urusis Formation, Schwarzrand Subgroup, UCLA 7376, Arimas farm, Namibia.

Diagnosis.—Centimeter-scale, porous, rugose, horn-shaped skeletons that appear to have been unmineralized or, perhaps, demineralized.

Description.—The holotype (Fig. 6.1, 6.4) is a narrow, conical object, 2 cm long, that has a sealed rounded base and about eight irregular, co-marginal rugae in the lower two-thirds of the structure; the open end of the skeleton was apparently circular but is now flattened by compaction that extends downward toward the rugose part of the cone; the cone surface is evenly granular, giving the impression of a fine mesh, which cannot be fully resolved because of the finite grain size of the matrix; a paratype (Fig. 6.2, 6.3) displays the mesh more clearly; the cells are 200–300 µm apart and appear to be packed like honeycomb; other specimens are more regularly rugose (Fig. 6.6, 6.7) and eight of 10 individuals on one small slab seem to be preferentially oriented, suggesting that the cones may have been tethered to the substrate (Fig. 6.5).

Etymology.—Named for Gerard J.B. Germs, in celebration of the fiftieth anniversary of the publication of his groundbreaking, University of Cape Town, Ph.D. dissertation on the stratigraphy and paleontology of the lower Nama Group (Germs, 1972a).

Materials.—Eight specimens (GSN F 1953–1960), each with one or several specimens from UCLA 7376.

Remarks.—Antcliffe et al. (2014) reviewed all of the then published reports of the oldest fossil sponges and recommended caution in making such claims. They proposed two selection criteria that should always be met and summarized a passing grade as: "The characters claimed for are useful for detecting sponges in the fossil record and have been reliably shown to be present in the particular candidate fossil." In their opinion, the oldest fossil sponges are siliceous hexactinellid spicules from the Fortunian of Iran (also China; Chang et al., 2017) and Archaeocyatha from the Tommotian (Cambrian Stage 2) of Siberia, a conclusion that has not been effectively challenged by subsequent reports of sponge-like fossils of Ediacaran or earlier ages (e.g., Turner, 2021). Antcliffe et al. (2014, p. 999) also concluded that "the ancestral archaeocyathan sponges must occur in the [Fortunian] *Purella antiqua* Zone and would have consisted of small, simple rounded cups, each provided with a single, weakly calcified wall, perforated by simple pores."

Arimasia germsi appears to pass these two selection criteria by having the sponge characters described in advance by Antcliffe et al. (2014) if our interpretation of the granular texture of the fossil is correct. The cell size of the wall mesh, 200–300 µm (Fig. 6.3), is comparable to the average interpore distance in single-walled Archaeocyatha, such as *Archaeolynthus contractus* Hill, 1965 (~330 µm; Hill, 1965, pl. 1, fig. 1), but is larger than the diameter of the pores, which in double-walled Archaeocyatha is commonly ~100 µm or less (Gravestock, 1984; Antcliffe et al., 2019). Thus, *Arimasia* may be viewed as an unmineralized, apparently single-walled archaeocyath, and perhaps also as a stem group demosponge, if that is where the Archaeocyatha fit into the Porifera (Antcliffe et al., 2014). There are also possible similarities to the unmineralized vauxiid sponges, which first appear in the Cambrian Stage 3 Chenjiang biota (Wei et al., 2021) and are regarded by some as being on the pathway to the keratose demosponges, now thought to be the monophyletic or paraphyletic sister group of the spiculate Heteroscleromorpha (Erpenbeck et al., 2012; Wörheide et al., 2012; Plese et al., 2021).

Although there is widespread agreement that the Archaeocyatha are hypercalcified aspiculate sponges (Rowland, 2001; Debrenne et al., 2012; Antcliffe et al., 2014) rather than some kind of calcified alga (Kazmierczak and Kremer, 2022), their position within the poriferan total group remains so uncertain as to be almost ignored (e.g., Botting and Muir, 2018). *Arimasia* may provide a way forward in that it is demonstrably older than any known spiculate sponge, was apparently unmineralized, and is similar in body form to the organic-walled vauxiids (Rigby, 1980, 1986; Botting et al., 2013; Luo et al., 2020; Wei et al., 2021), which Luo et al. (2021) have suggested might be demineralized archaeocyaths. Alternatively, *Arimasia*, *Vauxia*, and the archaeocyaths may all have been aspiculate stem group sponges, and therefore the vauxiids are not demineralized archaeocyaths (Luo et al., 2021) but, instead, were unmineralized members of the lineage leading to the aspiculate demosponges. This hypothesis would require the acquisition of siliceous spicules independently in the Hexactinellida and the Demospongiae, a proposal that has been vigorously rejected by nearly all sponge paleobiologists (e.g., Botting and Muir, 2018) but has recently received some molecular support (Aguilar-Camacho et al., 2019).

Class Erniettomorpha Pflug, 1972
Family Pteridinidae Richter, 1955
Genus *Pteridinium* Gürich, 1933

Type species.—*Pteridinium simplex* Gürich, 1933 from the Kliphoek Member of the Dabis Formation, Kuibis Subgroup, Aus district, Namibia, by monotypy.

https://doi.org/10.1017/jpa.2023.81 Published online by Cambridge University Press

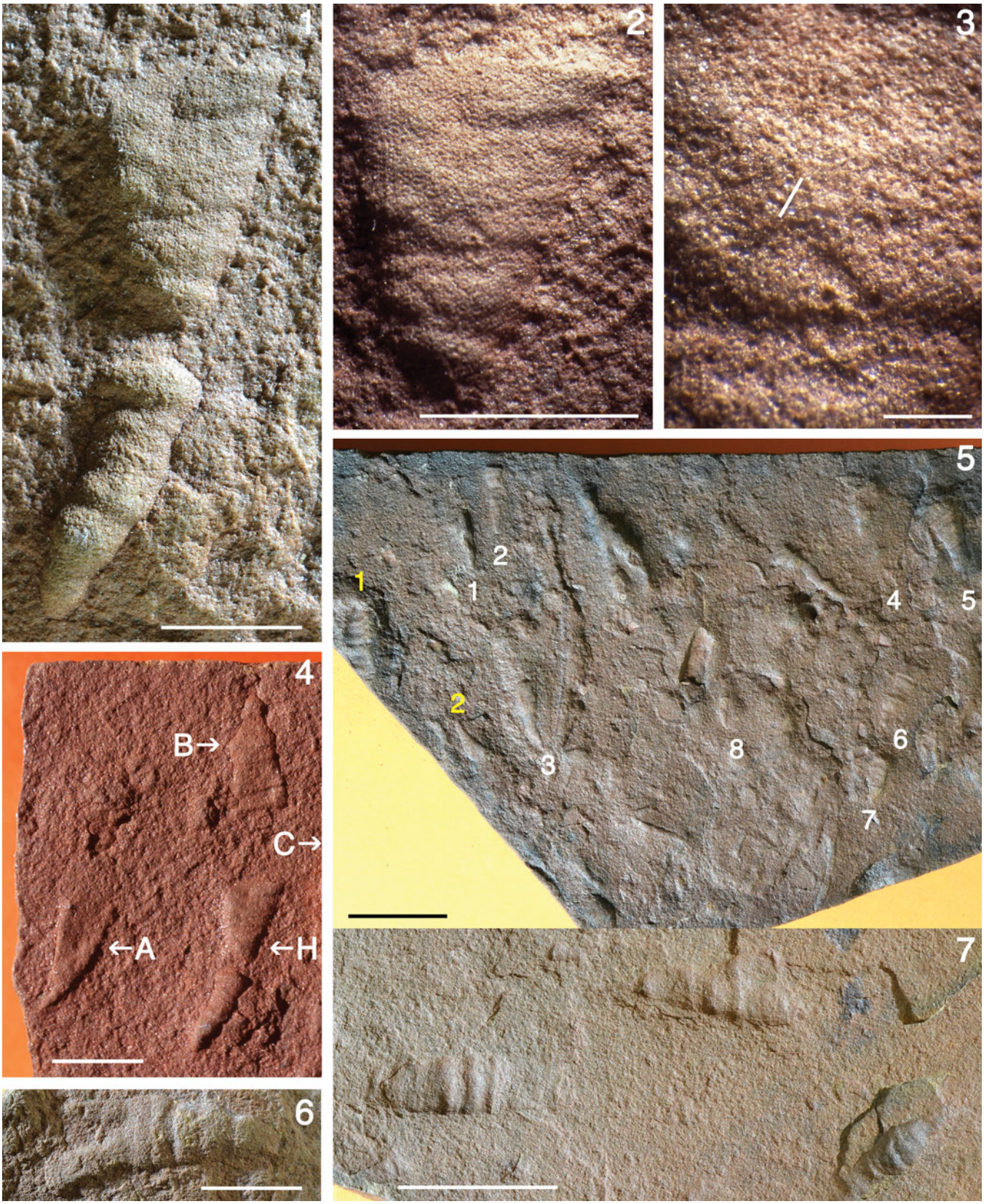

Figure 6. *Arimasia germsi* n. gen. n. sp., Huns Member, Urusis Formation, UCLA 7326, Arimas farm. (**1, 4**) Holotype, GSN F 1960H, showing rugose form, the apparently porous nature of the body wall, and other individuals (GSN F 1960A, GSN F 1960B, GSN F 1960C) on the same surface. (**2, 3**) GSN F 1960C, also showing the porous body wall. (**5**) A single surface with at least 10 specimens of *A. germsi,* eight of which (white numerals) are opening upward in this view, and the other two (yellow numerals) are facing downward, GSN F 1954. (**6**) External mold of one of the largest specimens, GSN F 1958. (**7**) Three, possibly current-aligned, specimens, GSN F 1955. (**1, 2**) scale bars = 5 mm; (**3**) horizontal scale bar = 2 mm; inclined scale bar = 1,000 µm; (**4, 6**) scale bars = 1 cm; (**5, 7**) scale bars = 2 cm.

https://doi.org/10.1017/jpa.2023.81 Published online by Cambridge University Press

Other species.—?*Paradoxides carolinaensis* St. Jean, 1973, from the Floyd Church Formation, Albemarle Group, Stanly County, North Carolina, USA; *Pteridinium nenoxa* Keller in Keller et al., 1974; *Inkrylovia lata* Fedonkin in Palij et al., 1979.

Diagnosis.—Frondose organisms, up to at least 0.4 m long, that are made of three equal-sized organic-walled vanes that are set lengthwise about an axis that extends from the curved proximal end to the acute distal growing tip; each vane is constructed from sealed tubular modules that meet alternatively or oppositely at the axis, depending on their order about it, and are concave toward the distal end of the frond; margins of the vanes are defined by smooth, thickened edges against which the modules terminate without narrowing.

Occurrence.—Kliphoek, Buchholzbrunn, and Mooifontein members of the Kuibis Subgroup and Nudaus, Nasep, Huns, and Spitskop members of the Schwarzrand Subgroup, Nama Group, Namibia (Fig. 2; Appendix); basal Ediacara Member, Rawnsley Quartzite, South Australia (Glaessner and Wade, 1966; Gehling and Droser, 2013); Floyd Church Formation, Albemarle Group, North Carolina, USA (St. Jean, 1973; Gibson et al., 1984; McMenamin and Weaver, 2002); Syuzma/Verkhovks member, Ust-Pinega Formation, Onega Peninsula, Russia (>552.85 ± 0.77 Ma; Keller et al., 1974; Fedonkin, 1981; Ivantsov and Grazhdankin, 1997; Grazhdankin, 2004; Ivantsov et al., 2019); Shibantan Member, Dengying Formation, China (<550.1 ± 0.06 Ma; Chen et al., 2014; Xiao et al., 2021; Yang et al., 2021); doubtfully, Ukraine (Fedonkin, 1983), Canada (Narbonne and Aitken, 1990), and Iran (Vaziri et al., 2021).

Remarks.—It is not clear why Pflug's (1972) class Erniettomorpha has been widely adopted in preference to his Pteridinomorpha, which has page precedence, but we follow that practice for the probable clade (Dececchi et al., 2017) that includes *Pteridinium* Gürich, 1933, *Ernietta* Pflug, 1966, *Phyllozoon* Jenkins and Gehling, 1978, *Swartpuntia* Narbonne, Saylor, and Grotzinger, 1997, and perhaps *Ventogyrus* Ivantsov and Grazhdankin, 1997, and *Miettia* Hofmann and Mountjoy, 2010. *Inkrylova lata*, the type species of *Inkrylova* Fedonkin in Palij et al., 1979, appears to be a junior synonym of *Pteridinium nenoxa* Keller in Keller et al., 1974. The relationships of these and other species of *Pteridinium* are discussed under the description of *P. simplex*. *Pteridium* Gürich, 1930 (Gürich, 1930b) was a nomen nudum replaced, perhaps unnecessarily, by *Pteridinium* Gürich, 1933; *Onegia* Sokolov, 1976 is a nomen nudum applied to Keller's species *nenoxa* by Sokolov (1976) and Grazhdankin (2004). As discussed under the genus *Ernietta* Pflug, 1966, the holotype of the type species, *E. plateauensis* Pflug, 1966, appears to be a specimen of *Pteridinium simplex*, so technically *Ernietta* becomes a subjective junior synonym of *Pteridinium*. However, we propose that an application be made to the International Commission on Zoological Nomenclature (ICZN) to replace the holotype of *E. plateauensis* with a neotype, the holotype of *Erniograndis sandalix* Pflug, 1972, to retain current usage of this well-established name.

Pteridinium simplex Gürich, 1933

Figures 7–9, 10.1–10.4, 11.1–11.3, 11.6–11.8, 19.1, 19.2, 19.7

1930b *Pteridium simplex* Gürich, p. 637, nomen nudum.
1933 *Pteridinium simplex* Gürich, p. 144, fig. 4a–c.
1955 *Pteridinium simplex*; Richter, p. 246, pls. 1–6, figs. 1–10, pl. 7, fig. 11.
1963 *Pteridinium simplex*; Glaessner, p. 8, pl. 1, figs. 1–4, pl. 2, fig. 1.
1966 non *Pteridinium* cf. *P. simplex*; Glaessner and Wade, p. 616, pl. 101, figs. 1–3.
1966 *Ernietta plateauensis* Pflug, p. 22, pl. 1, figs. 1–7.
1966 *Pteridinium simplex*; Cloud and Nelson, fig. 1A, C.
1972a *Pteridinium simplex*; Germs, p. 173, pl. 21, figs. 1, 2.
1972 *Ernietta plateauensis*; Pflug, p. 163, pl. 34, figs. 1–4, 6.
1977 non *Pteridinium simplex*; Keller and Fedonkin, p. 926, pl. 2, fig. 4.
2002 *Pteridinium simplex*; Grazhdankin and Seilacher, fig. 1, pl. 1, figs. 1–3.
2014a *Pteridinium simplex*; Meyer et al., figs. 2–6.
2022 *Pteridinium simplex*; Runnegar, p. 1103, fig. 9A.
2022 *Pteridinium simplex*; Darroch et al., figs. 2–5.
2022 non *Pteridinium simplex*; Darroch et al., fig. 7.

Neotype.—Gürich's (1933) specimens were lost during World War II so Richter (1955) nominated a neotype, a sandstone cast of part of a frond with two visible vanes (SMNH XXX 660f), probably from the Kliphoek Member, Kuibis Formation, on Plateau or Aar farm, Aus district, Namibia (Richter, 1955, pl. 1, fig. 1a, b; Darroch et al., 2022, fig. 1a, b).

Diagnosis.—A "three-vaned, ribbon-like frond" (Ivantsov et al., 2016, p. 540) in which the modules are less well expressed in the outer halves of the vanes.

Description.—Elongate, frondose organisms formed of three equal-sized, undivided vanes that radiate from a common axis and may exceed 0.4 m in length without signs of expansion or tapering in width; vanes are composed of curved to straight tubular modules that are commonly, but not always, more topographically expressed near the axis than the periphery; modules maintain a similar-sized cross section across the vane and terminate abruptly at the distal margins; vanes terminate axially in closed, polyhedral ends that either alternate with those of other modules in a zig-zag fashion or are directly opposed, depending on position around the axis (Fig. 8.8–8.10; Runnegar, 2022, figs. 9, 10); in two specimens with visibly narrowing vanes, the curvature of the modules is convex in the direction of narrowing and the angle of narrowing is 10° or less (Fig. 11.1, 11.2; Richter, 1955, p. 249, pl. 6, fig. 7; Runnegar, 2022, fig. 9a); whether the tapering of the vanes is unidirectional or bidirectional is unknown; vane margins are commonly obscure but when well preserved are delineated by a narrow differentiated edge (Figs. 9.2–9.4, 10.3) that was stiff enough to imprint other individuals (Fig. 7.3–7.5); vane curvature generally coaxial but inconsistent; two of the vanes are frequently opposite each other at the axis and either lie parallel to bedding or curve quasi-symmetrically to partially

https://doi.org/10.1017/jpa.2023.81 Published online by Cambridge University Press

embrace the third vane (Fig. 11.6–11.8), thus producing W-shaped cross sections (Fig. 7.5).

Materials.—Seven specimens (GSN F 1853–1859) from UCLA 7307; ~20 plaster casts of SMSWA specimens; ~20 specimens, mostly from Plateau and Aar farms in the SMNH collection (Richter, 1955); the Pflug (1970a) collection, plus numerous examples observed in the field at Aar farm and in the "museum" at Plateau farm, including the excavation and casting of the Seilacher slab and other specimens in 1993 (Fig. 10.1, 10.2; Crimes and Fedonkin, 1996; Seilacher, 1997, 2007; McMenamin, 1998; Grazhdankin and Seilacher, 2002; Ivantsov et al., 2019).

Taphonomy.—The numerous specimens that have been observed, extracted, and studied from the Amphitheatre site (UCLA 7307) on Aar farm (Figs. 3, 7–9, 10.1–10.4, 11.1–11.3; Richter, 1955; Grazhdankin and Seilacher, 2002; Vickers-Rich, 2007; Meyer et al., 2014a, b, Darroch et al., 2022) are all from a set of quartz sandstone beds that have been named the Aarhauser sandstone submember by Hall et al. (2013) (Fig. 3). The bed that was the source of the Seilacher slab is about 0.4 m thick, has a deeply erosive base (Fig. 7.2), a horizontally bedded to low-angle cross-stratified upper part (Fig. 8.1, 8.2, 8.4), a middle zone with cylindrical specimens of *Pteridinium* (Fig. 10.4; Crimes and Fedonkin, 1996, pl. 2c, d), and a thicker, poorly laminated lower part that is richly fossiliferous. *P. simplex* is widespread in the laminated to upper cross-stratified part, typically as long, straight segments of two-vaned fronds seen in plan view on bed surfaces, as W-shaped intersections on east–west joints, and as upright, stretched single vanes on the faces of north–south joints (Figs. 8.1, 8.2, 9.2–9.4; Darroch et al., 2022, fig. 5). Almost invariably, the axes of vanes seen on joint faces lie parallel to bedding and are commonly at the bottom of the vanes, even when the whole organism is twisted through 180° about a horizontal axis (Figs. 8.1, 8.2, 8.4, 8.6, 8.7, 9.6, 11.6–11.8). There is no evidence that the upright middle vane, the "chaperone wall" of Grazhdankin and Seilacher (2002), routinely switches places with one of the other vanes during the 180° folding, as shown in the sketch (Fig. 8.5) from Grazhdankin and Seilacher (2002), as previously noted by Meyer et al. (2014a). That would require improbable twisting about two different rotational axes. The other common U-turn is a hairpin bend (Figs. 9.5, 9.7, 9.8, 19.1, 19.2; Richter, 1955, pl. 7, fig. 11; Vickers-Rich, 2007, fig. 108; Meyer et al., 2014a, figs. 3–6), in which the fold axis is vertical rather than horizontal. One such U-turn, found in situ in 1993 (Fig. 9.5, 9.7, 9.8), was at the upstream end of the hairpin-shaped fossil, as shown by the orientations and of 10 flat-lying specimens measured on the top surface of the same outcrop (Fig. 3). Thus, most if not all of the examples of *P. simplex* found in the upper, laminated to cross-laminated layers of the Aarhauser sandstone appear to have been transported by northward-flowing high-velocity currents, as suggested previously (Jenkins, 1985; Elliott et al., 2011; Darroch et al., 2022).

A middle zone of closely packed tubular fossils is more problematical but is almost certainly a death association, perhaps created by close packing of enrolled, hairpin-shaped individuals (Fig. 10.4) rather than a population of sealed underground sausage-shaped organisms, as envisaged by Crimes and Fedonkin (1996). As the horizon is less accessible, it has not been well studied.

The lower layers are filled with *P. simplex* preserved in a somewhat different fashion, as can be seen from an extracted block in the Richter collection (Darroch et al., 2022, fig. 2). The lower part of this block, a similar specimen figured by Glaessner (1979b, fig. 11.1b), and the far more extensive Seilacher slab (Fig. 10.1–10.4; Seilacher, 1997, 2007; Grazhdankin and Seilacher, 2002) have doubly curved fronds that—to some—resemble inverted bathtubs or boats (Figs. 8.3, 9.2; Grazhdankin and Seilacher, 2002, text-fig. 1). These are the shapes that have given rise to the canoe model for *Pteridinium* (Pflug, 1970a; Buss and Seilacher, 1994; Ivantsov and Grazhdankin, 1997; Grazhdankin and Seilacher, 2002; Meyer et al., 2014b; Droser et al., 2017; Darroch et al., 2022) and to the hypothesis that *Pteridinium* lived on, in, or wholly within the sediment (Crimes and Fedonkin, 1996; Seilacher, 1997, 2007; Grazhdankin and Seilacher, 2002; Darroch et al., 2022). However, these lower layers also preserve specimens that are folded like tacos. In these cases, two oppositely directed vanes are bent through 180° about a horizontal axis, and for geometrical reasons, the third vane must follow one of the other two (Fig. 9.6). This cannot be a life orientation, so the fact that this postmortem topology is found among the canoes is evidence that all were transported before burial. As no one has described or illustrated convergence of the three vanes to form the "prow" or "stern" regions of any specimen of *P. simplex*, the canoe hypothesis is not supported by observation. Thus, we consider all of the material in the Aarhauser sandstone to have been transported by high-energy events. In this context, the experiments in computational fluid dynamics carried out by Darroch et al. (2022) may help understand the fact that in the laminated upper part of the Aarhauser sandstone, the horizontal laminae intersect the vertical or steeply inclined vanes with no trace of edge effects (Figs. 8.2, 8.4, 9.2–9.4; Crimes and Fedonkin, 1996; Elliott et al., 2011; Darroch et al., 2022). This would be possible if the sediment were moving by laminar rather than turbulent flow when transport is parallel to the vanes, as shown by the calculated streamlines (Darroch et al., 2022, fig. 10C). In this scenario, the only individuals to be trapped and buried were those that were concave enough to receive and retain sediment; presumably, all of the rest were blown away like discarded plastic shopping bags in the surf (see artwork by John D. Dawson in Monastersky and Mazzatenta, 1998). Additional support for frequent transport may come from widespread bed base rake and bump structures (Fig. 12), which we interpret as tool marks generated by *Pteridinium* or another erniettomorph.

Remarks.—*Pteridinium* is an uncommon fossil except at Aar and Plateau farms. It is, therefore, difficult to find populations large enough to compare with *P. simplex*. The next most frequent occurrences are from localities on the Onega Peninsula, Russia, but there the fossils are fragmentary and frequently deformed (Keller et al., 1974; Fedonkin, 1981, 1985; Palij et al., 1983; Ivantsov and Grazhdankin, 1997; Grazhdankin, 2004). Fortunately, the second species of

https://doi.org/10.1017/jpa.2023.81 Published online by Cambridge University Press

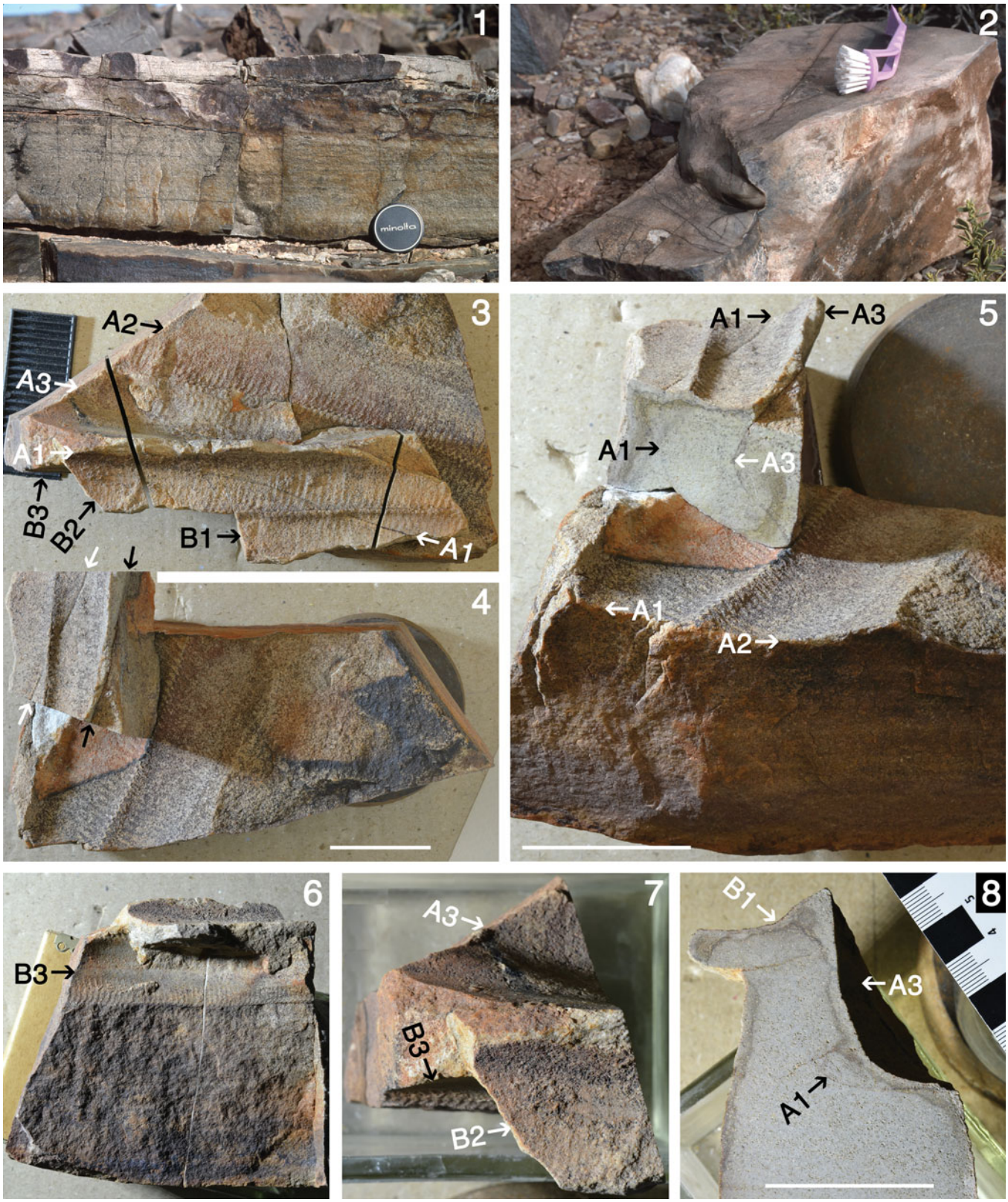

Figure 7. *Pteridinium simplex* Gürich, 1933, Aarhauser sub-member, Kliphoek Member, Dabis Formation, UCLA 7307, Aar farm. (**1**) A 25 cm thick bed of micaceous quartz sandstone overlain by dislodged joint blocks of the bed, many of which are fossiliferous. (**2**) Overturned piece of the same bed showing current scoured base. (**3**) Reassembled pieces of one joint block that contains two subparallel specimens of *P. simplex*, GSN F 1855A and GSN F 1855B, each composed of three vanes, A1, A2, A3, etc., lying with their axes parallel to bedding. (**4**) Two parts of the same block, viewed perpendicular to bedding, with the upper edges of vanes A1 and A3 indicated by white and black arrows, respectively. (**5**) Foreshortened oblique view of the reassembled block showing cross sections of vanes A1 and A3 on the sawn surface. (**6**) Lateral view of vane B3 with its lower edge parallel to bedding. (**7**) End piece viewed from the top to show the relative positions of vanes A3, B2, and B3. (**8**) Sawn edge of the end piece in (**7**) showing the cross-sectional curvature of vanes A1, A3, and B1. (**1**) Camera lens cover = 60 mm; (**2**) brush = 25 cm; (**3, 4**) scale bar = 5 cm; (**5**) scale bar = 3 cm but variable scales due to foreshortening; (**6–8**) scale bar = 3 cm.

https://doi.org/10.1017/jpa.2023.81 Published online by Cambridge University Press

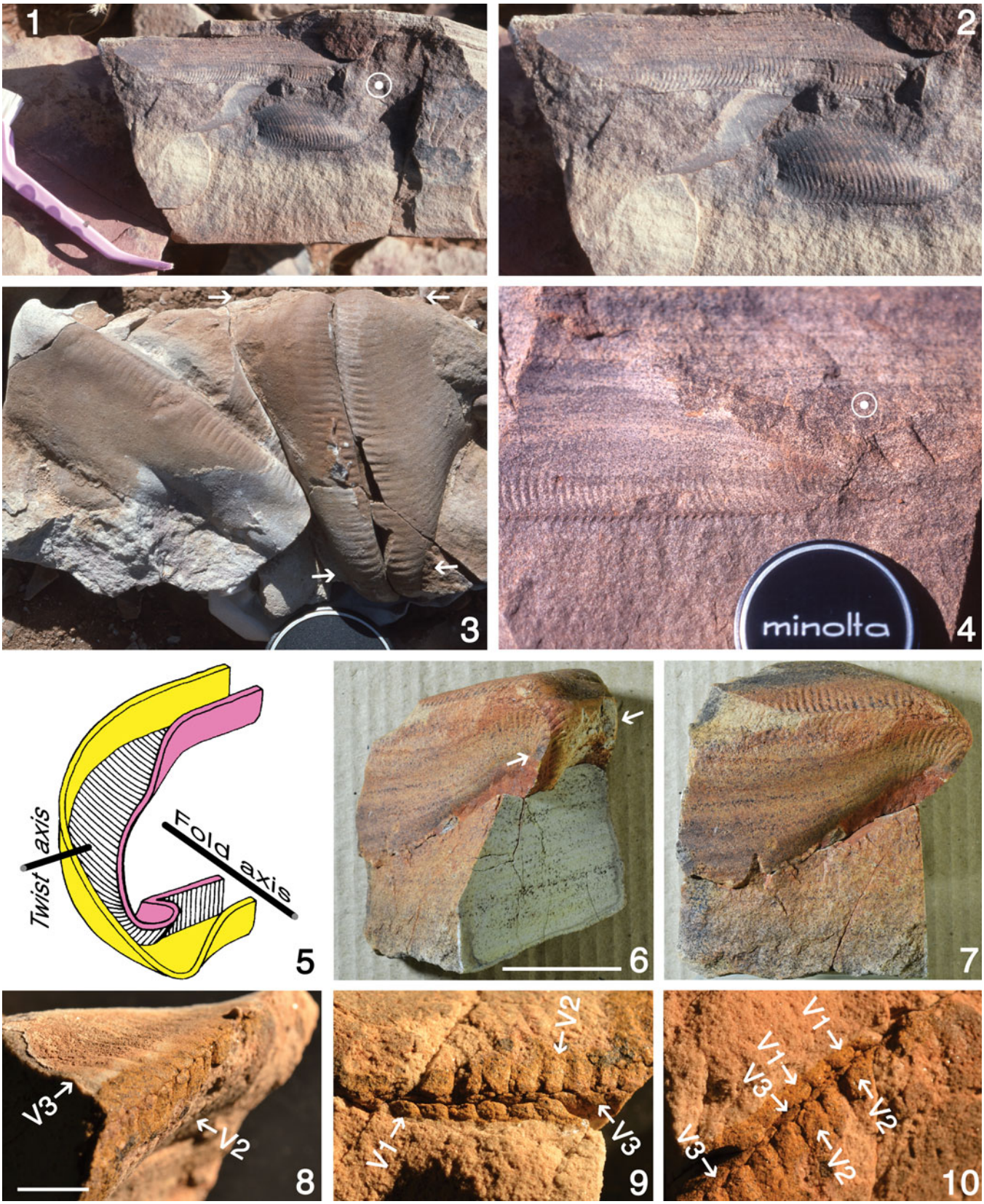

https://doi.org/10.1017/jpa.2023.81 Published online by Cambridge University Press

Figure 8. Folded specimens of *Pteridinium simplex* Gürich, 1933, Aarhauser sub-member, Kliphoek Member, Dabis Formation, UCLA 7307, Aar farm. (**1**) Field photograph of a dislodged but upright 20 cm thick joint block with a specimen of *P. simplex* folded about a horizontal axis (white dot with circle around it) and with longer upper part of the organism extending downstream. (**2**) Enlargement of (**1**) to show details of the limbs. (**3**) Field photograph of base of block excavated by the Seilacher team in 1993 (Seilacher, 1997) showing two similarly folded specimens of *P. simplex*, GSN F 758 and GSN F 576 (arrows indicate positions of horizontal fold axes), which became the basis for the "canoe" model for *Pteridinium* (Grazhdankin and Seilacher, 2002). (**4**) Field photograph of another dislodged joint block showing prominent horizontal lamination and one vane of a *P. simplex* that is tightly folded about a horizontal axis (white dot with circle around it). (**5**) Part of drawing (Grazhdankin and Seilacher, 2002, fig. 5C, republished with permission) used to explain both the canoe and vane substitution models for the growth of *Pteridinium*; note that vane substitution requires both twisting through 180° and folding about a horizontal axis. (**6**) Oblique view of small joint block that has been broken and sawn to reveal details of the kind of folds seen in (**1, 2, 4**), with the fold axis indicated by the arrows (GSN F 1857). (**7**) Same specimen as (**6**), lateral view. (**8–10**) Weathered fragment (GSN F 1856) that shows how the proximal ends of the three vanes, V1, V2, and V3, interlock; the modules of vanes V1 and V2 are opposite each other, whereas the modules of each alternate with those of V3 (**9, 10**). (**1**) Brush = 25 cm; (**3, 4**) camera lens cover = 60 mm; (**6, 7**) scale bar = 5 cm; (**8–10**) scale bar = 1 cm.

Pteridinium to be described, *P. carolinaensis* (St. Jean, 1973), seems to differ markedly from *P. simplex*, so we begin by examining the binary choice, *simplex* or *carolinaensis*? If all known specimens of *Pteridinium* can be comfortably referred to one of these two species, then this interim solution may serve until more quantitative information becomes available. If there are numerous intermediates that cannot be so allocated, then perhaps *P. simplex* should serve as the only known species of *Pteridinium* for the time being.

In a careful study of 18 specimens of *carolinaensis* and 25 specimens of *simplex* using modern morphometric methods, Meyer (2010) and Meyer and Xiao (2010) were unable to find any statistically significant differences between these two species on the basis of a landmark analysis designed to capture variability in size, vane shape, and module curvature. They therefore suggested that *P. carolinaensis* is a junior synonym of *P. simplex*. However, they could not incorporate rarely preserved features of the fossils, such as overall frond size and shape, in their analysis because these features are seen in too few specimens.

Perhaps the most striking feature of the seven specimens of *P. carolinaenis* that have been illustrated (St. Jean, 1973; Gibson et al., 1984; McMenamin and Weaver, 2002; Gibson and Teeter, 2011) is that six show terminations, even in specimens comparable in size (~20 cm) to many examples of *P. simplex*. Similar terminations are known from one specimen from the Spitskop Member (UCLA 7373) identified as *P. carolinaensis* by Narbonne et al. (1997) and from one of the ~50 then-known specimens of *P. nenoxa* Keller in Keller et al.,1974 (Fedonkin, 1981, pl. 5, fig. 2), but not from any of the numerous specimens of *P. simplex*. Whether this is a demographic difference is difficult to assess because all of the specimens in the Aarhauser sandstone at Aar could, conceivably, be members of a single long-lived cohort. Given the differences in frond size, module curvature, and module expression across the vanes, we continue to treat *simplex* and *carolinaensis* as separate species. *P. nenoxa* shares those characteristics with *P. carolinaensis* rather than *P. simplex* (Fedonkin, 1985), as do specimens of *Pteridinium* from Bed A (UCLA 7373) at Swartpunt farm (Figs. 10.5, 11.4, 11.5; Narbonne et al., 1997; Darroch et al., 2022, fig. 7), so we follow others in considering *nenoxa* to be a junior synonym of *carolinaensis* (Runnegar and Fedonkin, 1992; Narbonne et al., 1997; McMenamin and Weaver, 2002; Fedonkin et al., 2007). *Inkrylovia lata* Fedonkin in Palij et al., 1979 is probably a preservational variant of *nenoxa* resulting from expansion of the modules parallel to the axis as a result of soft sediment loading.

Pteridinium carolinaensis (St. Jean, 1973)
Figures 10.5, 11.4, 11.5, 11.9

1966 *Pteridinium* cf. *P. simplex* Gürich, 1933; Glaessner and Wade, p. 616, pl. 101, figs. 1–3.
1973 ?*Paradoxides carolinaensis* (*sic*) St. Jean, p. 204, pl. 3, figs. A–D.
1974 *Pteridinium nenoxa* Keller in Keller et al., p. 133, figs. 1, 2, 4, 5.
1976 *Onegia* ?*nenoxa* Keller; Sokolov, p. 141.
1977 *Pteridinium simplex*; Keller and Fedonkin, p. 926, pl. 2, fig. 4.
1979 *Inkrylovia lata* Fedonkin in Palij et al., p. 70, pl. 56, figs. 1–4.
1981 *Pteridinium nenoxa*; Fedonkin, p. 66, pls. 5–7, pl. 29, fig. 2.
1981 *Inkrylovia lata*; Fedonkin, p. 68, pls. 8, 9.
1983 *Inkrylovia lata*; Palij et al., p. 81, pl. 56, figs. 1–4.
1983 *Pteridinium nenoxa*; Palij et al., p. 81, pl. 58, fig. 3.
1985 *Pteridinium nenoxa*; Fedonkin, p. 99, pl. 11, figs. 1–4.
1985 *Inkrylovia lata*; Fedonkin, p. 100, pl. 12, figs. 3–5.
1992 *Pteridinium carolinaensis*; Runnegar and Fedonkin, fig. 7.5.9E.
1997 *Pteridinium carolinaensis*; Narbonne et al., p. 956, fig. 5.1–5.4.
2002 *Pteridinium carolinaensis*; McMenamin and Weaver, figs. 2–6.
2004 *Onegia*; Grazhdankin, fig. 4.
2022 *Pteridinium simplex*; Darroch et al., fig. 7.

Holotype.—Cast of distal end of frond (NCSM 4041; previously UNC 3062) from the Floyd Church Formation, Albemarle Group, Island Creek, Stanly County, North Carolina, USA (St. Jean, 1973, pl. 3A; Gibson et al., 1984, fig. 6; McMenamin and Weaver, 2002, fig. 2; Weaver and Ganis, 2013, fig. 4A), by original designation.

Diagnosis.—A three-vaned, leaf-like frond in which the modules are well expressed across the whole width of the vanes.

Description.—Frondose organisms apparently formed of three equal-sized, undivided vanes that radiate from a common axis; vane shape is approximately aerodynamic, with a pair of opposed vanes of larger specimens subtending an angle of ~20° at the distal end of the frond and rounded at the proximal end; vanes are composed of curved tubular modules that commonly taper in width across the vanes and terminate abruptly at the distal margins; vanes terminate axially in polygonal ends that alternate with those of other modules in a zig-zag fashion, so far as can be determined; when well preserved, vane margins are delineated by a narrow

https://doi.org/10.1017/jpa.2023.81 Published online by Cambridge University Press

Figure 9. Field and other images of a U-shaped specimen of *Pteridinium simplex* Gürich, 1933, GSN F 1858, that had been exposed by excavation during or before 1993. (**1**) U-shaped end piece (**5, 7, 8**) in place and with the trailing vanes, V1 and V2, extending northward in the direction of downstream transport; an extracted piece with part of V1 (**2–4**) is in the foreground. (**2–4**) Field images of V1 that show the modules leaning downstream and the linear distal edge of the vane. (**5**) U-turn with axis (AX) at periphery. (**6**) Plaster cast of a specimen folded like a taco about a horizontal axis, SMSWA 45730.1 now GSN F 1878. (**7, 8**) Three parts of the U-bend showing the curvature of the axis and the positions and orientations of V1 and V2 on both sides of the turn (downstream is toward the bottom of the page). (**1**) Hammer = 33 cm; (**3**) coin = 23 mm; (**4**) scale bar = 2 cm; (**5–8**) scale bar = 3 cm.

differentiated edge; vane curvature low to negligible, largely for taphonomic reasons; module curvature within vanes is convex toward the presumed proximal end of the frond (Fig. 10.5) and concave toward the opposite end (St. Jean, 1973; Gibson et al., 1984); consistency of vane curvature throughout suggests that the organism grew in only one direction.

https://doi.org/10.1017/jpa.2023.81 Published online by Cambridge University Press

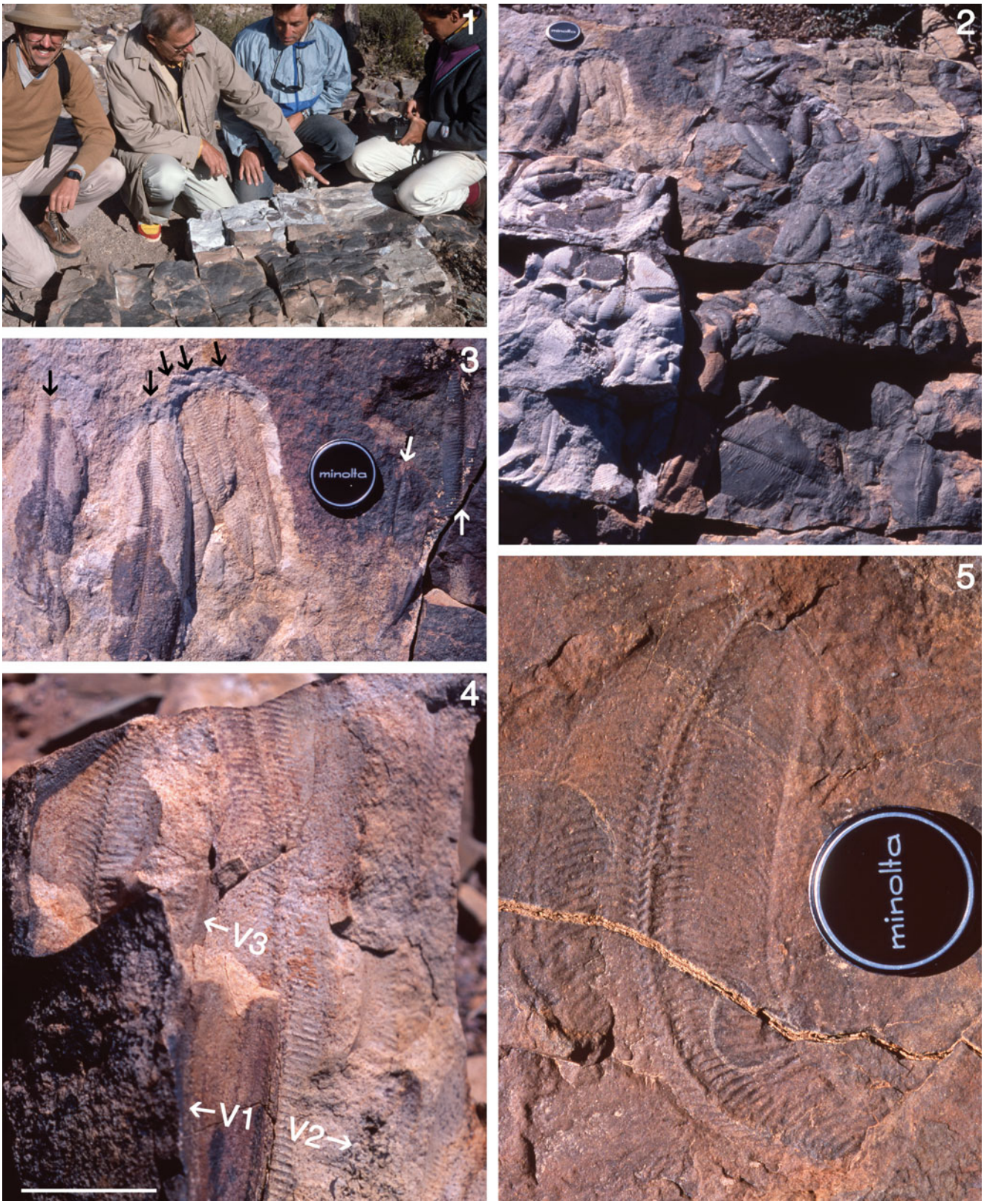

Figure 10. (**1–4**) Joint blocks of Aarhauser sandstone member, Aar farm (UCLA 7307), that had been split approximately in half parallel to bedding to reveal the lower sides of a large number of specimens of *Pteridinium simplex* Gürich, 1933 and then reassembled upside down for molding with silicone rubber by the Seilacher team (Seilacher, 1997). (**1**) Dolf Seilacher, second from left, with Mark McMenamin, Hans Luginsland, and Peter Seilacher viewing the "Seilacher slab" ready for molding, August 1993. (**2**) Richly fossiliferous two-thirds of the Seilacher slab (Seilacher, 1997, 2007, 2008), which inspired the "bathtub" or canoe models for *Pteridinium* living underground. (**3**) Seven aligned and four closely packed specimens of *P. simplex* seen in upper left corner of (**2**); in cross section, those in contact would resemble tubes. (**4**) Top of one of the joint blocks showing that the third vane (V3) may be underneath a pair of vanes (V1 and V2) exposed on the surface of the bed. (**5**) An in situ specimen of *Pteridinium carolinaensis* (St. Jean, 1973), Spitskop Member, UCLA 7373, Dundas Hill, Swartpunt farm. (**2, 3, 5**) Camera lens cover = 60 mm; (**4**) scale bar = 5 cm.

https://doi.org/10.1017/jpa.2023.81 Published online by Cambridge University Press

Materials.—Five reasonably complete specimens observed in the field at Dundas Hill, Swartpunt farm, three specimens described and illustrated by Narbonne et al. (1997), which were examined at Queen's University, and plaster casts of several specimens from White Sea localities kindly supplied by M.A. Fedonkin and the Museum of Paleontology, University of California, Berkeley.

Taphonomy.—All specimens of *P. carolinaensis* from the peri-Gondwanan Carolina terrane are from float (Meyer, 2010) so that only the nature of the sediments that enclosed them is known. The environment of deposition is thought to have been shallow marine adjacent to a volcanic arc, but there is little to indicate whether the fossils were preserved in place or transported before burial. According to Ivantsov and Grazhdankin (1997), the White Sea specimens of *P. nenoxa* are preserved in the Nama manner, and one actually stands vertically in the sediment (Fedonkin, 1981, pl. 29, fig. 2, 1985, pl. 11, fig. 1, 1992, fig. 26), although it is unclear why. The fossils are mostly biconvex, ovoid when viewed from below, and are preserved in sandstone that filled broad, erosive-based channels, similar to those seen in the Buchholzbrunn Member.

Remarks.—If the *Peridinium* from the Spitskop Member on Swartpunt farm is correctly identified as *P. carolinaensis*, then one specimen (Fig. 10.5) preserves the proximal end of the frond, as noted by Narbonne et al. (1997). The holotype, paratype, Rock Hole Creek, and Gleaning Mission Church specimens preserve the distal end of the fronds (Gibson et al., 1984, fig. 5; McMenamin and Weaver, 2002, fig. 4; Gibson and Teeter, 2011), and a small specimen from the Gleaning Mission Church has both (McMenamin and Weaver, 2002, fig. 5). These fossils show that the vanes of *P. carolinaensis* narrowed toward each end of the frond, but the curvature of the modules and overall shape of the frond remained unidirectional throughout growth. If *P. simplex* followed the same pattern of growth, then the specimen shown in Figure 11.1, 11.2 represents the proximal part of the frond, not its growing end.

Pteridinium sp.
Figure 11.10–11.13

Remarks.—Three specimens from the Nudaus Formation on Kyffhauser farm, north of the Osis ridge (Fig. 11.10, 11.12, 11.13), and one from the Buchholzbrunn Member, Namaland, west of Bethanie (Fig. 11.11) are referred to *Pteridinium* but not easily to either *P. simplex* or *P. carolinaensis* because of the narrowness of their modules.

Pteridinium tool marks?
Figure 12.1–12.8, 12.10, 12.11?

Description.—Marks on sandstone bed bases produced by a comb- or rake-shaped tool that had ~30 tines, each capable of producing rounded grooves, narrow channels, or pairs of closely spaced parallel scratches that are typically 2–5 mm apart. In one case, the paired grooves form a chevron-like pattern (Fig. 12.2).

Remarks.—Three examples, two from the Arimas (Fig. 12.3, 12.5A) and one from Kyffhauser (Fig. 12.4), are clearly erniettomorph in character. Presumably, they are impressions of parts of bodies or vanes thrust against the underlying eroded surface by the channel-filling sand that accompanied the transported bodies. In other cases, the tools merely raked or lightly scraped the surface. We interpret the rake marks as being due to the axes of *Pteridinium* fronds, rather than to bodies of *Ernietta*, because of the need for a wide head to the rake and because these structures extend well beyond the known stratigraphic range of *Ernietta* (Fig. 2; Darroch et al., 2021). Comparable tool marks have been reported from the Ingletonian of Yorkshire (Rayner, 1957), the Ordovician of Ohio (Osgood, 1970), the Silurian of Scotland (Trewin, 1979), and the Ordovician of Estonia (Vinn and Toom, 2016). Some are attributed to rolling hard fossils, such as crinoids and corals, but Rayner (1957) and Trewin (1979) were able to substantiate rake marks produced by graptolite stipes and their thecae, which served as the tines. These rake marks—if correctly interpreted—prove the presence of *Pteridinium* in the absence of body fossils, show that premortem transport was ubiquitous, and imply that the axes of the fronds were as stiff as graptolite stipes. The properties of the bump marks rule out both a spicular sponge source and a non-biological origin for these structures (Darroch et al., 2021). Tool marks attributed to *Pteridinium* were described by Fedonkin (1976) and Fedonkin in Palij et al. (1983) as the trace fossil *Suzmites volutatus* Fedonkin, 1976. Whether this name should be applied to the Namibian structures remains a matter for future investigation.

Genus *Swartpuntia* Narbonne, Saylor, and Grotzinger, 1997

Type species.—*Swartpuntia germsi* Narbonne, Saylor, and Grotzinger, 1997 from the Spitskop Member of the Urusis Formation, Schwarzrand Subgroup, Swartpunt farm, Witputs district, Namibia, by original designation and monotypy.

Other species.—None.

Swartpuntia germsi Narbonne, Saylor, and Grotzinger, 1997
Figures 13, 14.1–14.3, 14.6–14.8

1972a ?*Nasepia altae* Germs, p. 176, pl. 22, figs. 1–8.
1973 ?*Nasepia altae*; Germs, p. 8, fig. 2A–G.
1997 *Swartpuntia germsi* Narbonne, Saylor, and Grotzinger, p. 956, figs. 4, 6, 9, 10.
1998 ?*Swartpuntia*-like frond, Jensen, Gehling, and Droser, p. 568, fig. 2b, c.
2000 ?*Swartpuntia* cf. *S. germsi*; Hagadorn and Waggoner, p. 351, fig. 4.
2000 non cf. *Swartpuntia* sp., Hagadorn, Fedo, and Waggoner, p.735, fig. 3.1, 3.2.
2006 non ?*Swartpuntia* sp., Weaver, McMenamin, and Tacker, p. 130, figs. 8–10.
2013 non *Nasepia* sp., Gehling and Droser, fig. 2J.
2022 *Swartpuntia germsi*; Hoyal Cuthill, p. 1211, fig. 1a.
2022 non cf. *Swartpuntia*; Hoyal Cuthill, p. 1211, fig. 1b.
2022 *Swartpuntia germsi*; Nelson et al., fig. 6A, B, C?
2022 ?non cf. *Swartpuntia*; Meinhold et al., fig. 4b.

https://doi.org/10.1017/jpa.2023.81 Published online by Cambridge University Press

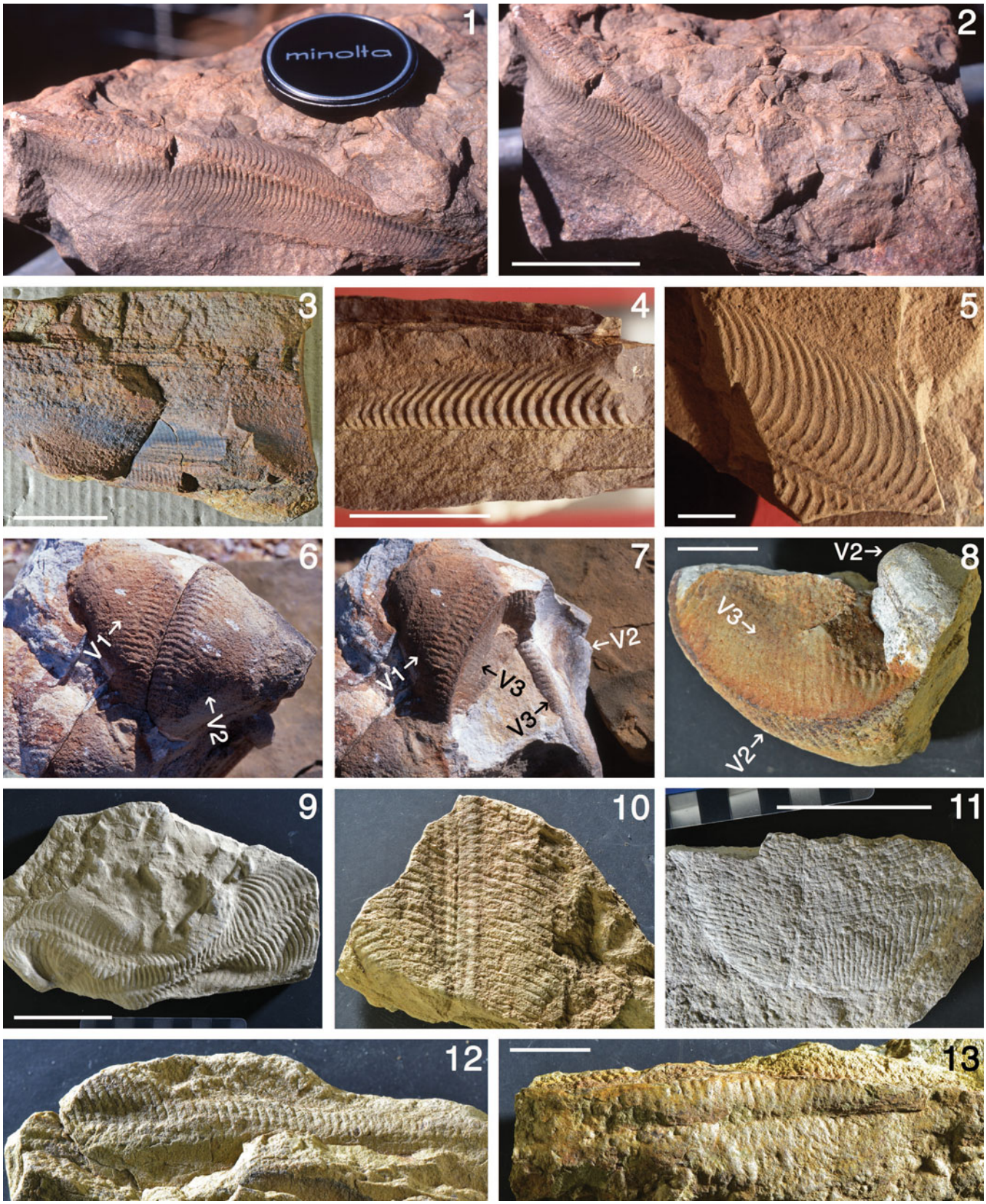

https://doi.org/10.1017/jpa.2023.81 Published online by Cambridge University Press

Figure 11. (**1–3, 6–8**) *Pteridinium simplex* Gürich, 1933, Aarhauser sub-member, Kliphoek Member, Dabis Formation, UCLA 7307, Aar farm. (**4, 5, 9–13**) Other occurrences of *Pteridinium* in southern Namibia. (**1, 2**) An unusual specimen of *P. simplex* that tapers proximally (right), Plateau farm collection, 1996, UCLA 7327.3 (plaster cast). (**3**) Severely weathered block of horizontally bedded sandstone with a fragment of one wide vane that preserves some of the distal edge, GSN 1859. (**4**) Vertically oriented vane of *Pteridinium carolinaenis* (St. Jean, 1973) for comparison with (**3**), GSN F 250, Spitskop Member, Urusis Formation, Dundas, Swartpunt farm, southern Namibia, photographed in Kingston, Canada, 1998. (**5**) Another specimen of *P. carolinaensis* from the same locality, GSN F 248, showing the distal edge of one vane well, photographed in Kingston, Canada, 1998. (**6, 7**) Field photographs, taken on Aar farm by Louis Mazzatenta in 1996, of a tightly folded and twisted specimen of *P. simplex*, with and without a removable piece, GSN F 1854 (**8**), that preserves vanes V2 and V3. (**8**) Another view of GSN F 1854 showing a configuration that has the topology implied by Grazhdankin and Seilacher's (2002) vane substitution hypothesis (Fig. 8.5). (**9**) *Pteridinium* cf. *P. carolinaensis* (St. Jean, 1973), plaster cast of SMSWA 45731 now GSN F 1905, "Uit Schwarzkalk" (Mooifontein Member, Zaris Formation), Kosis farm, near Helmeringhausen. (**10, 12, 13**) *Pteridinium* sp., three specimens, GSN F 1901, GSN F 1899, GSN F 1900, respectively, from UCLA 7320, Neiderhagen Member, Nundas Formation, Kyffhauser farm, that may be preservational variants of *P. simplex*. (**11**) *Pteridinium* sp., UCLA 7315, shale immediately below Mooinfontein Member, Buchholzbrunn Member, Dabis Formation, Namaland district, near Bethanien, showing axis with two vanes partly obscured by overfolding of another vane or individual, GSN F 1891. (**1**) Camera lens cover = 60 mm; (**2**) scale bar = 5 cm; (**3, 10, 11**) scale bars = 5 cm; (**4**) scale bar = 2 cm; (**5**) scale bar = 1 cm; (**6–8, 12, 13**) scale bars = 2 cm; (**9**) scale bar = 3 cm.

Holotype.—Incomplete frond displaying parts of three vanes, one of which appears to have both upper and lower surfaces preserved, GSN F 238-H, from fossil bed B, Spitskop Member, Urusis Formation, Schwarzrand Subgroup, Dundas Hill, Swartpunt farm, southern Namibia.

Description.—Cardioid to heart-shaped frond (Fig. 13.1), formed from at least three equal-sized vanes (Fig. 13.3) that are attached to a voluminous, knobbly axial structure (Fig. 14.6) so that the 50–100 narrow, tubular modules forming the distal parts of the vanes meet the axial structure at an angle of about 45°; those closer to the proximal end meet it nearly perpendicularly or even obtusely, and there is no evidence for a stem or stalk (Fig. 14.1, 14.8); confusion about the number of vanes arises because some appear to have been filled with fine sediment (Fig. 13.3; Narbonne et al., 1997, figs. 6, 7); in other cases, upper and lower surfaces of the vanes may be superimposed by composite molding so that the spacing of the modules may be halved.

Materials.—Four specimens from UCLA 7374 (GSN F 1886–1889) and one from UCLA 7376 (GSN F 1890) on Swartpunt and Swartkloofberg farms, respectively.

Remarks.—*Swartpuntia* was originally reconstructed as a vertically oriented, three-vaned frond supported by a stout cylindrical stem that was attached to an unseen holdfast in the sediment (Narbonne et al., 1997, fig. 11; Narbonne, 1998, fig. 1). Only the holotype was thought to show evidence for a distinct stem, but the feature interpreted as the stem (Narbonne et al., 1997, figs. 6, 7) may well be just an elevated section of the matrix. Hoyal Cuthill (2022, p. 1211) wrote: "It is notable . . . that the stalk originally described in *Swartpuntia* (Narbonne et al. 1997) is not clearly visible even in the classic Namibian material." We attempted to investigate this problem by collecting an in situ specimen preserved in relatively unweathered carbonate. Preparation of the proximal end revealed that opposing vanes are folded through ~90° across the axis of the putative stem and that the edge of one of the vanes can be followed to the axis (Fig. 14.1, 14.2, 14.8). There is no sign of a continuation of a voluminous axial structure beyond the margins of the frond.

The nature of the axial structure is not well understood, but it appears to have a surface formed of similarly sized, equally spaced, rounded projections that perhaps are arranged like the scales of a pineapple or the Fibonacci spirals of a pinecone (Fig. 14.6, 14.7). JGG found a possibly comparable axis at UCLA 7326 (Arimas), which became known as the "Arimas lycopod" (Fig. 14.5) because of its similarity to the bark of Paleozoic lycopods such as *Leptophloeum*. It was found at the same level as another float specimen (Fig. 12.9) with a fragment of a vane of *Nasepia altae* Germs, 1972 (Germs, 1972a, 1973), the only other example recovered subsequently from the type locality. Thus, the Arimas lycopod may be the decorticated axial structure of *Nasepia* judging from their co-occurrence and previously recognized similarities between the vanes of *Swartpuntia* and *Nasepia* (Fig. 14; Grotzinger et al., 1995; Narbonne et al., 1997). However, the syntypes of *Nasepia* are preserved in a carbonate conglomerate (Fig. 14.4), whereas the Arimas lycopod and the new *Nasepia* vane are both in blocks of sandstone, one of which also contains a poorly preserved specimen of *Archaeichnium* (Fig. 21.5). The only other penecontemporaneous fossil worthy of comparison with the Arimas lycopod seems to be *Gibbavasis kushkii* Vaziri, Majidifard, and Laflamme, 2018 (Vaziri et al., 2018, 2021) from the Ediacaran of Iran, but the similarities, although striking, are almost certainly superficial.

Swartpuntia has been positively or tentatively identified from the earliest Cambrian of South Australia (Jensen et al., 1998), the latest Ediacaran of Nevada and California (Hagadorn and Waggoner, 2000; Hagadorn et al., 2000), the early Cambrian of California (Hagadorn et al., 2000), the Ediacaran of North Carolina (Weaver et al., 2006), and the Spitskop Member just over the international border in South Africa (Nelson et al., 2022). Although the South African specimens are only parts of single vanes, their morphology and geographic and temporal proximity give confidence to the identifications. The same is not true for other reports, which should be treated skeptically on a case-by-case basis. The one American specimen that shows more than a fragment of a corrugated surface is LACNMH 12793 (Hagadorn and Waggoner, 2000, fig. 4.1, 4.2), which has two characters that may support an assignment to *Swartpuntia*: fine, dihedral linear striations that may be impressions of modules and an apparently knobbly axial structure. However, neither character is particularly convincing when compared with material from the type locality (Figs. 13, 14). The remainder of the referred specimens, including a sizeable surface from the Cambrian Poleta Formation of California (Hagadorn et al., 2000, fig. 3.2) may be pieces of erniettomorphs, but in the Cambrian at least, there are many other possibilities (e.g., MacGabhann et al., 2019; but see Hoyal Cuthill, 2022).

https://doi.org/10.1017/jpa.2023.81 Published online by Cambridge University Press

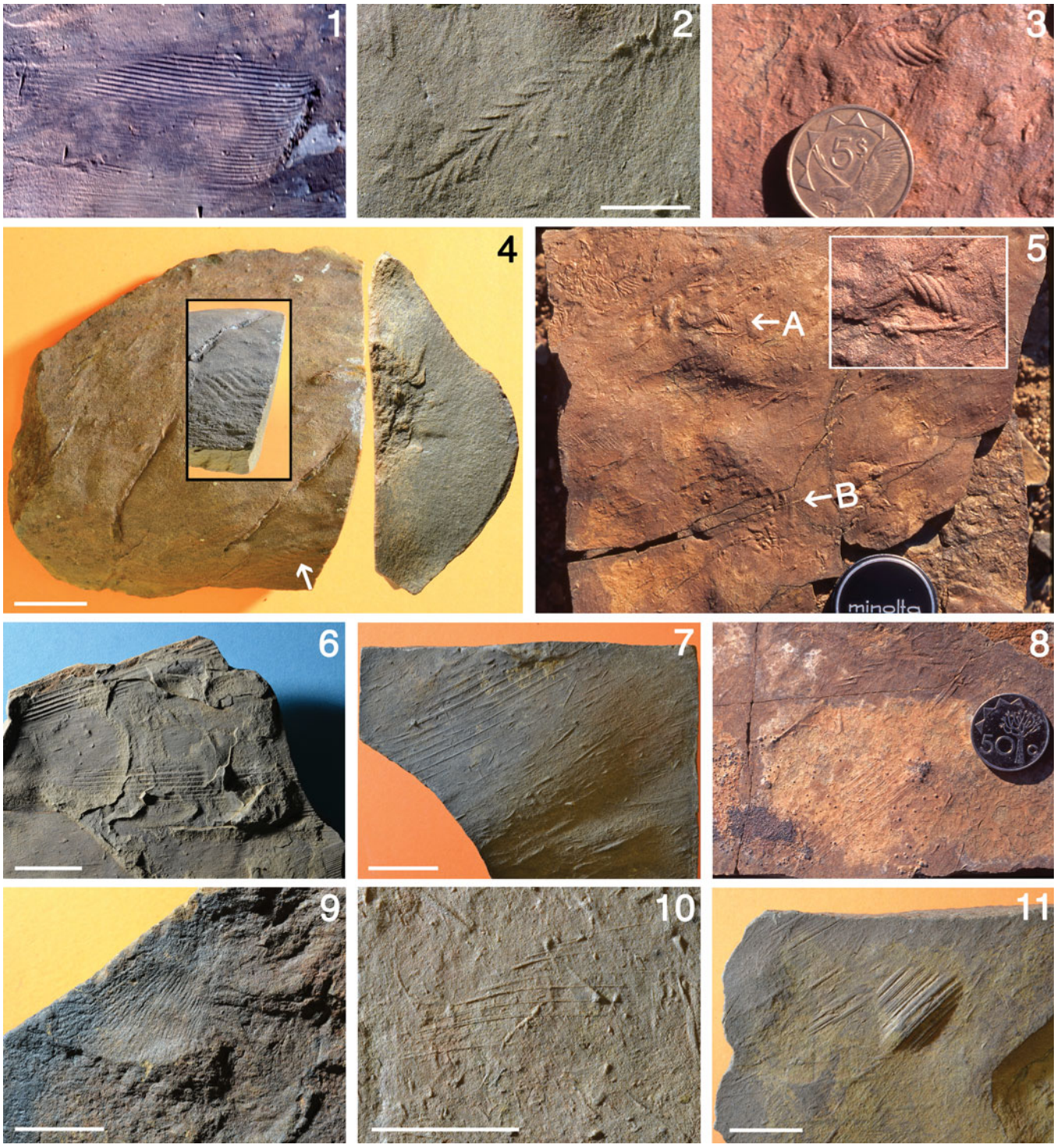

Figure 12. Tool and impact marks presumably left by erniettomorphs on the bases of flat, undulating, and incised sandstone beds, Huns (**2, 3, 5, 7, 8, 10, 11**) and Feldschuhhorn (**1, 6**) members, Urusis Formation and Neiderhagen Member, Nudaus Formation (**4**) on Arimas (UCLA 7309, 7326), Swartkloofberg (UCLA 7323) and Kyffhauser (UCLA 7320) farms, plus a vane of *Nasepia altae* Germs, 1972 from Arimas farm (**9**). (**1**) Broad comb-like toolmark, field photograph, Swartkloofberg, 1996. (**2**) Unique bilaterally symmetrical chevron-shaped tool mark, GSN F 1933. (**3**) Field photograph of an impact cast attributable to *Pteridinium*. (**4**) Lower surface and cross section of a shovel-shaped gutter cast, found by D.E. Erwin in 1995, showing *Pteridinium*-like impact mark on one side (arrow and insert), GSN F 1948. (**5**) Lower surface of large slab, left in field, showing a *Pteridinium*-like impact cast (arrow A and insert) and obscure impressions of several co-aligned specimens of *Archaeichnium* (arrow B), field photograph, 1996. (**6**) Hand specimen from same site as (**1**) showing similar comb marks, GSN F 1936. (**7**) Base of thin sandstone with evenly spaced bifid comb marks, GSN F 1924. (**8**) Another thin sandstone base with several sets of comb marks, one of which resembles the evenly spaced, bifid scratches of (**7**), field photograph, 1996. (**9**) Probable vane of *Nasepia altae* Germs, 1972 from the type locality but preserved in sandstone rather than limestone conglomerate (Fig. 14.4), GSN F 1909. (**10**) Third example of evenly spaced bifid comb marks, GSN F 1926. (**11**) Deep gouge mark on base of sandstone bed, which may or may not have been produced by a biological agent, GSN F 1932. (**1**) Comb approximately 3 cm wide; (**2**) scale bar = 1 cm; (**3**) coin = 25 mm; (**4, 6, 7, 9–11**) scale bars = 2 cm; (**5**) camera lens cap = 60 mm; (**8**) coin = 24 mm.

https://doi.org/10.1017/jpa.2023.81 Published online by Cambridge University Press

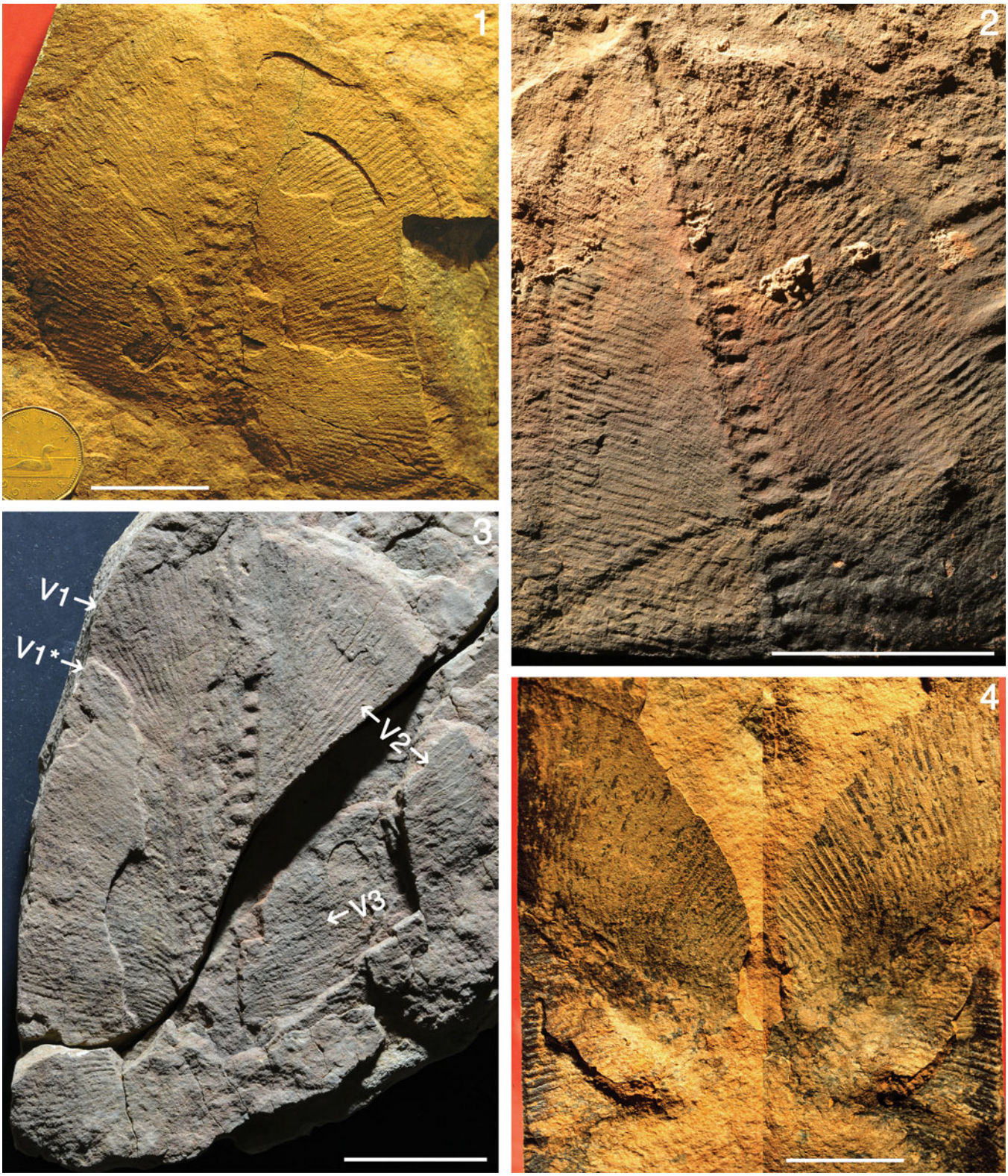

Figure 13. *Swartpuntia germsi* Narbonne, Saylor, and Grotzinger, 1997 from beds A, UCLA 7373 (**2**) and B, UCLA 7374 (**1, 3, 4**) of Narbonne et al. (1997), Spitskop Member, Urusis Formation, Dundas Hill, Swartpunt farm. (**1**) Paratype, GSN F 423, showing the cardioid shape of the vanes, no evidence of a stem, and preservation of the vane surfaces on at least three levels, photographed in Kingston, Canada, in 1998. (**2**) GSN F 1886, upper surface of bed and partly overlapped by a specimen of *Pteridinium carolinaensis* (St. Jean, 1973). (**3**) Topotype, GSN F 1887, showing preservation of three (V1–V3) or possibly four vanes if VI* is not just the other surface of vane V1. (**4**) Paratype, GSN F 245, part and counterpart, showing no sign of a stem but clear evidence for three vanes, as illustrated by Narbonne et al. (1997, fig. 9.2), photographed in Kingston, Canada, in 1998. (**1**) Scale bar = 3 cm and loonie = 26.5 mm; (**2**) scale bar = 5 cm; (**3, 4**) scale bars = 3 cm.

https://doi.org/10.1017/jpa.2023.81 Published online by Cambridge University Press

https://doi.org/10.1017/jpa.2023.81 Published online by Cambridge University Press

Figure 14. *Swartpuntia germsi* Narbonne, Saylor, and Grotzinger, 1997 from bed B, UCLA 7374 (**1, 2, 6–8**) Spitskop Member, Urusis Formation, Dundas Hill, Swartpunt farm, and UCLA 7376, top of Huns Member, Urusis Formation, Swartkloofberg farm (**3**), plus a paratype of *Nasepia altae* Germs, 1972 (**4**) and the "Arimas lycopod" (**5**), both from UCLA 7326, Huns Member, Urusis Formation, Arimas farm (**5**). (**1, 2, 8**) Three views of a three-dimensionally preserved specimen of *S. germsi*, GSN F 1888, which exposes the proximal parts of the frond folded through about 90° and displaying no evidence for a stem; arrows in (**8**) mark the edges of one vane; (**2**) is flipped horizontally to serve as a mirror image of (**1**). (**3**) GSN F 1890, stratigraphically oldest known specimen of *Swartpuntia*, found by M.L. Droser in 1996, preserved in silt-sized carbonate, with axis presumably embedded in the counterpart. (**4**) Paratype of *Nasepia altae* Germs, 1972 ISAM K1086, showing distal edge of one vane embedded in a limy matrix that includes rounded limestone clasts (arrow), photographed in Cape Town, South Africa in 1993. (**5**) The "Arimas lycopod" (enlarged in insert), GSN F 1910A, found by JGG in 1996, may be the decorticated axis judging from circumstantial evidence; the organization of its diagonal arrays of "leaf scars," analogous to those seen in lycopods, resembles that of the axial nodes of *Swartpuntia*, which are arranged in a similar fashion (**6, 7**, arrows). (**6, 7**) Topotype GSN F 1889 and paratype GSN F 247 (after Narbonne et al., 1997, fig. 10, republished with permission), of *S. germsi* that have well-preserved axial nodes. Scale bars = 2 cm except black bar in insert of (**5**) = 1 cm.

However, the *Swartpuntia*-like fossils discovered by Jensen et al. (1998) deserve further investigation; there is more than one specimen, which is an important first step, and they display bilateral symmetry, discrete margins, and subdivisions reminiscent of erniettomorphs. They also occur very close to the local base of the Cambrian, which may be equivalent in age to the Ediacaran–Cambrian boundary zone in both Namibia (Linnemann et al., 2019) and South Africa (Nelson et al., 2022).

Swartpuntia has been reported with *Vendoconularia* Ivantsov and Fedonkin, 2002, *Ventogyrus* Ivantsov and Grazhdankin, 1997, and *Calyptrina* Sokolov, 1965 from the Onega Peninsula of the White Sea area, northern Russia (Ivantsov and Fedonkin, 2002). According to Serezhnikova (2014), this association is approximately 550 million years old, which would make this the oldest record of the genus. However, until this material has been figured and described, affinity with the Nama occurrences cannot be evaluated. A frond-shaped fossil from northern Norway has been tentatively compared with *Swartpuntia* (Meinhold et al., 2022, fig. 4b). This too would represent an occurrence older than those of the Nama Group, but in view of the revised morphology of *Swartpuntia* presented here, this comparison now is unlikely.

In summary, *Swartpuntia* is a *Pteridinium*-like frond that probably had only three equal-sized vanes set about a knobbly, voluminous, axial structure, and it lacked any kind of stem or stalk. Its modules and vanes resemble those of the smaller frond, *Nasepia altae*, so the discovery of a lycopod-like fossil, similar to the axial structure of *Swartpuntia*, with *Nasepia* at its type locality provides circumstantial evidence for a close relationship between the two genera. *Swartpuntia/Nasepia* is known with certainty only from Namibia and nearby South Africa, but one fragmentary specimen from California may belong to *Swartpuntia*. All other identifications are based on specimens that are too fragmentary or too little studied to warrant confident assignment to the genus or even to the Erniettomorpha.

Family Erniettidae Pflug, 1972
Genus *Ernietta* Pflug, 1966

Type species.—*Ernietta plateauensis* Pflug, 1966 from the Buchholzbrunn Member of the Dabis Formation, Kuibis Subgroup, Aar farm, Aus district, Namibia, by original designation and monotypy.

Other species.—Numerous other generic and specific names, as well as two new orders, four families, and five subfamilies, were proposed by Pflug (1972) for material on Aar farm that is essentially topotypic. In preparing the Precambrian section of the Introduction volume of the *Treatise on Invertebrate Paleontology*, Glaessner (1979b) attempted to rationalize Pflug's excessive splitting by recognizing only two subfamilies and five genera: *Ernietta*, *Erniofossa*, *Ernionorma* (Erniettinae), plus *Erniobeta* and *Erniograndis* (Erniobetinae). Soon after, Richard Jenkins effectively overruled this assessment with the statement: "One of us (Jenkins) has examined Pflug's material and considers that all the specimens he refers to as the 'Erniettomorpha' belong to a single genus and species, *Ernietta plateauensis* Pflug" (Jenkins et al., 1981, p. 71). That interpretation has become the status quo. However, in his summary of the genus *Ernietta*, Glaessner (1979b, p. A101) wrote as follows: "Body compressed at base into U-shape; ribs strongly developed, separated by zig-zag median line; resembling a folded petaloid of *Pteridinium*."

When Pflug (1966) first described *E. plateauensis*, he thought he had the dorsal carapace of a soft-shelled worm or isopod-like arthropod but noted that the zig-zag dorsal suture was more like a structure found in *Pteridinium* than any animal except, perhaps *Dickinsonia*. One distinctive feature was a triangular mark at the topographical pole of the holotype, which he designated segment z (Fig. 19.1). This, he thought, was matched by segment 0 on the opposite side of the axis, and the segments were numbered away from these structures on both sides of the body. If segment z is a real feature of the anatomy, it is not seen in any other known specimens of *Ernietta*. It is, however, seen occasionally in U-shaped specimens of *P. simplex* (Fig. 19.2; Pflug, 1972, pl. 34, fig. 1), and it appears to be a tear of the seam between two modules on one side of the organism. Thus, Glaessner's diagnosis of *Ernietta* was more perceptive than he realized because the holotype of *E. plateauensis* (Fig. 19.1) is probably the tip of a tightly folded, U-shaped specimen of *P. simplex*.

One argument against this interpretation is that the discovery site "C" is described as "slate between Kuibis quartzite and black limestone in the lower part of the Nama system" (Pflug, 1966, p. 22), which clearly places it within the Buchholzbrunn Member (Fig. 3). This is the level where *Ernietta* abounds and *Pteridinium* is rarely seen (Fig. 2; Elliott et al., 2016). However, together with Bob Brain, Mark McMenamin, and Friedrich Pflüger, an attempt was made to recollect Pflug's locality C in 1993. Mark McMenamin found the only fossil, a vertical vane of *Pteridinium* (Fig. 19.7; McMenamin, 1998), at about the same stratigraphic level and geographic position as the holotype. So far as we know, Pflug's site C has not been resampled since that time; it is ~1.5 km east of the eastern edge of the geological maps of Plateau and Aar farms in Hall et al. (2013) and Elliott et al. (2016).

https://doi.org/10.1017/jpa.2023.81 Published online by Cambridge University Press

If the holotype of *E. plateauensis* is a small specimen of *P. simplex*, as seems likely, then *Ernietta* becomes a junior subjective synonym of *Pteridinium*. That is an undesirable outcome, given the long history of the use of *Ernietta* for a well-understood generic concept (Elliott et al., 2016; Ivantsov et al., 2016). However, the holotype of *E. plateauensis* is already an unsatisfactory standard because, as Pflug (1972, p. 139) noted: "From the collection area around point C [Pflug, 1966, fig. 1b] come the [holotype and paratype] specimens of the genus *Ernietta* and the specimens numbered 393, 399 of *Erniotaxis*. Almost all other pieces, with the exception of an *Erniobeta* colony, were found in collection area E, F." (~2 km south of the southern edge of the maps of Plateau and Aar and farms in Hall et al. [2013] and Elliott et al. [2016]). As discussed in the following, *Erniotaxis* is an unusual juvenile form of *Ernietta*, and a "colony of *Erniobeta*" could mean many things. Thus, it is very difficult to obtain a population of individuals of *E. plateauensis* on the basis of the topotypic principle that all similar specimens from a bed or set of beds at one place are likely to be conspecific. Without such a sample to assess intraspecific variability, application of the name *plateauensis* is difficult. For both of these reasons, we recommend that the holotype of another of Pflug's species, *Erniograndis sandalix* Pflug, 1972, be designated the neotype of *E. plateauensis*. This recommendation will need the approval of the ICZN before it can take effect; in the meantime, community input is invited. There are precedents for this type of action to preserve useful names.

If there are to be other valid species of *Ernietta*, then *Namalia villiersiensis* Germs, 1968 has priority over all of Pflug's species except *plateauensis*. Again, the holotype of *N. villiersiensis* (Germs, 1968, fig. 1, 1972a, pl. 23, fig. 1) is not ideal in terms of preservation and the availability of topotypic material, but even worse, it may be missing (it could not be found at the ISAM in 1993). The type locality, Buchholzbrunn, has yielded the juvenile specimens of *Ernietta* shown in Figure 16, but they are preserved in a very different fashion from the holotype of *Namalia villiersiensis*. A better comparison is with the sandstone cast of a fossil—similar to those commonly attributed to *Namalia villiersiensis* or *Kuibisia glabra* Hahn and Pflug, 1985 (Hahn and Pflug, 1985a)—from the Aarhauser sandstone at Aar (Fig. 19.8, 19.9). This specimen was uncovered by the Seilacher team during their excavation in 1993. Thus, *Namalia villiersiensis* may be the senior synonym of *Kuibisia glabra*, and both may or may not be conspecific with *Ernietta plateauensis* (Jenkins et al., 1981; Runnegar and Fedonkin, 1992; Vickers-Rich, 2007; Ivantsov et al., 2016; but see Grazhdankin and Seilacher, 2002). The apparent differences between *N. villiersiensis*/*K. glabra* and neotypic *Ernietta plateauensis* may be due to preservation in coarse sandstone instead of siltstone.

Returning to Glaessner's (1979b) revision of Pflug's taxa, do his generic categories help break up *Ernietta* into distinct morphotypes? His subfamily Erniobetinae comprised two genera, *Erniobeta* and *Erniograndis*. A swift survey of Pflug's material may be obtained from the reproductions of his 13 *Palaeontographica* plates by Vickers-Rich (2007). Excluding plate 34, which deals mainly with *E. plateauensis*, 10 of the plates are devoted to specimens that generally resemble the shapes shown in Figure 19.3–19.6. The remaining two plates, 38 and 39, illustrate the Erniobetinae—*Erniobeta* and *Erniograndis*—which are bulky, internal molds of large specimens such as the proposed neotype for *plateauensis* (Fig. 15.3; Pflug, 1972, pl. 38, 1, 2, 4; Vickers-Rich, 2007, fig. 124; Elliott et al., 2016, fig. 3). Thus, the Erniobetinae sensu Glaessner (1979b) may serve as a population concept for *E. plateauensis* if the proposed neotype is eventually adopted.

Pflug's plates 31 and 32 may best summarize the second morphotype, which Glaessner included in his subfamily Ernietinae; whether this morphotype may be specifically distinct from *plateauensis* is discussed in the following under the species description. Finally, plate 37, which shows specimens Pflug referred to *Erniotaxis*, is very different from all the others. *Erniotaxis* was one of five of Pflug's generic names that Glaessner (1979b, p. A102) dismissed as "unrecognizable." Our discovery of this morphology on Twyfel farm, where it is associated with larger and more normal specimens (Fig. 17), allows us to show that *Erniotaxis* is a young growth stage that is allometrically different from larger individuals. The modified generic name "erniotaxid" may therefore serve as informal shorthand for this juvenile morphotype. Finally, we agree with Elliott et al. (2016) that *Erniocarpus sermo* Pflug, 1972 is not a specimen of *Ernietta* and suggest that while *Erniocarpus orbiformis* Pflug, 1972 may be, *Erniocentrus centriformis* Pflug, 1972 is certainly not.

Diagnosis.—Sack-shaped, organic-walled bodies, oval or stadium shaped in cross section and U to V shaped in lateral profile, formed of tubular modules that meet in a zig-zag suture at the base, are attached to the outer wall, generated an inner wall by packing together during growth, and terminate distally in either stubby lobes or conical tips.

Occurrence.—Kliphoek and Buchholzbrunn members, Dabis Formation, Kuibis Subgroup, Nama Group, Namibia (Fig. 2; Appendix); Lower Member, Wood Canyon Formation, Nevada, USA (Horodyski et al., 1994; Smith et al., 2017, 2022; Runnegar, 2022).

Ernietta plateauensis Pflug, 1966
Figures 15–17, 19.3–19.6, ?19.8, ?19.9

1966 non *Ernietta plateauensis* Pflug, p. 22, pl. 1, figs. 1–7.
1968 ?*Namalia villiersiensis* Germs, figs. 1, 2.
1972a *Ernietta plateauensis*; Germs, p. 174, pl. 21, figs. 4–9.
1972a ?*Namalia villiersiensis*; Germs, p. 177, pl. 23, figs. 1–7.
1972 non *Ernietta plateauensis*; Pflug, p. 163, pl. 34, figs. 4, 9.
1972 *Erniodiscus rutilus* Pflug, p. 158, pl. 27, figs. 3, 4.
1972 *Erniodiscus clypeus* Pflug, p. 158, pl. 27, fig. 1.
1972 *Erniaster apertus* Pflug, p. 159, pl. 28, figs. 1–3, 5–7.
1972 *Erniaster patellus* Pflug, p. 159, pl. 29, figs. 1, 4, 8.
1972 *Erniofossa prognatha* Pflug, p. 159, pl. 27, figs. 2, 6, 7.
1972 *Ernionorma abyssoides* Pflug, p. 160, pl. 29, figs. 6, 7, 10–12.
1972 *Ernionorma peltis* Pflug, p. 160, pl. 30, figs. 1, 7, pl. 29, figs. 2, 5.
1972 *Ernionorma clausula* Pflug, p. 160, pl. 31, figs. 2, 3.
1972 *Ernionorma rector* Pflug, p. 161, pl. 32, figs. 4, 6–9.
1972 *Ernionorma corrector* Pflug, p. 161, pl. 32, figs. 1–3, 5.

https://doi.org/10.1017/jpa.2023.81 Published online by Cambridge University Press

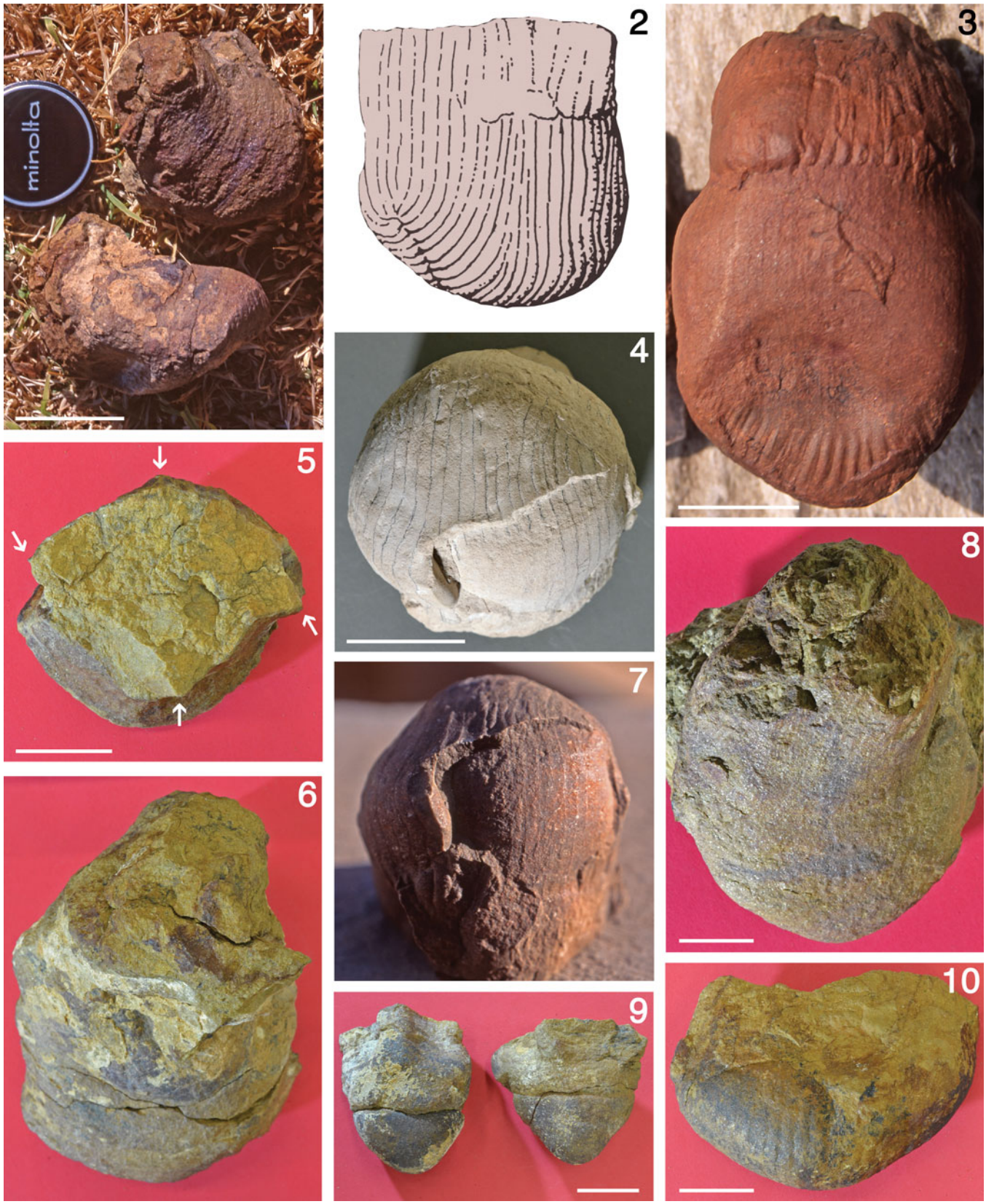

https://doi.org/10.1017/jpa.2023.81 Published online by Cambridge University Press

Figure 15. *Ernietta plateauensis* Pflug, 1966, Buchholzbrunn Member, Dabis Formation, Plateau farm (**2, 4, 7**) and approximately the same stratigraphic level, UCLA 7378, Twyfel farm (**1, 5, 6, 8–10**). (**1**) Classic "sock in a rock" preservation, found in place and photographed in the field, both specimens numbered GSN F 1876. (**2**) Colorized version of one of five sketches based on plaster cast, YPM 204 508, of specimen in the "museum" at Plateau farm after Seilacher et al. (2003, fig. 11), copyright 2003, the Palaeontological Society of Japan, republished with permission. (**3**) GSN F 389, holotype of *Erniograndis sandalix* Pflug, 1972, and proposed neotype for *E. plateauensis*, photographed in Lich, Germany, 1993, GSN F 389. (**4**) Duplicate of the plaster cast used as the model for (**2**), UCLA 7327.2, gifted by the Seilacher team, was used to count the 70+ modules (Fig. 18.6) after tracing the between-module seams with a soft pencil. (**5, 6**) Two excavated specimens, GSN F 1863 and GSN F 1864, that share rhomboidal distal cross sections (corners indicated by arrows in (**5**)), viewed from above. (**7**) Photograph taken in 1993 of the specimen used to make the casts used for (**2**) and (**4**). (**8–10**) Four other excavated specimens, GSN F 1865, GSN F 1866, GSN F 1867, GSN F 1868, respectively, that show the typically pointed shape of the toe and, in the smaller specimens, evidence for growth interruptions. (**1**) Scale bar = 5 cm; (**2, 4, 7**) scale bar = 3 cm; (**3**) scale bar = 3 cm; (**5, 6, 8–10**) scale bars = 2 cm.

1972 *Ernionorma tribunalis* Pflug, p. 161, pl. 31, figs. 4–8.
1972 *Erniobaria baroides* Pflug, p. 162, pl. 31, figs. 11, 12, pl. 32, figs. 10, 11.
1972 *Erniobaris gula* Pflug, p. 162, pl. 33, figs. 1, 2, 4.
1972 *Erniobaris epistula* Pflug, p. 162, pl. 31, figs. 9, 10.
1972 *Erniobaris parietalis* Pflug, p. 162, pl. 33, figs. 3, 5, 6.
1972 *Erniopelta scrupula* Pflug, p. 163, pl. 33, figs. 7, 10.
1972 *Ernietta aarensis* Pflug, p. 163, pl. 34, figs. 5, 7, 8.
1972 *Ernietta tsachanabis* Pflug, p. 164, pl. 34, figs. 10–12.
1972 *Erniocarpus carpoides* Pflug, p. 164, pl. 35, figs. 5–9.
1972 *Erniocoris orbiformis* Pflug, p. 164, pl. 36, figs. 1–4.
1972 *Erniotaxis segmentrix* Pflug, p. 165, pl. 37, figs. 1–8, pl. 35, fig. 10.
1972 *Erniograndis sandalix* Pflug, p. 165, pl. 38, figs. 1, 2, 4, pl. 35, fig. 1.
1972 *Erniograndis paraglossa* Pflug, p. 166, pl. 38, fig. 3, pl. 39, figs. 7–9, 11.
1972 *Erniobeta scapulosa* Pflug, p. 166, pl. 39, fig. 6.
1972 *Erniobeta forensis* Pflug, p. 166, pl. 39, figs. 2–5, 10.
1981 *Ernietta plateauensis*; Jenkins, Plummer, and Moriarty, fig. 5A–E.
1985a ?*Kuibisia glabra* Hahn and Pflug, p. 5, pl. 2, 3.
2016 *Ernietta plateauensis*; Ivantsov et al., figs. 5, 6.
2016 *Ernietta plateauensis*; Elliott et al., p. 1019, figs. 3–5 (with additional synonymy).
2017 *Ernietta*; Smith et al., fig. 3.
2022 *Ernietta plateauensis*; Runnegar, p. 1104, fig. 3.

Holotype.—Tip of U-shaped internal mold (GSN F 429; previously Pflug no. 227) from the Buchholzbrunn Member, Aar farm, Aus district, Namibia by original designation (Fig. 19.1; Pflug, 1966, pl. 1, figs. 1–3, 1972, pl. 34, fig. 4).

Proposed neotype.—Nearly complete internal mold (GSN F 389; previously Pflug no. 192) from the Buchholzbrunn Member, Aar farm, Aus district, Namibia (Fig. 15.3; Pflug, 1972, pl. 38, figs. 1, 2, 4; Vickers-Rich, 2007, fig. 124; Elliott et al., 2016, fig. 3; Maloney et al., 2020, fig. 3A).

Description.—Body sack-like, composed of as many as 70 tubular modules arranged side by side around the circumference and joined proximally (ventrally) in a zig-zag seam; body cross section is elliptical to stadium shaped; basal profile at right angles to the zig-zag seam is U shaped or rounded V shaped, and parallel to the seam it is U shaped; upper part of body usually truncated postmortally, with the upper parts frequently assuming the cross-sectional shape of a four-pointed star (Fig. 15.5) that is aligned with the symmetry axes; modules are approximately constant in width for any growth stage until they approach the distal (dorsal) margin, where they start to separate from each other and taper toward pointed ends (Smith et al., 2017, fig. 3d; J.G. Hall et al., 2020, fig. 1b; Runnegar, 2022, fig. 3a; possibly Narbonne, 2005, fig. 4b); modules are circular in cross section in the tapering tips, square to rectangular in cross section throughout much of the upper part of the body, and triangular to D shaped near the base, where they are in contact with each other only at the outer wall (Fig. 17.6); rare internal molds (Fig. 15.7) show that the sides of adjacent modules approached each other during growth and then coalesced about one-third of the way to the top of the body.

Materials.—Numerous specimens (GSN F 1860–1877, 1880, 1881) from UCLA 7317 and UCLA 7378 on Buchholzbrunn and Twyfel farms and rare specimens from UCLA 7312, UCLA 7313, UCLA 7314, UCLA 7315, and UCLA 7381, all west of the road from Bethanie to Helmeringhausen (Fig. 1).

Ontogeny.—Two sizeable blocks of sandstone, each part of a sand-cast gutter fill, were found on the floor of a small road metal quarry in the Buchholzbrunn Member on Buchholzbrunn by SJ and BR in 1995 (UCLA 7317; Fig. 16). The lower surfaces of these blocks preserve numerous small specimens of *Ernietta* that were transported with the sand and settled first, presumably because they behaved hydrodynamically like pebbles. The fossils are not well preserved, but they do display the modules well enough for them to be counted and compared with specimen size (Fig. 18.6). The smallest identifiable specimen, ~4 mm in diameter (E in Fig. 16.4, 16.5, 16.7), appears to have four modules (Fig. 16.7), although only three are visible in the gutter cast. An even smaller object to the upper left of it (Fig. 16.7) is preserved in the same fashion and may be an ~1 mm larval stage with only one module, such as the tiny White Sea specimens of *Dickinsonia costata* Sprigg, 1947 illustrated by Ivantsov and Zakrevskava (2022, pl. 1, figs. 1, 2). The subsequent growth of *E. plateauensis* is summarized in Figure 18.6, which is a plot of countable module number versus body size (length + width/2). The largest individual measured was a plaster cast of a specimen in the Plateau "museum" collection (Fig. 15.4, UCLA 7327.2, YPM 204 508; Seilacher et al., 2003, fig. 11, bottom row; Seilacher, 2007, fig. 1) that has ~70 modules. Thus, body size is a reasonable predictor of module number (Fig. 18.6), although Ivantsov et al. (2016) found a fairly constant number of modules (~26) in a cohort of similar-sized individuals preserved in a gutter cast. Presumably, modules are added at one or both ends of the zig-zag seam (Ivantsov et al., 2016),

https://doi.org/10.1017/jpa.2023.81 Published online by Cambridge University Press

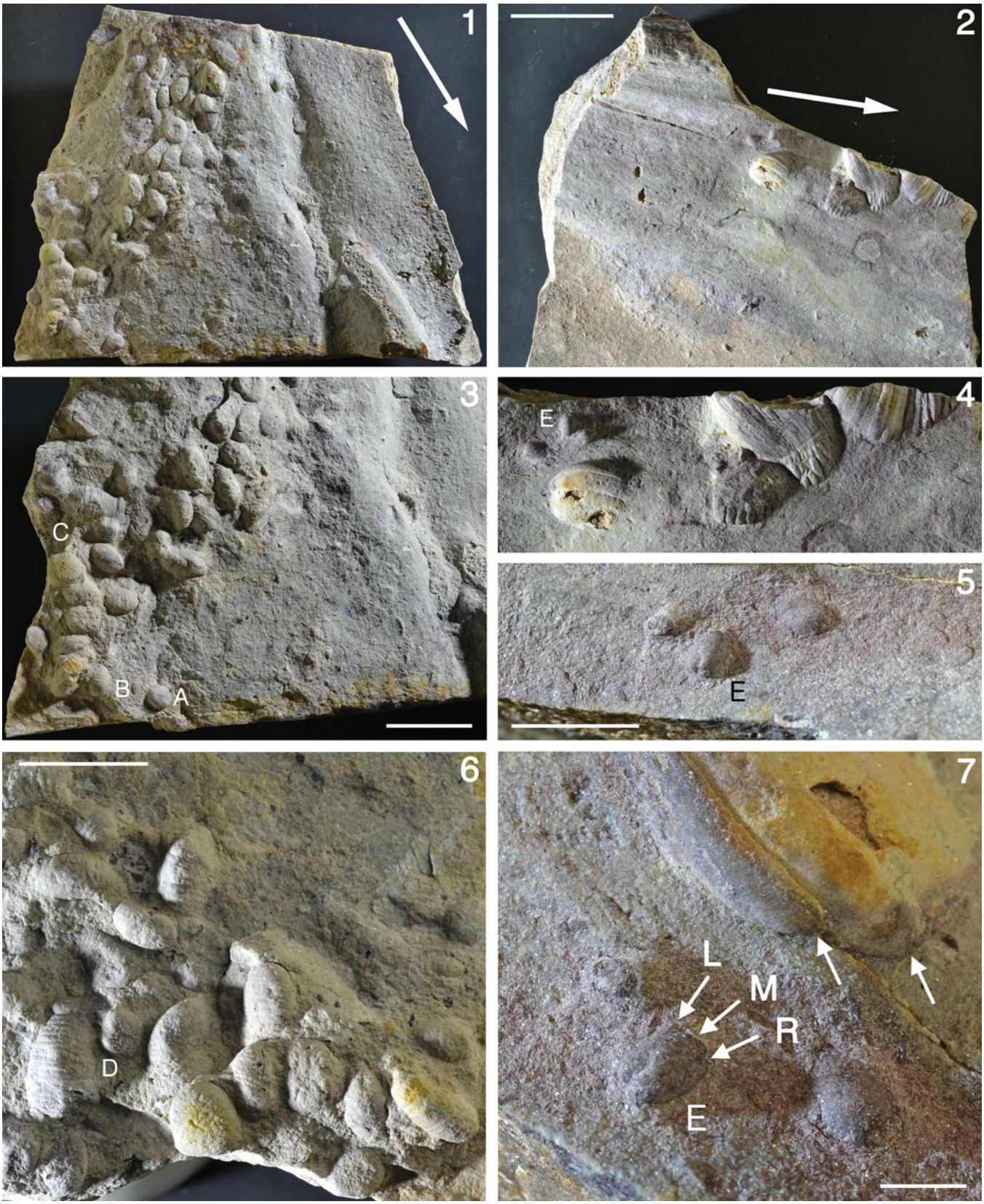

Figure 16. Juvenile specimens of *Ernietta plateauensis* Pflug, 1966 preserved on the bases of two sizeable pieces of a gutter cast, found on the floor of a small road metal quarry, Buchholzbrunn Member, Dabis Formation, UCLA 7317, Buchholzbrunn farm, near Goageb. (**1**) Whole block, GSN F 1860. (**2**) Part of second block, GSN F 1861; arrows indicate directions of current flow. (**3, 6**) Enlargements of GSN F 1860 with individuals used for module counts (Fig. 18.6) indicated by letters. (**4, 5, 7**) Enlargements of parts of GSN F 1861 with smallest identifiable individual labeled E and three of its four modules indicated by L, M, and R (other arrows point to the ends of the modules of a larger individual); the bump above E in (**7**) may be the base of a tiny one-module postlarva (Fig. 18.6). (**1, 2**) Scale bar = 5 cm; (**3, 4, 6**) scale bars = 2 cm; (**5**) scale bar = 1 cm; (**7**) scale bar = 5 mm.

https://doi.org/10.1017/jpa.2023.81 Published online by Cambridge University Press

but it has not been possible to identify the most recently added modules in those areas because of inadequate preservation. At the base of the body, the modules terminate in separate, rounded ends (Fig. 15.7), so it is not obvious how new modules are generated; they may even be intercalated around the body during growth, as might be recorded by impressions of vertical seams on internal molds (Fig. 15.2, 15.4, 15.7; Jenkins et al., 1981, fig. 5B). However, these structures are better attributed to changes in module width and shape during growth, as discussed in the following.

One of Pflug's (1972) taxa, *Erniotaxis segmentrix*, is a puzzling set of small objects that Glaessner (1979b) dismissed as "unrecognizable" and Elliott et al. (2016, p. 1024) thought were "part of the midline of a fragmentary *Pteridinium* fossil." Our discovery of two similar small specimens on Twyfel farm (Fig. 17.1–17.4) validates Pflug's recognition of the importance of his find, and the two small collections reveal the same features of the internal anatomy of young examples of *E. plateauensis* (Fig. 16.1–16.5). The striking feature of both is the depth of the walls of the modules and their concave lateral surfaces. In these specimens, the inner edges of the modules are blade-like and close to the axis of the body (Fig. 17.2). The concavity of their lateral walls suggests that there may have been open space between the modules and that they were in contact only at the outer wall. This morphology is seen more clearly in a larger but still youthful specimen from the same site (Fig. 17.6), which is best understood as an inverted fragment of the lower part of the specimen shown in Figure 17.10 (in both examples, the modules taper distally). In these specimens, the modules were filled with carbonate following burial, so the whole structure is preserved in three dimensions and could in one case be separated from the internal mold (Fig. 17.6). The two halves of this specimen show clearly that, at an early growth stage, the modules were D shaped in cross section and in contact with each other only at the seams of the outer wall, best seen in the external mold (Fig. 17.6, left) and modeled in Figure 18.7, 18.8. Larger, more mature individuals have modules that are wholly in contact laterally, resulting in square to rectangular cross sections (Fig. 15.4; Pflug, 1972, pl. 38, fig. 3; Jenkins et al., 1981, fig. 6C; Elliott et al., 2016, fig. 4.2), except toward their growing terminations, where the modules separated and assumed a hydrostatic (circular) cross section (Runnegar, 2022, fig. 3a). There are also some contentious components of the growth of *Ernietta*: (1) whether there were two or more layers of modules in the body wall; (2) the nature of the growing terminations of the body; (3) the significance of waist-like constrictions that are seen in many specimens, including the proposed neotype; (4) whether sand was incorporated into the body during life. These matters are reviewed in the following under remarks.

Taphonomy.—An evocative metaphor for the preservation of a mature individual of *Ernietta* is not a "rock in a sock" (Seilacher, 1992) but rather a "sock in a rock" (Knoll, 2003, p. 166; Fig. 15.1). Is this morphology the result of mass flow transport and burial or a life orientation? A recent consensus is the latter based on in situ specimens from localities west of the Aar homestead (Elliott et al., 2016) and sites on Weigkrup and Hansburg farms (Bouougri et al., 2011; Maloney et al., 2020), which are close to our localities UCLA 7378 and UCLA 7379 on Twyfel and Weigkrup (Fig. 1). Perhaps the best evidence for this interpretation is the fact that nearly all specimens are oriented with their zig-zag seams down and occur in clusters that are thought to have developed in depressions in the seafloor. However, some of these group occurrences appear to be secondarily transported (Ivantsov et al., 2016). At Twyfel, we also found that rare specimens in the same bed as the upright clusters are inverted, a configuration that is difficult to explain in an in situ community. Given the high probability that transported specimens partly filled with sand would aggregate seam downward in depressions, the life orientation of any of these clusters is questionable.

The carbonate infilling of the modules of the specimen shown in Figure 17.6 is unusual and previously unreported from Namibia. As the specimen is unique, no preparation of it was undertaken, so the identification of the fill, based on microscopic examination of fractured surfaces, is tentative. Another specimen found with it (Fig. 17.10) seems to be preserved in the same way and could be examined with computed tomography in the future. A possibly similar style of preservation has been reported by Ivantsov (2018) from the Ediacaran of Siberia.

Remarks.—Jenkins et al. (1981, fig. 6) published a reconstruction of *Ernietta* based on Pflug's material, which Jenkins had examined in Giessen with Pflug's assistance. Two key observations, based on an unfigured syntype of *Erniograndis sandalix* (Pflug no. 182), were the presence, near the base, of a small piece of sediment that had filled the interior of a second outer palisade of modules and an "enigmatic 'budding' suture" that encircled the upper part of the internal mold and is also present in the holotype (Fig. 15.3; Pflug, 1972, pl. 38, figs. 1, 2, 4; Vickers-Rich, 2007, fig. 124; Elliott et al., 2016, fig. 3; Maloney et al., 2020, fig. 3A) and several other specimens from Aar (e.g., Fig. 15.2). Jenkins also sketched three cross sections of *Ernietta* on the basis of sawn specimens, including a paratype of *E. sandalix* (Pflug, 1972, pl. 39, fig. 1; Jenkins et al., 1981, fig. 5B), which is shown as displaying a voluminous inner layer of modules crossed by rare septa and a tiny, attached fragment of a second layer of modules. Pflug's (1972, pl. 39, fig. 1) figure of the paratype shows a thick layer of white sediment near the base of the organism, comparable to that illustrated by Ivantsov et al. (2016, fig. 6E, F) in a similar sawn section, and two or three linear features that could be the intersections of septa. However, their convexity is in the opposite direction to the septa shown in Jenkins's sketch, and the thickness of the adhering second layer of modules is negligible. Furthermore, the other two cross sections sketched by Jenkins each have only one layer of modules. Thus, evidence for a second layer of modules is limited to a few fragments adhering to the bases of syntypic specimens of *E. sandalix* (e.g., Elliott et al., 2016, fig. 4.2) and an image of the polished sawn surface of GSN F-1243 from the Teapot locality on Aar (Elliott et al., 2016, fig. 5.3), which show two layers of honeycomb-like cells. Given that the orientation of the polished surface with respect to the fossil is not clear, that the section may intersect part of the ventral zig-zag seam, and that some mineralized cracks may mimic mineralized organic

https://doi.org/10.1017/jpa.2023.81 Published online by Cambridge University Press

Figure 17. Juvenile and small specimens of *Ernietta plateauensis* Pflug, 1966, Buchholzbrunn Member, Dabis Formation, UCLA 7378, Twyfel farm (**1–4, 6, 7, 9, 10**); UCLA 7308, Aar farm (**5**); and UCLA 7313, Klipdrif farm (**8**). (**1–4**) Unusual, globose specimens preserved in carbonate that resemble the *Erniotaxis segmentrix* morph (**5**) in having extraordinarily wide walls between adjacent modules (**2**) and highly curved outer walls, GSN F 1869 (**1–3**) and GSN F 1870 (**4**). (**5**) Holotype of *Erniotaxis segmentrix* Pflug, 1972, no. 396 now GSN F 449, photographed in Lich, Germany, in 1993. (**6**) Part and counterpart of a specimen with carbonate-filled modules that are convex in both outward and inward directions and are in lateral contact only at the outer surface (arrows); GSN F 1874. (**7, 9**) Excavated block shown in original orientation with two visible specimens of *E. plateauensis*, one of which is removable and is shown in inverted orientation in (**9**). (**8**) A deformed specimen found with other individuals in a small channel ~3 m below the first limestone of the Mooifontein Member, GSN F 1956. (**10**) Rare example of preservation of the outer surface of the organism as a result of carbonate-filled modules, GSN F 1872. Scale bars = 1 cm.

https://doi.org/10.1017/jpa.2023.81 Published online by Cambridge University Press

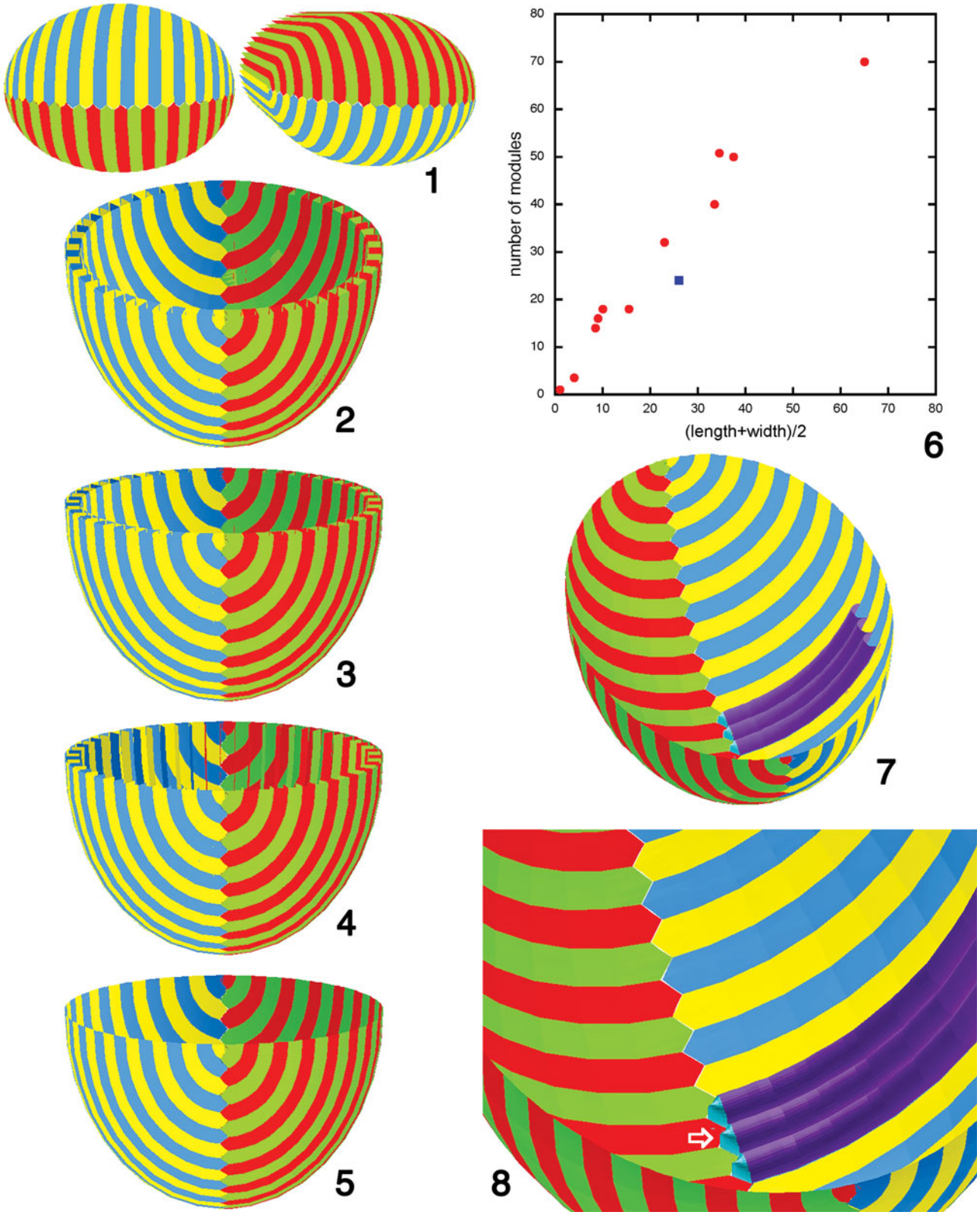

Figure 18. Growth of *Ernietta*. (**1–5, 7, 8**) Super3D models. (**6**) Scatter plot of size versus number of modules in *Ernietta plateauensis* Pflug, 1966 (filled circles); the holotype of *E. plateauensis*, thought to be a deformed specimen of *Pteridinium simplex*, is represented by the filled square. (**1**) Perspective view of two identical copies showing how the modules interdigitate along the proximal seam. (**2–5**) Orthographic views of the base of the model tilted about X by 30° (**2**) and 20° (**3, 4**) showing the progressive deconstruction of the model, which is based on rectangular modular cross sections found in mature individuals of *Ernietta* from Nevada. (**7, 8**) The basal part of the external layer of the model and three modules of the kinds seen in immature individuals from Namibia (Fig. 17.6), where the cross sections are D-shaped and end proximally in wedge-shaped terminations (arrow), reminiscent of the youthful modules of the erniotaxid morphotype (Fig. 17.2); it is assumed that the D-shaped modules merge distally into mature box-shaped ones.

https://doi.org/10.1017/jpa.2023.81 Published online by Cambridge University Press

walls, it also does not provide strong support for the dual- or multiple-wall hypothesis that forms the basis for the remarkably similar reconstructions of Jenkins et al. (1981, fig. 6A) and Ivantsov et al. (2016, fig. 7). Because there is no evidence for more than a single wall in the great majority of specimens of *Ernietta* (Fig. 17.6; Pflug, 1972; Hall et al., 2020; Runnegar, 2022) or *Namalia* (Grazhdankin and Seilacher, 2002), caution is recommended until a complete individual or population of individuals showing evidence for more than one palisade wall becomes available. We tentatively attribute those few specimens that have some evidence of more than one layer near their bases to abnormal development, regeneration after injury, or some unidentified taphonomic process.

This suggestion may also apply to Jenkins's encircling suture, which interrupts the modules so severely that they may be significantly narrower above it and not in register with the modules below it (Fig. 15.2, 15.3; Jenkins et al., 1981, fig. 5B), details not captured in the reconstructions (Jenkins et al., 1981, fig. 6A; Ivantsov et al., 2016, fig. 7). Perhaps an explanation for these sutures is that they also represent a response to traumatic injury, such as truncation of the top of the organism by storm surge, followed by subsequent regrowth. This may explain why the suture is lower down in specimens from Twyfel (Fig. 15.9) than in those from Aar (Fig. 15.3).

The nature of the growing ends of the modules is another feature of the two reconstructions that deserves reassessment. In Jenkins's reconstruction, the modules terminate in lappet-like edges, which border a pair of wide lips formed from three concentric palisades of modules (Jenkins et al., 1981, fig. 6A). Ivantsov et al. (2016, fig. 7) show two concentric rows of similar lappets that flare outward, away from the symmetry axis. These reconstructions contrast with the ones by Monastersky and Mazzatenta (1998), based on undescribed specimens of *Ernietta* from Nevada (Horodyski et al., 1994), which have the modules terminating in narrowly tapering cones with pointed ends (Runnegar, 2022, fig. 3a). The holotype of *Kubisia glabra* has lappet-like terminations (Ivantsov et al., 2016, fig. 8D), adding support for the Jenkins–Ivantsov reconstruction, but another specimen of *Ernietta* from Namibia seems to have distal terminations like the Nevada examples (Narbonne, 2005, fig. 4b; Smith et al., 2017, fig. 3d; Hall et al., 2020, fig. 1b; Runnegar, 2022, fig. 3a). Does this mean that *Ernietta* could withdraw and collapse its tentaculate terminations like anemones exposed at low tide, or that there are two distinct, co-existing morphotypes? These questions deserve further investigation.

As mentioned previously, Glaessner's (1979b) *Erniettinae*, best exemplified by the specimen shown in Figure 19.4, 19.5, may prove to be another distinct morphotype/species of *Ernietta*. If so, Pflug's *Ernionorma abyssoides* may be the name to use, which is why we re-illustrate an epoxy cast of the holotype (Fig. 19.3; GSN F 485; Pflug no. 280). This morphotype is commonly found as basal pieces formed of numerous closely spaced modules (Fig. 19.5, white dots) but may also have highly variable module widths (Fig. 19.6). A morphometric analysis of populations tied to the type localities for the holotypes of *E. sandalix* and *E. abyssoides* will be needed to answer this question.

A fourth area of concern for understanding the biology and taphonomy of *Ernietta* is the long-standing questions as to whether they were epibenthic or endobenthic, whether they received sediment passively in their body cavities during life or actively incorporated sediment into their body tissues to enable them to remain upright if disturbed. There is no doubt that many are preserved with their modules filled with sediment, which is often coarser and better sorted than the matrix that surrounds them (Pflug, 1972; Ivantsov et al., 2016; Hall et al., 2020). This is particularly noticeable in Nevada, where the modules of corrugated bodies or their degraded bag-like remnants are full of clean quartz sand, quite unlike the deep-water, silty matrix in which they are interred (Hall et al., 2020). This suggests that only those bodies that were torn and filled with coarse grains during high-velocity transport were preserved. However, Ivantsov et al. (2016) opted for a division of function along the length of the modules, with active incorporation of sand in their basal parts, a fluid-filled hydrostatic function for their middle parts, and an aerobic/osmotic function for their distal parts. Evidence for sediment incorporation came from longitudinal thin and polished sections, which showed a wide zone of clean quartz sand between the outer and inner walls and sequential fill of less coarse sediment within the body cavity (Ivantsov et al., 2016, fig. 6E, F), similar to the sawn section illustrated by Pflug (1972, pl. 39, fig. 1; Jenkins et al., 1981, fig. 6B). However, the problem with these cross sections compared with internal molds of the *E. sandalix* type is that there is the paucity of partitions attributable to septa—even allowing for the small angles between sections and septa—and the distance between the inner and outer walls is proportionally large compared with the module depths recorded by internal molds. These discrepancies raise the possibility that, although the inner and outer walls were largely intact, the walls and septa had been sufficiently breached to allow coarse suspended grains to enter the wall cavity during transport. Thus, the Namibian and Nevadan specimens may have been preserved under similar conditions. The highly structured nature of the filling of the body cavity of a Namibian specimen (Ivantsov et al., 2016, fig. 6B, C) may provide a reason to doubt this interpretation, but it may also be explicable by waning storm surge sedimentation if the bodies had sufficient mechanical strength to remain open during burial.

Subkingdom Eumetazoa Bütschli, 1910
Phylum Cnidaria? Verrill, 1865
Family Mackenziidae? Conway Morris, 1993
Genus *Archaeichnium* Glaessner, 1963

Type species.—*Archaeichnium haughtoni* Glaessner, 1963 from the Kuibis? or Schwarzrand Subgroup, Karasburg district, Namibia, by monotypy.

Other species.—None. Two species of *Archaeichnium* erected on Paleozoic material, *Archaeichnium kunmingensis* Luo in Luo et al. (1994), from the lower Cambrian of Yunnan, China, and *Archaeichnium*(?) *xizangensis* Yang in Yang et al. (1983), from the Upper Carboniferous of Tibet, are trace fossils with longitudinal striations.

Diagnosis.—Narrow conical organism with about 10–12 longitudinal ridges that may be the edges of, and internally

https://doi.org/10.1017/jpa.2023.81 Published online by Cambridge University Press

Figure 19. *Ernietta plateauensis* Pflug, 1966, Buchholzbrunn Member, Dabis Formation, UCLA 7308, Aar farm (**1, 3**) and approximately the same stratigraphic level, UCLA 7379, Wegkruip farm, plus *Pteridinium simplex* Pflug and *Namalia villiersiensis* Germs, UCLA 7307, Aarhauser sub-member, Kliphoek Member, Dabis Formation, Aar farm (**2, 7–9**). (**1**) Plaster cast of holotype of *Ernietta plateauensis* Pflug, 1966, no. 227 now GSN F 429, probably a deformed and torn specimen of *P. simplex* (**2**) that should be replaced by a neotype such as the holotype of *Erniotaxis segmentrix* Pflug, 1972 (Fig. 15.3). (**2**) Plaster cast of a deformed and torn specimen of *P. simplex*, SMSWA 45370.2 now GSN F 1879, that shows a similar triangular lesion to the one in the holotype of *Ernietta plateauensis*, which Pflug (1972) termed an "apicostomatous aperture"; however, note that there are three vanes (V1–V3) preserved in this specimen. (**3**) Underneath view of epoxy cast of the holotype of *Ernionorma abyssoides* Pflug, 1972, no. 280 now GSN F 485, donated by H.D. Pflug, for comparison with specimens from Wegkruip farm (**4–6**); (**4, 5**) Underneath and lateral views of a weathered but otherwise well-preserved internal mold with the number of visible modules indicated by white dots, GSN F 1880. (**6**) Four similar-sized specimens to illustrate variations in module size and number, GSN F 1881, GSN F 1882, GSN F 1883, GSN F 1884, respectively. (**7**) Fragment of one vane of a specimen of *P. simplex*, embedded in a horizontally bedded sandstone, found by M.A.S. McMenamin at or near the type locality of *E. plateauensis*, field photograph, 1993, GSN F 2209 (McMenamin, 1998, p. 85, fig. 5.3). (**8, 9**) Two views of a specimen resembling the holotype of *Namalia villiersiensis* that was excavated by the Seilacher team at Aar farm, field photographs, 1993, GSN F 612 (Grazhdankin and Seilacher, 2002, text-fig. 9F–H). (**1, 3–6**) Scale bars = 1 cm; (**2, 7–9**) scale bars = 2 cm; (**7**) coin = 23 mm.

https://doi.org/10.1017/jpa.2023.81 Published online by Cambridge University Press

septate, pleated body wall, possibly enclosed in similarly corrugated unmineralized epitheca.

Archaeichnium haughtoni Glaessner, 1963
Figures 20, 21

1960 ?archaeocyathid Haughton, p. 38, pl. 3–5, pl. 3, fig. 1;.
1963 *Archaeichnium haughtoni* Glaessner, p.117, pl. 3, figs. 1, 2.
1978 *Archaeichnium haughtoni*; Glaessner, figs. 1, 2.
2000 non cf. *Archaeichnium* sp., Hagadorn and Waggoner, p. 351, figs. 3.5, 3.6.
2013 non *Archaeichnium* sp., Gehling and Droser, fig. 2M, N.
2016 microbially induced crack, Buatois and Mángano, fig. 2.7c.
2022 indeterminate trace fossils, Turk et al., p. 9, figs. 9.1, 9.2, 9.4, 9.5.

Holotype.—One of several specimens probably preserved in convex hyporelief on a small slab of sandstone, ISAM K4812, ostensibly from the Nababis Formation, Kuibis Subgroup, on Gründoorn farm, near the Ham River, ~60 km east of Karasburg, southern Namibia (Fig. 20.1; Haughton, 1960, pl. 4, 5; Glaessner, 1963, pl. 2, fig. 1, 1978, fig. 1), but possibly from the younger Schwarzrand Subgroup in the same section (near 19.295356°E, 28.094153°S); by original designation and monotypy.

Description.—Longitudinally ridged, tubular fossils that taper gradually or rapidly to a closed end (Figs. 20.5, 21.1), which may have been fixed to the substrate (Fig. 21.1, 21.4); the greatest diameter is typically ~5 mm, and the tubes may exceed several cm in length; the number of longitudinal ridges is ~10–12 assuming that external molds, which have ~3.5 ridges (Fig. 21.6), represent about a third of the circumference; perimortem kinks (Fig. 21.2) and twists (Fig. 20.1) in the tubes suggest that they were unmineralized and flexible; a remarkable specimen (Fig. 20.3, 20.4, 20.6, 20.8) shows either an impression of the side of one ridge or the side view of a flange that either extended outward from the ridge crest or is an internal extension from the body wall; the structure has evenly spaced, radially oriented ridges that are about 0.5 mm apart and of similar length that may have provided structural support or had some other function (see Remarks); rare external molds suggest that, in life, the ridges were narrow and stiff and the intervening wall segments were concave so that the cross section resembled a concave or parabolic star with 10–12 points (Fig. 21.6).

Materials.—Six pieces of sandstone from Arimas (UCLA 7309), two from the Holoog River (UCLA 7325), and one from Kyffhauser (UCLA 7320), most having more than one specimen of *Archaeichnium*, plus an image of a specimen (Fig. 21.6) figured by Buatois and Mángano (2016, fig. 2.7c), generously provided by Luis Buatois.

Remarks.—The holotype and other specimens on the same surface are tubular fossils that are longitudinally ridged and may or may not taper to pointed ends. Haughton (1960) thought the pointed ends were closed and possibly attached to the seafloor; Glaessner (1963, 1978) rejected Haughton's comparisons to archaeocyathids and thought that the tapering of the tubes was caused by their trajectory out of the bedding plane. We are confident that the tubes tapered to closed ends because they overlay surfaces sealed by microbial mats before being buried by event sands and do not leave those surfaces (Fig. 21.1, 21.2).

Glaessner (1978) thought *Archaeichnium* was some kind of agglutinated sand worm tube, and Turk et al. (2021, 2022) have compared it to priapulid burrows, but it is clear from the specimen discovered by JGG at Arimas (Fig. 20.6) that *Archaeichnium* must be a body fossil, not a trace fossil. Presumably, the ladder-like feature preserved in this specimen is part of a tubular and perhaps pleated body wall. As it associated with one of the longitudinal ridges, it may be one of numerous similar structural elements, each comprising part of one of the ridges. If the external molds shown in Figure 20.7, 20.8 do represent casts of the exterior of *Archaeichnium*, on the basis of their co-occurrence, then all of the wall complexity would presumably lie inside this unmineralized epitheca. Thus, the ladder-like feature (Fig. 20.6) may have extended inward from the ridge crest in the form of a longitudinal septum. An associated external mold (Fig. 20.7) is another similar-sized, tubular object, but it also has ~8 longitudinal corrugations and regularly spaced commissural flanges. It may represent an external mold of a piece of the epitheca of *Archaeichnium* such that each longitudinal corrugation would house a projecting flange.

We also tentatively assign several specimens on the base of the slab from Kyffhauser (UCLA 7320; Fig. 21.3, 21.4) to *Archaeichnium*, although they may represent a completely different organism. However, they are conical, taper to a pointed and apparently attached end, are longitudinally ridged, and are comparable to *Archaeichnium* in size but not in length. Apart from their length/width ratios, they are similar to other specimens of *Archaeichnium* (e.g., Fig. 21.5). Whether the Kyffhauser specimens are assigned to *Archaeichnium* makes little difference to the biological interpretation of the fossil. In that context and starting from first principles, *Archaeichnium* appears to have had radial symmetry and a stiff but flexible body wall and probably lived attached to the substrate. Some of the Kyffhauser specimens somewhat resemble the Cambrian demosponge *Takakkawia* Walcott, 1920 (Rigby, 1986; Botting 2012), but the lengths of the longer ones and the flexibility of the walls effectively rule out a poriferan affinity. Perhaps a more plausible possibility is some connection with those "Precambrian macroorganisms" (Protechiuridae; Ivantsov and Fedonkin, 2002; Ivantsov et al., 2019) that possess unmineralized conical thecae. Although most are vastly different (e.g., *Protechiurus edmondsi* Glaessner, 1979a), there are intriguing similarities to some (e.g., *Vendoconularia triradiata* Ivantsov and Fedonkin, 2002) in the pleating of the walls, the hint of duodeciradial symmetry, and the possibility of longitudinal flanges. Ivantsov et al. (2019) pointed out some similarities of the protechurids to conulariids and anabaritids and suggested that all three groups might be basal scyphozoans, so a cnidarian affinity for *Archaeichnium* is one potentially viable possibility. The reconstruction of the putative Ediacaran anthozoan *Auroralumina attenboroughii* (Dunn et al., 2022) is also similar in some respects to *Archaeichnium*, most notably in its

https://doi.org/10.1017/jpa.2023.81 Published online by Cambridge University Press

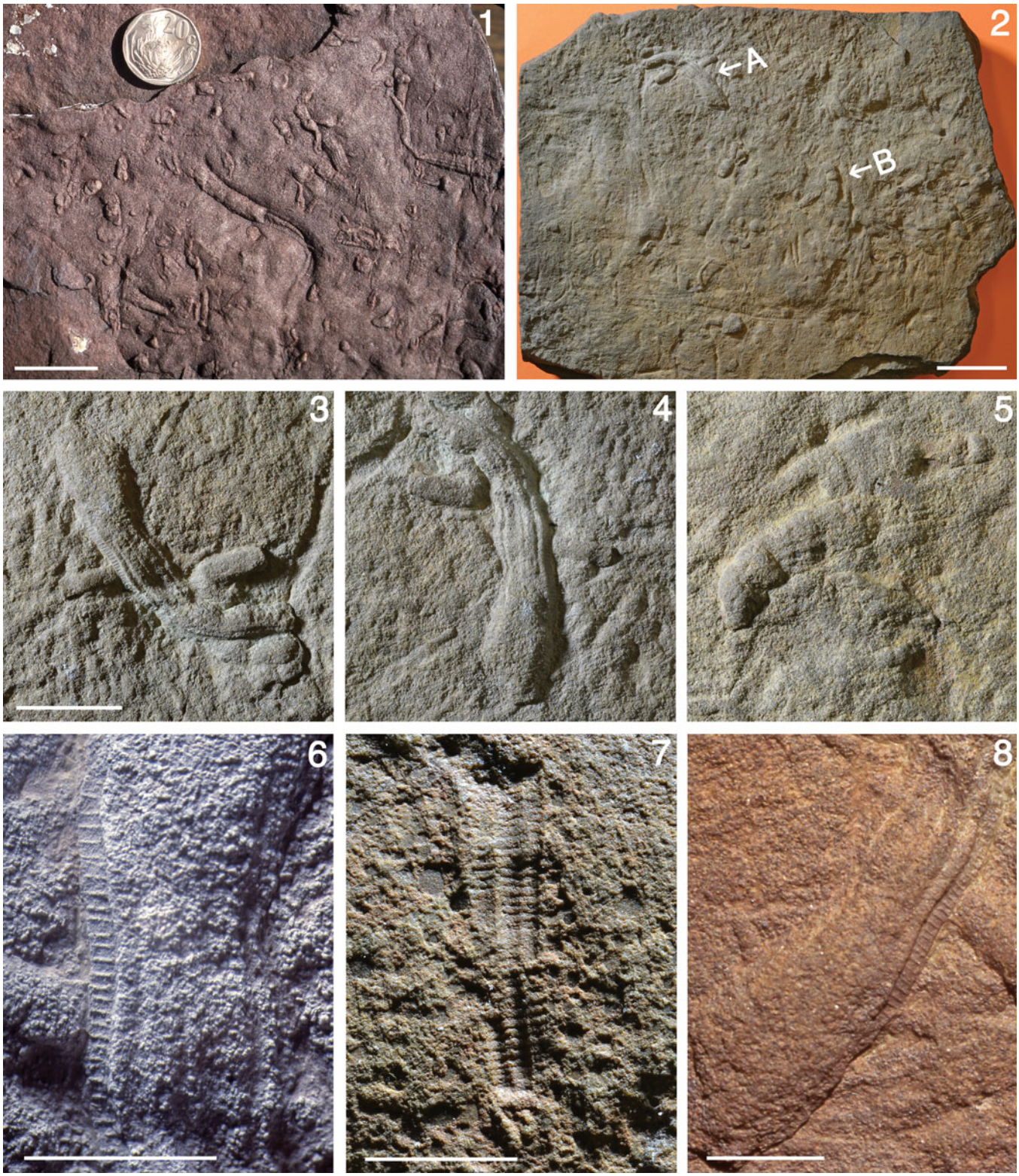

Figure 20. *Archaeichnium haughtoni* Glaessner, 1963, Nakop Member, Nababis Formation, Gründorn farm (57) (**1**) and Huns Member, Urusis Formation, UCLA 7309, Arimas farm (**2–8**). (**1**) Holotype of *A. haughtoni*, ISAM K4812, photographed in Cape Town, South Africa, in 1993. (**2**) Sandstone slab with two specimens, GSN F 1904A (**3, 4, 6, 8**) and GSN F 1904B (**5**), that reveal much of the anatomy of the form. (**3, 4, 6, 8**) Four views of GSN F 1904A taken with different lighting and equipment to show the nature of the body wall and its construction. (**5**) End piece showing likely origin of growth. (**7**) A co-occurring external mold that is longitudinally fluted and may represent a cast of the cuticle or tube of *Archaeichnium*. (**1**) Coin = 19 mm; (**1, 2**) scale bars = 2 cm; (**3–5**) scale bar = 1 cm; (**6–8**) scale bars = 5 mm.

https://doi.org/10.1017/jpa.2023.81 Published online by Cambridge University Press

Figure 21. *Archaeichnium haughtoni* Glaessner, 1963, Huns Member, Urusis Formation, UCLA 7309, Arimas farm (**1**), UCLA 7325, Holoog River (**2**), and Neiderhagen Member, Nudaus Formation, Kyffhauser farm (**3–6**). (**1**) Four longitudinally striated individuals with pointed terminations (arrows), presumed to be the origins of growth, on the base of a 3 cm thick sandstone bed with "old elephant skin" texture, GSN F 1906. (**2**) Two specimens from the Holoog River, one of which is severely kinked (insert), GSN F 1962 and GSN F 1975, respectively. (**3**) Superb bed base, GSN F 1939, found by D.E. Erwin in 1995, with at least eight tethered and current-oriented individuals, six facing right and two facing left, with the three best-preserved ones indicated by arrows and shown in (**4**). (**4**) Three panels enlarged from (**3**) to show left-facing (top, GSN F 1939A) and right-facing individuals (middle, GSN F 1939B, bottom GSN F 1939C). (**5**) External mold, GSN F 1949. (**6**) An external mold, photographed in the field and then discarded, figured as a pseudofossil by Buatois and Mángano (2016, fig. 2.7c) that clearly shows the pleated nature of the body wall; image kindly provided by Luis Buatois, rotated through –90° so that it appears in positive rather than negative relief. (**1**) Scale bar = 2 cm; (**2, 2 insert, 3, 5, 6**) scale bars = 1 cm; (**4**) scale bar = 5 mm.

https://doi.org/10.1017/jpa.2023.81 Published online by Cambridge University Press

longitudinally pleated cup and stem. A third, and perhaps even better, cnidarian comparison is with the Cambrian Stage 4 "tubicolous enigma" *Gangtoucunia aspera* Luo and Hu in Luo et al., 1999, which is thought to be a sessile, tube-dwelling stem or early crown medusozoan (G. Zhang et al., 2022). Some specimens of *Gangtoucunia aspera* have 16–19 mesenteric septa that appear to extend along the length of the body. The tube is phosphatic and densely annulated like some Schwarzrand Subgroup tubes (Fig. 23), so it is possible that our speculative association of a radially fluted tube (Fig. 20.7) with the longitudinally ridged and possibly septate body of *Archaeichnium* may prove to be correct.

Another, and more likely, possibility is a relationship to the Burgess Shale and Chenjiang mackenziids *Mackenzia* Walcott, 1911 (Conway Morris, 1993) and *Paramackenzia* Zhao et al. 2021. Each has an elongate, sausage-shaped body with 10–20 longitudinal elements that are thought to be radial septa, either of the cnidarian type (Conway Morris, 1993) or the kind found between the modules of *Ernietta* (Zhao et al., 2021). However, in *Paramackenzia*, each septum houses shallowly inclined tubular structures that are ~1–2 mm long, ~1 mm apart, and ~0.25 mm in diameter, which are comparable in organization and dimensions to the ladder-like feature of *Archaeichnium* (Fig. 20.6). The tubular structures are thought to represent pore canals that were used to pump water into the body cavity of an *Ernietta*-like organism (Zhao et al., 2021), and some are filled with sediment, giving them the kind of topographic relief seen in the ladder-like feature of *Archaeichnium*. Although Zhao et al. (2021) advanced a strong case for *Ernietta*-like modular construction of *Paramackenzia*, the presence of an inner body wall is still debatable. Conway Morris's (1993, p. 610) description of the body wall of *Mackenzia* is closer to our concept of *Archaeichnium* (see Fig. 21.6): "It is conjectured that in life the circumference of the body was not simple but thrown into relatively deep folds and intervening ridges, the expression of which is now seen in the elevated lines and displaced margins. Further support for this comes from the distal end of some specimens which have a lobate appearance." Thus, it is possible that even the mackenziids are total group cnidarians, although the inferred pore–canal system of *Paramackenzia* has no counterpart in the Cnidaria. Nevertheless, for all of these reasons, we tentatively refer *Archaeichnium* to the Cnidaria while acknowledging that new discoveries are needed to further explore that possibility.

Tubular fossils

Remarks.—It is well known that the terminal part of the Ediacaran is replete with tubular fossils preserved in different ways: organic films, which may or may not be phosphatic or phosphatized; composite molds in siliciclastic sediments; calcareous skeletons, frequently originally aragonitic and recrystallized; and siliceous replicas of originally calcareous skeletons. Although the nature of the inhabitants of most of these tubes remains uncertain, the time immediately before the "Cambrian explosion" has become known as "Wormworld" (Schiffbauer et al., 2016; Darroch et al., 2018; Chai et al., 2021) or—less restrictively—as "tube world" (Budd and Jackson, 2015). The Nama biota is characteristic in that the dominant fossils through much of the succession are vendotaeniids (Cohen et al., 2009), mineralized tubes of *Cloudina* (Grant, 1990; Yang et al., 2022), composite molds of the bodies of *Archaeichnium*, and a variety of smooth or annulated tubes typically filled or cast in positive or negative hyporelief by sandy event beds (Figs. 20–23).

Order Sabelliditida Sokolov, 1965

Remarks.—Similarities in the collar-in-collar construction of the tubes of *Saarina hagadorni* (Selly et al., 2020) and *Cloudina hartmannae* Germs, 1972 (Germs, 1972b) (Yang et al., 2020, 2022) have given rise to the term "cloudinomorph" as a group name. If these similarities are thought to be due to relatedness rather than convergent similarity, then the family and group names Saarinidae, Sabelliditidae, and Sabelliditida (Sokolov, 1965) should take precedence over Cloudinidae Hahn and Pflug, 1985 (Hahn and Pflug, 1985b) and cloudinomorph.

Siboglinid annelid worms abound in Russian Arctic waters because of the widespread availability of methane from seafloor clathrates and cold seeps (Karaseva et al., 2022). Discovery of this biodiversity (Ivanov, 1954, 1963) led to temporary acceptance of the phylum Pogonophora for the gutless siboglinids (Pleijel et al., 2009) and presumably to Sokolov's (1965, 1967) hypothesis that his Ediacaran genera *Calyptrina*, *Paleolina*, and *Saarina*—as well as *Sabellidites* Yanishevsky, 1926—are Precambrian examples of the phylum. A recent in-depth study of the tubes of *Sabellidites* has supported Sokolov's hypothesis (Moczydłowska et al., 2014), but the discovery by Schiffbauer et al. (2020) of a one-way gut in a cloudinomorph—which may be either *Saarina* or the related genus *Costatubus* (Selly et al., 2020)—would reinforce molecular evidence that the Siboglinidae are a significantly younger, highly derived clade of the Annelida (Hilário et al., 2011; Vrijenhoek, 2013; Georgieva et al., 2019, 2021; Capa and Hutchings, 2021). However, *Eoalvinellodes annulatus* (Little et al., 1999) is a pyritized annulated worm tube from a Silurian fossil hydrothermal vent site in Russia (Georgieva et al., 2019), which may imply that it had a chemosymbiotic lifestyle. Some other tube-dwelling polychaetes that inhabit vents and seeps obtain nutrients from bacterial symbionts in their respiratory crowns (Goffredi et al., 2020), a less-derived mode of chemosymbiosis that may have been in operation lower in the annelid tree. Thus, a non-siboglinid annelid affinity for the sabelliditid tubes remains a prime possibility and is compatible with the existence of a non-siboglinid, tube-dwelling polychaete (*Dannychaeta*) in a Cambrian Stage 3 fauna in China (Chen et al., 2020).

Landing et al. (2021) have also argued for extending the stratigraphic range of siboglinid and sabellid polychaetes into the Ediacaran on the basis of their reinterpretation of the early Cambrian stem gastropod *Pelagiella exigua* (Resser and Howell, 1938), which preserves two fan-shaped arrays of chitinous chaetae (Thomas et al., 2020). Their new sabellid genus *Pseudopelagiella* is based on *P. exigua* but is considered characteristic of species such as *Pelagiella subangulata* (Tate, 1892), which have triangular apertures (e.g., Mghazli et al., 2023) and an inner shell layer made from foliated aragonite (Runnegar in Bengtson et al., 1990, fig. 169B). The presence of an identical microstructure in *Aldanella attleborensis* (Shaler and Foerste, 1888; Qiang et al., 2023), which Landing et al. (2021) accept

https://doi.org/10.1017/jpa.2023.81 Published online by Cambridge University Press

as a stem gastropod, and in the stem lineage bivalves *Fordilla troyensis* (Barrande, 1881) and *Pojetaia runnegari* (Jell, 1980; Runnegar and Pojeta, 1992; Vendrasco et al., 2011), makes the probability that species referred to "*Pseudopelagiella*" are annelids rather than mollusks vanishingly small.

Bobrovskiy et al. (2022) have recently redescribed one of Sokolov's sabelliditid species, *Calyptrina striata* Sokolov, 1967, and have extracted biomarker molecules from an organically preserved specimen of its tube. The proportion of cholestane, the diagenetically derived end product of cholesterol, was ~9% in *Calyptrina*, a little less than the background average for the Lyamtsa locality (~11%; Bobrovskiy et al., 2020) and thus very different from the much higher average amount (~50%) found in large specimens of *Dickinsonia* from the same site (Bobrovskiy et al., 2018). Furthermore, the ratio of two cholestane isomers (5ß/5α) was extraordinarily high (~4) in *Dickinsonia* but similar to that expected from diagenesis (~0.65) in *Calyptrina*. Conversely, other lighter and heavier steranes from *Calyptrina* have unusually low 5ß/5α ratios (~0.2) compared with *Dickinsonia*, where the average value (~0.7) is indistinguishable from the diagenetic expectation. Bobrovskiy et al. (2022) used these and other data to conclude that almost all of the steranes in *Dickinsonia* were derived from cholesterol in body tissue that had been decomposed by anaerobic bacteria rather than from dietary cholesterol in a one-way gut, the usual source of 5ß-cholestane in younger paleobiological, archaeological, and forensic contexts (Runnegar, 2022). *Calyptrina*, they suggested, had lost its tissue cholesterol by not being decomposed by anaerobes, and the low 5ß/5α ratios of its other steranes was due to the processing of dietary sterols derived from algal food sources by aerobic bacteria. This complex argument depends on many questionable assumptions, including a comparison with *Kimberella* (Glaessner and Wade, 1966), which they assumed to be a bilaterian with an alimentary canal. If that assumption is incorrect, then the case for a gut in *Calyptrina*, based on biomarkers, is even weaker. Given that 88% of the total steranes detected in *Calyptrina* come from green algae and that the clay underlying *Calyptrina* is similar to bulk rock extracts from the White Sea area (Bobrovskiy et al., 2020, table S1, 2022, table S1), perhaps the simplest explanation is that the part of the tube analyzed was not inhabited at the time of fossilization.

Family Saarinidae Sokolov, 1965
Calyptrina Sokolov, 1965

Type species.—*Calyptrina partita* Sokolov, 1965 by original designation.

Other species.—*Calyptrina striata* Sokolov, 1967 from the Syuzma beds of the Ust-Pinega Formation (>552.85 ± 0.77 Ma) in a borehole at Obozerskaya (40.31°E, 63.45°N), ~200 km south of Arkhangelsk, Russia (Sokolov, 1967; Stankovskiy et al., 1983; Xiao et al., 2002; Ivantsov et al., 2019; Bobrovskiy et al., 2022).

Coarsely and regularly annulated tubes, cf. *Calyptrina striata* Sokolov, 1967
Figure 22.2–22.6

Description.—Sand-filled tubes, ~5 mm in diameter and up to 10+ cm long, that were probably originally circular in cross section, now slightly flattened, are in places ornamented with regularly spaced well-separated circumferential ridges, which presumably strengthened the tube wall.

Material.—Eleven sandstone gutter casts, each containing several to many individual tubes, from Kyffhauser (UCLA 7320) and single specimens, possibly of the same form, on bed bases from Arimas (UCLA 7309) and the Holoog River (UCLA 7325).

Remarks.—It is not known whether the corrugated parts of these tubes represent a different stage of growth from the smooth and seemingly thicker parts or are due to differences in preservation. However, there is little doubt that these corrugated tubes are neither body fossils nor trace fossils but rather the secreted dwelling structures of a worm-shaped animal. Rare specimens from the Holoog River (Fig. 22.5) and Arimas (Fig. 22.6) are tentatively included in this form taxon.

A variety of sparsely annulated tubular fossils have been assigned to *Calyptrina striata*, which was based on a single compressed pyritized specimen (Sokolov, 1967; Bobrovskiy et al., 2022, fig. S4H, I). The redescription of the species from numerous White Sea examples preserved in different ways (Bobrovskiy et al., 2022) revealed that the apertural part of the tube had regularly spaced wall thickenings that were robust enough to leave deep grooves in external molds and are clearly visible in mineralized compressions (Bobrovskiy et al., 2022, fig. S4D, H, I).

Between the thickened annulations, the wall has fine longitudinal costae that would not be visible in our material because of the grain size of the sandstone gutter casts. Bobrovsky et al. (2022) also provided excellent evidence that the apertural end of the tube projected above the seafloor during life and that the longer, buried portion of the tube ran horizontally and changed character gradationally along its length to become finely and regularly annulated or finely and irregularly annulated, features we found in tubular fossils from other localities (Fig. 23.1–23.3, 23.6, 23.9). However, as there is no direct evidence for a biological connection between these variously ornamented tubes, we describe the finely annulated ones separately. Annulated structures from Ediacara identified as the meniscuate trace fossil *Taenidium* cf. *T. serpentinum* (Heer, 1877) by Jenkins (1995) are superficially similar to *C. striata* but are consistently short and banana shaped (Reid et al., 2017) and probably not circular in cross section.

Family uncertain
Genus *Sinotubulites* Chen, Chen, and Qian, 1981

Type species.—*Sinotubulites baimatuoensis* Chen, Chen, and Qian, 1981, from the Shibantan Member of the Dengying Formation, Shibantan of Yichang City, China, by original designation.

Remarks.—We tentatively refer some regularly annulated tubular fossils to this species, which is based on rather poorly preserved type material and has been identified from Ediacaran deposits in many parts of the world (Yang et al.,

https://doi.org/10.1017/jpa.2023.81 Published online by Cambridge University Press

https://doi.org/10.1017/jpa.2023.81 Published online by Cambridge University Press

Figure 22. Coarsely and regularly annulated tubes, cf. *Calyptrina striata* Sokolov, 1967 (**2–6**), smooth tubes (**1, 7**), and two important specimens of *Archaeichnium haughtoni* Glaessner, 1963 (**8, 9**) from the Neiderhagen Member, Nudaus Formation, UCLA 7320, Kyffhauser farm (**1–4**), the Huns Member, Urusis Formation, UCLA 7325, Holoog River (**5, 7**), and UCLA 7309, Arimas farm (**5, 8, 9**). (**1**) Bed base with sandstone casts of numerous small, short, conical tubes plus one wider, coarsely annulated, kinked tube (arrow), GSN F 1941. (**2**) Base of gutter with sandstone cast of one coarsely annulated tube, GSN F 1944. (**3**) Top of tube-filled gutter cast, found by D.H. Erwin in 1995, with one annulated tube indicated by the arrow, GSN F 1943. (**4**) Top, end, and base of small section of a gutter cast with one enclosed coarsely annulated tube indicated by the arrow, GSN F 1945. (**5**) Cast of irregular annulated tube on bed base, Holoog River, GSN F 1973. (**6**) A somewhat similar structure, Arimas, GSN F 1934. (**7**) Small sandstone slab with casts, many presumably current-aligned smooth tubes, GSN F 1976. (**8**) Recognizable specimen of *Archaeichnium haughtoni* that is on the same surface as the "Arimas lycopod" (Fig. 14.5), thus demonstrating co-occurrence of these two taxa, GSN F 1910. (**9**) Quartz filling of *Archaeichnium haughtoni* that gives some information about its cross-sectional shape before burial and compaction, GSN F 1919. (**1, 3, 4, 7**) Scale bars = 2 cm; (**2, 5, 6, 8, 9**) scale bars = 1 cm.

2022). As currently diagnosed, the species is a form taxon that is sufficiently broadly defined to accommodate the Namibian material for the time being. There are also some similarities to *Wutubus annularis* (Chen et al., 2014) as discussed in the following.

Finely annulated tubes, cf. *Sinotubulites baimatuoensis* Chen, Chen, and Qian, 1981
Figure 23.1–23.3, 23.6, 23.9

2021 Tubular and annulated body fossils, Darroch et al., fig. 4a, f.

Description.—External molds preserved in calcareous siltstone and sandstone of a an originally cylindrical finely annulated tube, having either dispersed irregular narrow ridges (Fig. 23.1, 23.2) or tightly packed narrow annulations (Fig. 23.3, 23.6, 23.9); length of tube at least 140 mm, diameter 2–6 mm; longest known tube appears to taper from ~3.5 to ~2 mm; severely kinked specimen (Fig. 23.1) demonstrates that the tube wall was unmineralized and flexible.

Material.—One large, kinked specimen from Swartkloofberg (UCLA 7377), three slabs with five specimens from Zaris (UCLA 7383), five slabs with one or more specimens from Zaris Pass (UCLA 7384C), and eight slabs from the Holoog River (UCLA 7325), only some of which may be tentatively included in this category.

Remarks.—There are similarities to some specimens of *Calyptrina striata* (e.g., Bobrovskiy et al., 2022, figs S2E, S4C), but in the absence of examples with widely spaced coarse rugae, membership of that species is unlikely. *Sinotubulites baimatuoensis* has fewer distinctive features, being simply an irregularly to regularly annulated tube, but we tentatively refer these Namibian tubes to that form species. *Wutubus annularis* (Chen et al., 2014) is also similar, but some specimens taper rapidly to a closed apex that is presumed to be the site of attachment to the substrate. Our material tapers far more slowly (Fig. 23.6), and there is no evidence for a closed end. *Annulatubus flexuosus* (Carbone et al., 2015) is more regularly annulated and fits better with the *Sekwitubus–Corumbella–Shaanxilithes* morphotype according to the analysis by Dunn et al. (2022).

Regularly annulated tubes, cf. *Sekwitubulus annulatus* Carbone et al., 2015
Figure 23.4, 23.5, 23.7, 23.8

1972c *Taenidium* sp., Germs, pl. 2, fig. 2.
2016 *Shaanxilithes*; Darroch et al., fig. 6d.
2021 Tubular and annulated body fossils, Darroch et al., fig. 4b, c, d.
2022 Tubular body fossils, Turk et al., fig. 11.2–11.4.

Description.—Cylindrical tubes, 2–3 mm in diameter, ornamented with regularly spaced angular ridges that are not obviously collar shaped, are not tapered, and do not appear to have been mineralized.

Material.—About half a dozen short pieces of tubular fossils found as external molds on the bases of slabs from Arimas (UCLA 7309), the Holoog River (UCLA 7325), and Zaris (UCLA 7383).

Remarks.—There are many similarly ornamented tubular structures in the Ediacaran, and the morphology persists to the present, as exemplified by the living terebellid annelid *Glyphanostomum pallescens* (Georgieva et al., 2019). *Sekwitubulus annulatus* is a comparable, incompletely known regularly annulated tubular fossil from the Blueflower Formation, northwest Canada, described by Carbone et al. (2015), who compare it with previously described Ediacaran genera.

Other body fossils and body traces
Figure 24.1, 24.3, 24.4, 24.6–24.9

Remarks.—We illustrate but do not describe specimens of *Aspidella* sp. and *Beltanelliformis brunsae* Menner in Keller et al., 1974 from Aar (UCLA 7307) and *Palaeopascichnus* sp. from the Namaland (UCLA 7315) for the sake of completeness. One locality has yielded three specimens of *Pseudorhizostomites* (Sprigg, 1949; Fig. 24.6), best interpreted as the removal trace of a frond (Tarhan et al., 2015). We also show two examples of scratch circles (Osgood, 1970; Jensen et al., 2018), one of which is on a bed base and has a conical plug at its center (Fig. 24.7) that resembles structures described (Darroch et al., 2021) as the conical burrows *Conichnus* (Männil, 1966) and *Bergaueria* (Prantl, 1946) and presumably was the entrance to the home of the producer. Other blister-like structures on bed bases (Fig. 24.5) are best interpreted as incipient syneresis cracks.

Ichnofossils

Remarks.—The Ediacaran ichnofossil record of Namibia has recently been reviewed by Darroch et al. (2021) and Turk

https://doi.org/10.1017/jpa.2023.81 Published online by Cambridge University Press

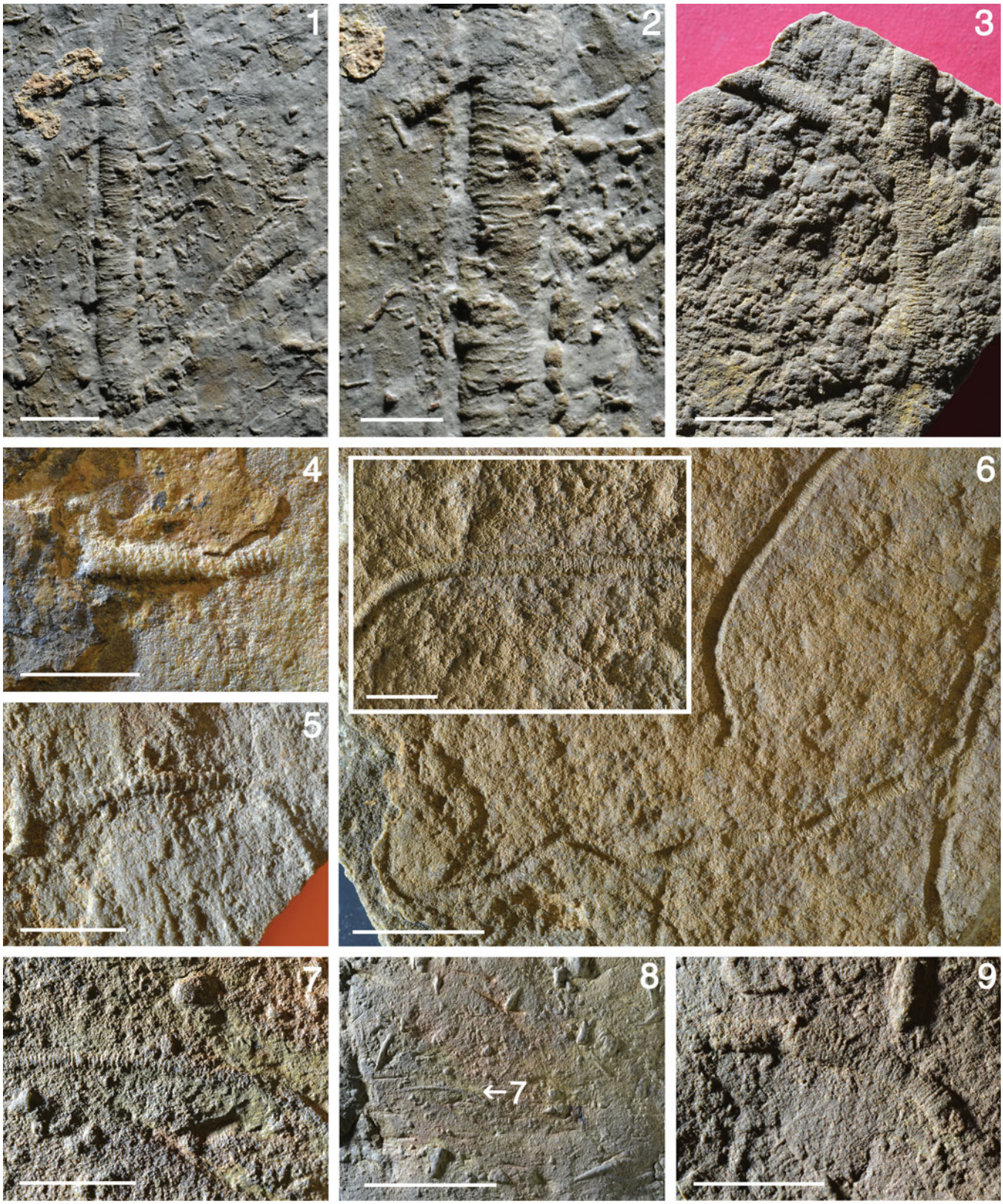

Figure 23. Various annulated tubes, cf. *Sinotubulites baimatuoensis* Chen, Chen, and Qian, 1981 (**1–3, 6, 9**) and cf. *Sekwitubulus annulatus* Carbone et al. (**4, 5, 7, 8**), Feldschuhhorn Member, Urusis Formation, UCLA 7377, Swartkloofberg farm (**1, 2**), Urikos Member, Zaris Formation, UCLA 7383 and UCLA 7384C, Zaris farm and Zaris Pass (**3, 5, 6**), and Huns Member, Urusis Formation, UCLA 7309, Arimas farm (**4, 7, 8**) and UCLA 7325, Holoog River (**9**). (**1, 2**) Two views of a kinked tube on a presumed lower fine-grained carbonate bed surface, GSN F 1935. (**3**) Two finely annulated tubes on the lower surface of a carbonate slab that has OES texture, GSN F 1982. (**4**) Small piece of crisply annulated tube, GSN F 1918. (**5**) Another crisply annulated tube, GSN F 1984. (**6**) Bed base casts of finely annulated tubes (seen in positive relief in insert), GSN F 1966. (**7, 8**) Narrow annulated tube, seen in bed base context in (**8**), GSN F 1953. (**9**) Section of finely annulated tube, bed base, GSN F 1971. (**1, 3, 5, 6 insert, 7, 9**) Scale bars = 1 cm; (**2, 4**) scale bars = 5 mm; (**6**) scale bar = 2 cm; (**8**) scale bar = 5 cm.

https://doi.org/10.1017/jpa.2023.81 Published online by Cambridge University Press

et al. (2022). Our contribution is focused on bilaterian traces from the Kliphoek Member (Fig. 24.11–24.13) and evidence for a substantial infauna of small animals during Schwarzrand time (Figs 25.5, 26.1–26.8). We also discuss the evidence for the first occurrence of treptichnids in the Nama succession and briefly review ichnological arguments for and against treating the upper part of the Spitskop Member as earliest Cambrian.

Ichnogenus *Archaeonassa* Fenton and Fenton, 1937

Type ichnospecies.—*Archaeonassa fossulata* Fenton and Fenton, 1937 from the Cambrian Series 3, Stage 5, Mt. Whyte Formation, Alberta, Canada (Fenton and Fenton, 1937; Yochelson and Fedonkin, 1997), by monotypy.

Archaeonassa isp.
Figure 24.10

1982 ?*Nereites* sp., Crimes and Germs, p. 900, pl. 2, fig. 8.
2021 *Archaeonassa* Fenton and Fenton; Darroch et al., fig. 9 g.
2022 *Archaeonassa*; Turk et al., p. 6, fig. 7.1.

Remarks.—A single specimen, GSN F 1979, from the base of the Huns Member at Holoog River (UCLA 7325) shows the characteristic U-shaped end of this groove and ridged trace; better examples were illustrated by Turk et al. (2022, fig. 7.1) from their Canyon Roadhouse site. *Archaeonassa* Fenton and Fenton, 1937 ranges from the late Ediacaran to the present (Jensen, 2003; Uchman and Martyshyn, 2020).

Ichnogenus *Ariichnus* new ichnogenus

Type ichnospecies.—*Ariichnus vagus* n. igen. n. isp. from the Huns Limestone Member, Urusis Formation, Arimas farm, Southern Namibia.

Diagnosis.—As for the type species by montypy.

Etymology.—Contraction of *Arimas* (farm) and *ichnos*, Greek for footprint or track.

Ariichnus vagus new ichnospecies
Figures 25.2, 26.1, 26.2, 26.4–26.8

1972a thin, straight, or curved thread-like trails, Germs, p. 208, pl. 26, fig. 5.
1972b very thin, straight, or curved thread-like trails, Germs, p. 866, pl. 1, fig. 5.
2000 smaller ?trace fossils, Jensen et al., fig. 2.
2021 sub-millimeter scale burrows, Darroch et al., p. 15, fig. 9b, c.
2022 meiofaunal traces, Turk et al., p. 11, fig. 8.

Holotype.—Burrow shown in insert of Figure 26.6, on slab GSN F 1931, from the Huns Limestone Member, Urusis Formation, Arimas farm, Southern Namibia.

Diagnosis.—Narrow, subhorizontal, dichotomously branching burrows that follow irregular paths and occasionally cross over each other.

Description.—Narrow, subhorizontal cylindrical burrows, ~0.3 mm in diameter, exhibiting occasional Y-shaped junctions that multiply the total number of terminations away from the burrow entrance; in the holotype, adjacent branches are irregular in the forward direction and cross each other without intersecting (see also Darroch et al., 2021, fig. 9c, right arrow; Turk et al., 2022, fig. 8.3); numerous circular cross sections presumably represent vertical segments that connect the subhorizontal tunnels into a complex three-dimensional network.

Etymology.—Latin, *vagus* (roving, wandering), in reference to the paths of the primary branches of the burrows.

Material.—Six sandstone gutter casts, GSN F 1924–1931, from the same locality, each with numerous examples of microburrows intersected and cast by the sandstone channel fills plus the specimen collected by Germs at Arimas.

Remarks.—The three-dimensional geometry of these microburrow systems is difficult to reconstruct from the curved two-dimensional surfaces on which they are observed. It does, however, appear that they formed systems with true branching and are not merely the result of coincidental interference. The surface expression resembles planar sections of *Chondrites* burrow systems seen in thin and polished sections and core slices (Ekdale and Bromley, 1982; Bromley and Ekdale, 1984; Baucon et al., 2020). The diameter of the burrows is smaller than that of most ichnospecies of *Chondrites* but overlaps with *Chondrites intricatus* (Brongniart, 1828), in which the strings are smaller than 1 mm (Fu, 1991); Ekdale and Bromley (1982) and Uchman (1999) also recorded occurrences with a burrow diameter as narrow as 0.2–0.3 mm. The wandering pathways their primary branches seem to follow (Fig. 26.6; Darroch et al., 2021, fig. 9c; Turk et al., 2022, fig. 8.3) distinguish *Ariichnus vagus* from all previously described ichnospecies of *Chondrites*.

Reconstruction of the three-dimensional geometry is problematic because of the small size and style of preservation, but it appears to be less complex than is typical for *Chondrites*, so attribution of the new ichnospecies to *Chondrites* was not desirable. It should be noted that this would have been the first Ediacaran record of *Chondrites*, earlier reports of this age having been rejected (Jensen and Runnegar, 2005; L. Zhang et al., 2022). The ichnogenus is rare also in the Cambrian, without a single accepted Terreneuvian or Series 2 occurrence (Mángano and Buatois, 2014; but see Baucon et al., 2022 for possible exception). *Chondrites* from the Teltawongee Group of New South Wales, Australia (Webby, 1984), sometimes cited as Terreneuvian (e.g., L. Zhang et al., 2022), is in strata of poorly constrained age. Webby (1984) considered the occurrence to be no older than early or middle Cambrian, on the basis of the trace fossils, and they remain the main criteria for the maximum depositional age of the group, with minimum depositional ages obtained from cross-cutting volcanics dated at 505 and 515 Ma (Johnson et al., 2016).

An alternative ichnogeneric assignment of the Nama material could have been to *Pilichnus,* an ichnogenus that Uchman (1999) erected as part of the *Chondrites* group of branched

https://doi.org/10.1017/jpa.2023.81 Published online by Cambridge University Press

https://doi.org/10.1017/jpa.2023.81 Published online by Cambridge University Press

Figure 24. Miscellaneous body fossils and trace fossils. (**1**) *Aspidella* sp., Aarhauser sub-member, Kliphoek Member, Dabis Formation, UCLA 7307, Aar farm, GSN F 1894. (**2**) *Aspidella terranovica* Billings, 1872, Fermeuse Formation, St. John's Group, Ferryland, Avalon Peninsula, Newfoundland, UCLA 7335.1, for comparison with (**1**). (**3**) *Beltanelliformis brunsae* Menner in Keller et al., 1974, characteristic closely packed aggregate, top of Kliphoek Member, Dabis Formation, UCLA 7311, Kliphoek farm. (**4**) *Palaeopascichnus* sp., base of very thin sandstone, Buchholzbrunn Member, Dabis Formation, UCLA 7315, Namaland district, near Bethanien, GSN F 1892. (**5**) Lens-shaped blisters, possibly sandstone casts of syneresis cracks, base of bed, same locality as (**4**). (**6, 9**) radially grooved disks reminiscent of *Pseudorhizostomites* Sprigg, 1949, bed base and counterpart cast of bed base, same locality as (**4**), GSN F 1893 and GSN F 1895, respectively. (**7**) Sandstone cast of scratch circle and funnel-shaped hole made by rotating tethered object, Huns Member, Urusis Formation, UCLA 7309, Arimas farm, GSN F 1912. (**8**) Concentric scratch circles on ripple-marked bed top, same locality as (**7**), GSN F 1917. (**10**) *Archaeonassa* isp., positive relief, Urusis Formation, UCLA 7325, Holoog River, GSN F 1979. (**11**) *Gordia* isp. in positive hyporelief, thin sandstone bed, Urikos? Member, Zaris Formation, UCLA 7384A, Zaris Pass, GSN F 1970. (**12**) *Helminthopsis* isp., sinuous channel, either a trace or a body fossil, on a rippled bed top, same locality as (**7**), GSN F 1915. (**13, 14**) *Gordia* isp., two small slabs from the same bed with possibly the oldest known trace fossils from the Nama Group, Kliphoek Member, Dabis Formation, UCLA 7378, Twyfel farm, GSN F 1920 and GSN F 1921, respectively; the trace fossils occur with syneresis cracks, e.g., left of center in (**13**). (**1–9, 11, 12**) Scale bars = 2 cm; (**10, 13, 14**) scale bars = 1 cm.

structures. The Cretaceous type material has straight to winding strings 0.15–0.35 mm wide, with dichotomous branches. Subsequent reports have extended this ichnogenus to the Terreneuvian (e.g., Buatois and Mángano, 2012). The latest Ediacaran *Pilichnus* from the Tamengo Formation, Brasil (Adôrno, 2019) has larger dimensions and rare branching. A possible difference of the Nama material from *Pilichnus* is that the orientation of *Pilichnus* is mainly along a horizontal plane, although comparison of this ichnogenus with modern traces has been made with more vertically oriented traces (Hertweck et al., 2007).

At the type locality, the microburrows are preserved on the sides and bases of sandstone gutter casts such as the one from the Buchholzbrunn Member seen in outcrop (Fig. 26.3). The Arimas gutter casts were float samples, but the level from which they came is well constrained (Fig. 4; Turk et al., 2022). The microburrows are confined to certain parts of the channel walls and are not found below or above the presumed bioturbated interval that is ~3 cm deep and lies 1–2 cm below the surface (Fig. 26.7, 26.8). This distribution eliminates all four of the hypotheses proposed by Turk et al. (2022) for their formation: opportunistic colonization of exposed sediment in gutters, selective preservation in gutters of a ubiquitous infauna, lithologic contrast between gutter-filling sandstone and guttered substrate, and reborrowing of the channel surface by small animals carried with the eroding fluid. However, they also said that "small bilaterian traces … might be more widespread in these intervals than is currently recognized," as we suggest. As the tops of the channel sands are rippled (Fig. 26.5), the original height of the seafloor was probably lower than the tops of the channel-filling sand (Fig. 26.1, 26.3, 26.5, 26.8). Nevertheless, it is clear that the microburrowed interval began at least 1 cm below the sediment–water interface and continued downward for ~3 cm. This suggests that the tracemakers were exploiting a particular part of the redox gradient and, like *Chondrites*, may have been adapted to dysaerobic conditions (Bromley and Ekdale, 1984; Savrda and Bottjer, 1987).

Parry et al. (2017) described a dense occurrence of "meiofaunal ichnofossils" from the terminal Ediacaran of Brazil and identified them as *Multina minima* Uchman (2001), an Eocene species of *Multina* Orlowski in Orlowski and Zylinska, 1996 from the late Cambrian of the Holy Cross Mountains, Poland (Orlowski and Zylinska, 1996). However, both of these ichnospecies of *Multina* are meshes, not networks, and even *M. minima* has a much larger tunnel diameter than the Brazilian meiofaunal burrows. There is a better size comparison with the Namibian structures, but although the Brazilian traces are described as having "rare dichotomous branches" (Parry et al., 2017, p. 1456; Adôrno, 2019), the tomographic reconstructions show little evidence for branching. On the basis of the small diameter of their narrowest burrows, Parry et al. (2017) were able to exclude most bilaterian phyla as possible tracemakers and opted for a nematode-like worm that lacked the ability to move by peristalsis. We think that is unlikely for the Namibian microburrows because of the irregularity of the trajectories of the tunnels. Nematodes move by bending their bodies in a sinusoidal fashion and either make sinusoidal traces (Balinski and Sun, 2015) or generate "meioturbation" rather than well-defined burrows (Schieber and Wilson, 2021). Thus, it seems more likely that the Namibian microburrows were produced by small animals using hydrostatic processes. The significance of a sizeable bioturbated zone, well below the sediment–water interface and apparently decoupled from the widely assumed Ediacaran microbial mat communities, is explored under Discussion. Another kind of subterranean trace fossil community is indicated by *Planolites*-like burrows intersected by a gutter cast in the top of the Nasep Member on Swartkloofberg (UCLA 7322; Fig. 25.5). Thus, it seems that by the close of the Ediacaran, some bioturbation had moved well below the level of microbial mats. Although probably morphologically distinct, the Nama microburrows compare to, and predate, Fortunian material of *Olenichnus irregularis* Fedonkin in Sokolov and Iwanowskii (1985) from Siberia that Marusin and Kuper (2020) interpreted as complex three-dimensional endobenthic tunnel systems made by bilaterians.

Trace fossils are rarely preserved in pot and gutter casts and, if present, are thought to be post-depositional (Myrow, 1992; Jensen, 1997; Mángano et al., 2002). However, the *Planolites*-like burrows from the Nasep Member are interrupted by the gutter cast wall (arrow, Fig. 25.5), and the microburrows from Arimas were clearly exposed by the erosive action that created the gutters. By contrast, the body fossils, which are occasionally preserved in gutter casts or on the bases of channels (Figs. 12.3–12.5, 16, 21.3, 21.4, 22.4), are thought to have been transported by the eroding events and are, like the tool marks, synchronous with them.

Ichnogenus *Gordia* Emmons, 1844

Type ichnospecies.—*Gordia marina* Emmons (1844) from an Ordovician "fine flagging stone" (calcareous turbidite) of the Giddings Brook slice, Taconic Allochthon (Landing, 2012), at "Mr. M'Arthur's quarry," Jackson, New York, by monotypy.

https://doi.org/10.1017/jpa.2023.81 Published online by Cambridge University Press

Figure 25. Ediacaran and Cambrian trace fossils. (**1**) *Treptichnus* isp? and *Helminthopsis* isp., GSN F 1937, base of thin sandstone slab with continuous and intermittent traces preserved in convex hyporelief, both possibly made by the same organism, and comparable to the traces shown in (**2**), ~160 m above base of Huns Member, Urusis Formation, UCLA 7371, Arimas farm. (**2**) *Treptichnus* isp. and numerous microburrows, *Ariichnus vagus* n. igen. n. isp., all preserved in convex hyporelief, ISAM K4366, Huns Member, Urusis Formation, Arimas farm, found by G.J.B. Germs before 1972, photographed in Cape Town, South Africa, in 1993. (**3, 4**) *Treptichnus pedum* (Seilacher, 1955), lower bed surfaces, Nomtsas Formation, UCLA 7324, Sonntagsbrunn farm, GSN F 1951 and GSN F 1952, respectively. (**5**) Subhorizontal burrows excavated and filled by sediment filling a gutter as evidenced by breaks in the continuity of the borrows (arrow), GSN F 1923, found by A.J. Kaufman in 1995, Nasep Member, Urusis Formation, UCLA 7322, Swartkloofberg farm. (**6**) *Gordia* isp., looping traces on the top surface of a rippled slab, GSN F 1925, Huns Member, Urusis Formation, UCLA 7326, Arimas Farm. (**1–4**) Scale bars = 1 cm; (**5, 6**) scale bars = 2 cm.

https://doi.org/10.1017/jpa.2023.81 Published online by Cambridge University Press

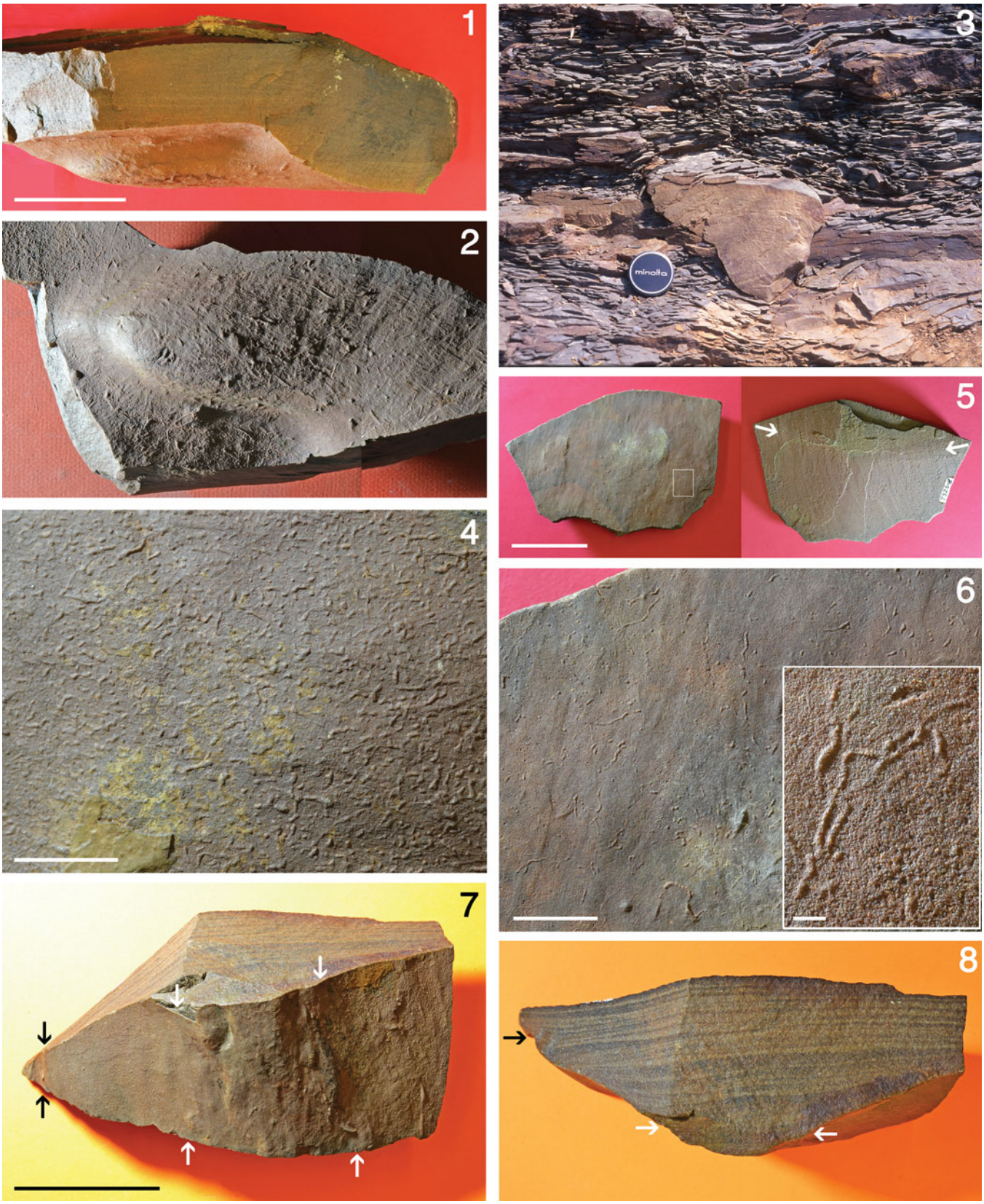

https://doi.org/10.1017/jpa.2023.81 Published online by Cambridge University Press

Figure 26. Gutter casts and microburrows of *Ariichnus vagus* n. isp., Buchholzbrunn Member, Dabis Formation, UCLA 7314, Namaland district (**3**) and Huns Member, Urusis Formation, UCLA 7326, Arimas farm (1, 2, 4–8). (**1, 2**) GSN F 1911, sandstone cast of large gutter, viewed from side and bottom, with microburrow traces on the shallower parts of the cast. (**3**) Cross section of a sandstone-filled gutter cast, embedded in a thin sandstone event bed, and comparable to samples found as float elsewhere. (**4**) GSN F 1929, flat base of an event bed that cast erosional intersections with many microburrows. (**5**) Upper and lower surfaces of a channel cast topped by hummocky stratification (rectangle shows location of the holotype; arrow indicates ripple crest), GSN F 1931; lower surface enlarged in (**6**). (**6**) GSN F 1931, enlargement of lower surface of channel (**5, 6**) showing numerous casts of microburrows; insert is an enlargement of the holotype, which is on another part of the same surface (**5**). (**7, 8**) GSN F 1927, oblique and cross-sectional views of a well-formed channel that has cast microburrows above the level of the white arrows and below the level of black arrows, a stratigraphic interval of ~3 cm. (**1, 2, 5, 7, 8**) scale bars = 5 cm; (**3**) camera lens cap = 60 mm; (**4, 6**) scale bars = 1 cm; (**insert in 6**) scale bar = 1 mm.

Gordia ispp.
Figures 24.11, 24.13, 24.14, 25.6

1972a worm tracks, Germs, pl. 27, fig. 4.
1972b bundled and individual cylindrical tubes, Germs, pl. 2, fig. 5.
2021 *Gordia*, Darroch et al., p. 8, fig. 7g.
2022 *Gordia*, Turk et al., p. 8, fig. 7.6

Material.—Three small slabs from Twyfel, GSN F 1920–1922, one specimen from Arimas, GSN F 1925, and other examples observed in the field.

Remarks.—*Gordia* is one of four Ediacaran ichnogenera/behaviors identified in simple horizonal trails (Buatois and Mángano, 2016) and is characterized by common self-crossings. The examples we illustrate are typical, but those from the Kliphoek Member on Twyfel (Fig. 24.11, 24.13, 24.14) are older than previous records from Namibia and extend this kind of behavior downward from the Schwarzrand Subgroup (Darroch et al., 2021, fig. 18b) into the Kuibis Subgroup. There has been some difference of opinion about the stratigraphic position of the fossiliferous intervals on Twyfel, Weigkrup, Hansburg, and Zuurberg farms (Bouougri et al., 2011; Maloney et al., 2020), but we agree with Maloney et al. (2020) in identifying these horizons as either upper Kliphoek Member or Bucholzbrunn Member rather than Kanies Member. Thus, these specimens of *Gordia* isp. and some associated finer trails are the oldest known trace fossils from Namibia. A looped trace from the Huns Member on Arimas (Fig. 25. 6) may also be referred to *Gordia* isp., but it is clearly different in detail from the Twyfel examples.

Ichnogenus *Helminthopsis* Heer, 1877

Type ichnospecies.—*Helminthopsis magna* Heer, 1877 by subsequent designation of Ulrich (1904, p. 144) or *Helminthopsis abeli* Książkiewicz, 1977 (Han and Pickerill, 1995) or *Helminthopsis hieroglyphica* Wetzel and Bromley, 1996.

Remarks.—Wetzel and Bromley (1996) proposed *Helminthopsis hieroglyphica* to retain Heer's generic name, which was based on material that should be referred to other ichnogenera, so *H. hieroglyphica* Wetzel and Bromley, 1996 has gained acceptance as the replacement type species (e.g., Šamánek et al., 2022).

Helminthopsis isp.
Figures 24.12, 25.1

Material.—Only two possible examples of many similar structures are illustrated. The long continuous trace in Figure 25.1 is best characterized as the form genus *Helminthopsis* but may, in fact, have been generated by the producer of *Treptichnus* isp? (Fig. 25.1, arrows).

Remarks.—According to Buatois and Mángano (2016, p. 41) "*Helminthopsis* displays a tendency to meander," so we refer simple cylindrical traces with this property to *Helminthopsis*. However, as noted by many others, it may be difficult to distinguish such ichnofossils from tubular body fossils. The specimen shown in Figure 25.1 is fairly clearly a trace fossil and may, in fact, be a variety of *Treptichnus*, which occurs next to it on the same slab. The one shown in Figure 24.12 is more ambiguous, and there are many more poorly preserved traces like this in the Schwarzrand Subgroup that could be either trace or body fossils.

Ichnogenus *Streptichnus* Jensen and Runnegar, 2005

Type ichnospecies.—*Streptichnus narbonnei* Jensen and Runnegar, 2005 from UCLA 7375, uppermost Spitskop Member, Urusis Formation, Swartpunt farm, southern Namibia, by original designation and monotypy.

Streptichnus narbonnei Jensen and Runnegar, 2005

2005 *Streptichnus narbonnei* Jensen and Runnegar, figs. 2, 3.
2019 *Streptichnus narbonnei*, Linnemann et al., fig. 4b.

Holotype.—One of two adjoining slabs, GSN F 626 (Jensen and Runnegar, 2005, fig. 2b), from the Spitskop Member, Urusis Formation, UCLA 7375, 13 m below the summit of Dundas Hill, Swartpunt farm, southwestern Namibia.

Remarks.—The complexity of the *Streptichnus* burrow system is comparable to that of *Treptichnus pedum*, so Linnemann et al. (2019) advocated lowering the Ediacaran–Cambrian boundary to just below the level of *Streptichnus* in the Dundas Hill section on Swartpunt (Fig. 5). However, the subsequent discovery of *Streptichnus* in the Shibantan Lagerstätte of South China (Xiao et al., 2021; Mitchell et al., 2022) confirms that it is associated with typical Ediacaran taxa.

Ichnogenus *Treptichnus* Miller, 1889

https://doi.org/10.1017/jpa.2023.81 Published online by Cambridge University Press

Type ichnospecies.—*Treptichnus bifurcus* Miller, 1889 from the Carboniferous, Gzhelian, Mansfield Formation of Indiana (Maples and Archer, 1987), by original designation and monotypy.

Treptichnus pedum (Seilacher, 1955)
Figure 25.3, 25.4

1972a *Phycodes pedum*; Germs, pl. 27, figs. 7, 8.
1972b *Phycodes pedum*; Germs, pl. 2, figs. 7, 8.
1982 ?*Neonereites biserialis* Seilacher, Crimes and Germs, p. 897, pl. 2, fig. 7.
1982 *Phycodes* cf. *P. pedum*; Crimes and Germs, p. 901, pl. 2, fig. 9.
2012 *Treptichnus pedum*; Wilson et al., figs.10–15.

Holotype.—Specimen figured by Seilacher (1955, p. 387, fig. 4a) from the early Cambrian Neobulus shale (Khussak Formation), Salt Range, Pakistan (Buatois, 2018).

Material.—Three specimens from the Nomtsas Formation on Sonntagsbrunn, GSN F 1950–1952.

Remarks.—See Wilson et al. (2012) for a full description of this species and its occurrence in Namibia.

Treptichnus isp.
Figure 25.1, 25.2

1972a Discontinuous trails with three ridges, Germs, p. 208, pl. 26, figs. 5, 7, pl. 27, fig. 1.
1972b Trails with three parallel ridges, Germs, pl. 1, figs. 5, 7, pl. 2, fig. 1.
2000 *Treptichnus*; Jensen et al., fig. 2A–E.
2016 treptichnids; Buatois and Mángano, fig. 4b, c.
2020 treptichnids; Mángano and Buatois, fig. 2a.
2021 burrow similar to *Torrowangea* Webby; Darroch et al., fig. 9a.
2021 treptichnid-type traces; Darroch et al., fig. 13a–e.

Materials.—A single slab from Arimas, ISAM K4366, described originally by Germs (1972a, b) and another similar-sized slab collected by us (Fig. 25.2) from Arimas (UCLA 7371).

Remarks.—Germs's discovery slab was not in place, so the stratigraphic level from which it was derived is uncertain. Germs (1972b, fig. 2) showed the horizon as being immediately beneath the base of the Huns Limestone Member as he then defined it, which would probably place it above the level of UCLA 7326 (Fig. 4). Jensen et al. (2000) placed Germs's specimen lower down in the Arimas section on the basis of field observations of similar traces by JGG in 1993, and Turk et al. (2022, fig. 4) indicated a comparable level, just below their "gutter cast horizon" (= UCLA 7326). Buatois and Mángano (2016, fig. 4) suggested that treptichnids occur even lower down, well below the first prominent limestone bed, in the vicinity of UCLA 7309 (Fig. 4). The only sample in our collection we can confidently place in the stratigraphic section is the one shown in Figure 25.1, which was removed from outcrop by SJ in 1996. The similar slab collected by Germs could easily have moved downslope from that level. Thus, UCLA 7371 (Fig. 4) is the oldest certain occurrence of *Treptichnus* in Namibia.

We refer these traces to *Treptichnus* because of the great range of preservational variants found in some examples of the type species, including structures that closely resemble Germs's "discontinuous trails with three ridges" (Getty et al., 2016, fig. 4.1, 4.2). In any case, *Treptichnus* is a form taxon, which could have been produced by different kinds of animals in the Ediacaran and the Cambrian, so our use of the generic name does not necessarily imply biological continuity across the eon boundary.

Results

Stratigraphy.—Recently published U–Pb ages for the Witputs subbasin (Linnemann et al., 2019; Nelson et al., 2022) have allowed us to postulate a hiatus of ~2 million years at the base of the Schwarzrand Subgroup south of the Osis arch (Fig. 1), but there is little biostratigraphic evidence for this break (Fig. 2). Our carbon isotope data from a section at Mamba, just north of the Osis arch, confirms the correlation of the peak of the OMKYK positive excursion, first identified by Grotzinger et al. (1995), with the top of the Mooifontein Member in the heart of the Witputs subbasin (Fig. 3). On the basis of these correlations, we propose a revision of the sequence stratigraphic terminology for the Nama Group (Fig. 2). We also constrain and extend the stratigraphic and geographic ranges of the key Ediacaran taxa: *Archaeichnium*, *Ernietta*, *Pteridinium*, *Swartpuntia*, and *Treptichnus* (Fig. 2). A conservative estimate for the first appearance of the genus *Treptichnus* is at the top of the Huns Limestone Member, higher than previously thought (Fig. 4), but the diagnostic basal Cambrian species of *Treptichnus*, *T. pedum*, has not been found below the Nomtsas Formation. Suggestions to lower the eon boundary to beneath *Streptichnus narbonnei* (Linnemann et al., 2019) are not supported by the recent discovery of *Streptichnus* with characteristic Ediacaran taxa in the Shibantan Lagerstätte of South China (Xiao et al., 2021: Mitchell et al., 2022).

Taphonomy and paleoecology.—All of the evidence presented here indicates that few if any of the Ediacaran soft-bodied organisms were preserved in life orientation in their original habitats. That includes specimens from the Aarhauser sandstone at Aar excavated by Seilacher and his team that formed the basis of the canoe hypothesis for *Pteridinium* (Ivantsov and Grazhdankin, 1997; Seilacher, 1997; Grazhdankin and Seilacher, 2002) as well as the beds with abundant *Ernietta* on Aar, Twyfel, Wegkruip, Hansburg, and Zuurberg farms that have been used to propose and model a totally infaunal or partly buried lifestyle for *Ernietta* (Crimes and Fedonkin, 1996; Meyer et al., 2014a, b; Elliott et al., 2016; Ivantsov et al., 2016; Gibson et al., 2019; Hall et al., 2020; Maloney et al., 2020). All of the unmineralized tubular fossils we have studied appear to have been transported or perhaps toppled (Fig. 21.4) by water motion, as are most specimens of *Cloudina*. The only taxa that are unquestionably

https://doi.org/10.1017/jpa.2023.81 Published online by Cambridge University Press

in situ are the trace fossils, *Palaeopascichnus*, and frond holdfasts such as *Aspidella* and *Pseudorhizostomites*.

Tool-marked bed bases are a prominent feature of the Nama Group succession. Comb and rake structures previously attributed to the transport of spicular sponge skeletons (Darroch et al., 2021) are shown to be bump and drag marks of erniettomorphs, most probably vanes of *Pteridinium*. Microscopic trace fossils on gutter casts are referred to new ichnogenus and ichnospecies *Ariichnus vagus*. These microburrows were produced by tiny animals that seem to have inhabited a 2–3 cm thick dysaerobic zone that began ∼1 cm below the sediment–water interface.

Taxonomy.—The holotype of the type species of *Ernietta*, *E. plateauensis*, appears to be a small, deformed specimen of *Pteridinium simplex*, and we recommend that it be replaced by a neotype, the holotype of *Ernietta sandalix*, to retain the use of Pflug's iconic generic name. The discovery of a problematicum—the Arimas lycopod—at the type locality of *Nasepia*, and its resemblance to the axis of *Swartpuntia*, raises the possibility that *Swartpuntia* is either a junior synonym or close relative of *Nasepia*. New evidence suggests that *Swartpuntia* lacked a stem and holdfast, which puts it closer in body plan to *Pteridinium* than previously thought.

Paleobiology.—*Arimasia germsi* n. gen. n. sp. from the Huns Limestone Member is described as a simple sponge, which may have resembled an unmineralized, one-walled archaeocyath. We suggest that *Arimasia*, the Archaeocyatha, and the unmineralized vauxiid sponges may all have been aspiculate stem members of the Demospongiae. This hypothesis requires the independent origin of siliceous spicules in the Hexactinellida and the Demospongiae (Aguilar-Camacho et al., 2019).

Juvenile specimens of *Ernietta* from Buchholzbrunn (Fig. 16) show that growth proceeded from a stage with four or fewer tubular modules to an observed maximum of ∼70 modules in the largest specimens (Fig. 18.6). The evidence for more than one layer of modules in the body wall is limited, so *Ernietta* is considered to be an epifaunal, bag-shaped organism formed of a single layer of tubular modules that were generated at the outer wall and coalesced in a proximal to distal direction during growth. New modules may have arisen at the ends of the zig-zag basal seam and/or by intercalation. Growth interruptions, which are obvious on many internal molds, are attributed to zones of damage and repair during life.

Archaeichnium haughtoni, previously thought to be an archaeocyath, an agglutinated worm tube, or a trace fossil, is shown to be a body fossil with a complicated, pleated body wall that resembles to some extent the polyp-like bodies of the Cambrian animals *Mackenzia* and *Paramackenzia* (Zhao et al., 2021). Consequently, *Archaeichnium* and the mackenziids are tentatively considered to be anemone-like cnidarians rather than *Ernietta*-like vendobionts.

Three different kinds of unmineralized, annulated tubes are illustrated and briefly described as possible examples of *Calyptrina*, *Sinotubulus*, and *Sekwitubulus*. Those identified as "cf. *Calyptrina striata* Sokolov" compare well to White Sea examples of that species illustrated and analyzed for biomarkers by Bobrovskiy et al. (2022). Although the biomarker argument for a one-way gut in *Calyptrina* is debatable, there is a developing consensus that at least some of these Ediacaran tubular structures were produced by annelid grade worms.

Discussion

Glaessner (1979b, p. A96) tentatively referred Pflug's "Petalonamae" to four families, Pteridiniidae, Rangeidae, Charniidae, and Erniettidae "until clear distinctions between observable and hypothetically postulated characters can be drawn." The removal of the Rangeomorpha as an order of Octocorallia (Jenkins, 1985) or more plausibly as a plesion of the Eumetazoa (Dunn et al., 2022) leaves *Pteridinium*, *Ernietta*, *Swartpuntia*, and their candidate synonyms *(Namalia*, *Nasepia*, *Inkrylovia*, *Kuibisia*) as another potentially monophyletic clade, the Erniettomorpha (Pflug, 1972; Erwin et al., 2011). However, finding shared derived characters to support a monophyletic Erniettomorpha as distinct from other Ediacaran fronds has been challenging to impossible (Dececchi et al., 2017; Hoyal Cuthill and Han, 2018). If our interpretation of the anatomy of *Swartpuntia germsi* is correct, then it is far more similar to *Pteridinium carolinaensis* than previously suspected, and the question about the monophyly of the Erniettomorpha reduces to whether *Pteridinium* and *Ernietta* are closely related and whether *Phyllozoon* (Jenkins and Gehling, 1978; Gehling and Runnegar, 2022)—or any other taxon—is another member of this clade. The synapomorphies identified by Dececchi et al. (2017) for *Ernietta*, *Pteridinium*, and *Swartpuntia*—"undifferentiated tubular elements (modules) that are parallel to each other and all of the same width"—also apply to *Phyllozoon* but are insufficient to assess possible ingroup relationships. As these taxa show little if any sign of whole-body differentiation, their position outside the Rangeomorpha and/or Arboreomorpha seems secure. But are they similar to each other as a result of inheritance, convergence, or merely simplicity?

Unique features of some or all erniettomorphs include tubular modules that coalesce during early growth (*Ernietta*) and are in contact laterally via linear not planar seams (*Ernietta*, *Pteridinium*, *Phyllozoon*) as well as triradial symmetry about a unipolar growth axis (*Pteridinium*, *Swartpuntia*). The apparently bipolar growth of *Ernietta* may be an attribute of its topology, and it is conceivable that *Ernietta* inherited the unipolar patterning of most Ediacaran fronds (Runnegar, 2022). Thus, the bipolarity of *Ernietta* may be an adaptation to an epibenthic lifestyle, as it apparently was for *Fractofusus* within the Rangeomorpha (Gehling and Narbonne, 2007; Dececchi et al., 2017). If so, the case for a monophyletic Erniettomorpha remains viable but barely so. In the remaining part of this brief discussion, we address two interwoven topics, both ultimately dependent on taphonomy: paleoecology and extinction.

Pteridinium has been found only in distal mass-flow deposits in South Australia even though it must have persisted during the deposition of the classical Ediacara-style bedforms of the Ediacara Member (Glaessner and Wade, 1966; Wade, 1971; Gehling and Droser, 2013). So where did it live, given that many richly fossiliferous beds have been sequentially excavated at the Nilpena Ediacara National Park (Droser et al., 2019) without revealing a single specimen of *Pteridinium*? The same question could be asked about *Ernietta* in Namibia and Nevada

https://doi.org/10.1017/jpa.2023.81 Published online by Cambridge University Press

(Smith et al., 2017; Hall et al., 2020), some of which are filled with clean quartz sand quite unlike the downslope silty matrix in which they are found. Perhaps the answer lies with *Phyllozoon*, which seems to have inhabited sites that were below storm wave base in South Australia (Gehling and Runnegar, 2022) or with unsuspected anchoring structures that are in plain sight, such as one of the many "triradialomorphs" (Hall et al., 2020). Conversely, where are the discoidal holdfasts and epibenthic recliners that are so characteristic of South Australian and Avalonian assemblages? The obvious answer is differential extinction between the White Sea and Nama assemblages (Darroch et al., 2015, 2018; Evans et al., 2022), but the almost complete absence of Ediacara-style bed surfaces in Namibia (UCLA 7315 being a notable exception) suggests that differential preservation may be just as important. If only the mass-flow deposits in South Australia were fossiliferous, then Ediacara and Nilpena would be "Nama" rather than "White Sea" sites (Gehling and Droser, 2013). Last but not least, increasingly sophisticated phylogenomic studies continue to require substantial Precambrian histories for the crown group clades such as the Cnidaria (McFadden et al., 2021) and the Ecdysozoa (Shi et al., 2022; for a contrary view, see Holmes and Budd, 2022). Although magnificently exposed, the Nama succession is sparsely fossiliferous and thus may represent only a small sample of late Ediacaran biodiversity.

Acknowledgments

For assistance in the field and elsewhere, we thank J.E. Almond, R. Birenheide, C.K. (Bob) Brain, M.L. Droser, D.H. Erwin, G.J.B. Germs, J.P. Grotzinger, A.J. Kaufman, A.H. Knoll, M.A.S. McMenamin, G. Narbonne, G. Oertel, V. Rai, B.Z. Saylor, A. (Dolf) Seilacher, and M.R. Walter. H. Mocke, B. Hoal, G. Schneider, H-K. (Charlie) Hoffmann, M. Dunaiski, C. Kangueehi, N. Mieze, and Sidney—(unrecorded)—all of the Geological Survey of Namibia, generously provided field assistance, logistical support, and curatorial assistance. We are grateful to A. and L. Vollersten, Helmeringhausen Hotel, M. and K. van der Merwe, Rosh Pinah Guesthouse, W. van der Merwe, Bahnhof Hotel at Aus, and A. and G. Porteus, Hammerstein Rest Camp, for welcoming hospitality. Landowners or managers at the following farms kindly allowed access to their properties and in many cases assisted with local advice and communications: H. Erni, Aar (16), W. Erni, Plateau (38), P.F. Cilliers, Chamis Sud (49), J. and H. Gaugler, Dabis (15), Mrs. van der Merwe, Grünau (14), J. Scholtz, Klipdrif (134), E. Dreyer and J. Richter, Kyffhauser (18), D.C. Jankowitz, Saraus (18), W. van der Westhuizen, Swartpunt (74), R. Magson, Donker Gange (161), K. van Staaden, Wegkruip (130), Christoff, Zaris (103), M. and R. Field, Zebra River (122), and the owners of Buchholzbrunn (142), Mamba (125), Mooifontein (50), and Vrede (140). Funding was provided by A. Seilacher from his 1992 Crafoord Prize, the U.S. National Science Foundation (EAR-9627924), the Division of Physical Sciences, UCLA, the Leverhulme Trust, and the National Environment Research Council, U.K. Field and laboratory assistance was supplied by the Geological Survey of Namibia, and permission to collect and export the material studied was obtained with the approval of landowners via applications and permits from the Ministry of Mines and Energy, the Ministry of Trades and Industry, and the National Monuments Council of Namibia, with the assistance of staff at the Geological Survey of Namibia. S. Moran, North Carolina Museum of Natural Sciences, kindly helped track down all known specimens of *Pteridinium carolinaensis* and supplied curatorial information. H. Mocke received and curated the collection at the National Earth Sciences Museum in Windhoek, and L. Buatois, A. Ivantsov, and a third anonymous reviewer provided many helpful comments on the manuscript.

Declaration of competing interests

The authors declare none.

Author contributions

Fieldwork was carried out in 1993 by JGG and BR, in 1995 by SJ and BR, and in 1996 by JGG, SJ, MRS, and BR; stratigraphic sections were measured by JGG, MRS, and BR; samples for carbon isotope analysis were collected by MRS and BR and prepared for analysis by MRS; the fossils were studied at UCLA by JGG, SJ, and BR; BR carried out all of the photographic work, prepared the illustrations, and wrote the manuscript; all authors reviewed the manuscript and contributed to its final form.

Data availability statement

Supplemental dataset 1—Tabulated carbon isotope samples and analyses.

Data available from the Dryad Digital Repository: https://doi.org/10.5061/dryad.fxpnvx0zj

References

Adams, E.W., Schröder, S., Grotzinger, J.P., and McCormick, D.S., 2004, Digital reconstruction and stratigraphic evolution of a microbial-dominated, isolated carbonate platform (Terminal Proterozoic, Nama Group, Namibia): Journal of Sedimentary Research, v. 74, p. 479–497.

Adôrno, R.R., 2019, *Taxonomy, paleoecology and chronobiostratigraphy across the Ediacaran–Cambrian boundary: Tamengo and Guaicurus formations* [D. Geol. thesis]: Brasilia, University of Brasilia, 213 p.

Aguilar-Camacho, J.M., Doonan, L., and McCormack, G.P., 2019, Evolution of the main skeleton-forming genes in sponges (phylum Porifera) with special focus on the marine Haplosclerida (class Demospongiae): Molecular Phylogenetics and Evolution, v. 131, p. 245–253.

Antcliffe, J.B., Callow, R.H.T., and Brasier, M.D., 2014, Giving the early fossil record of sponges a squeeze: Biological Reviews, v. 89, p. 972–1004.

Antcliffe, J.B., Jessop, W., and Daley, A.C., 2019, Prey fractionation in the Archaeocyatha and its implication for the ecology of the first animal reef systems: Paleobiology, v. 45, p. 652–675.

Balinski, A., and Sun, Y., 2015, Fenxiang biota: a new Early Ordovician shallow-water fauna with soft-part preservation from China: Science Bulletin, v. 60, p. 812–818.

Barrande, J., 1881, Système Silurien du centre de la Bohême, Vol. 6. Classes de Mollusques, Ordes des Acéphalés: Paris and Prague, Chez l'auteur et éditeur, 342 p.

Baucon, A., Bednarz, M., Dufour, S., Felletti, F., Malgesini, G., et al., 2020, Ethology of the trace fossil *Chondrites*: form, function and environment: Earth-Science Reviews, v. 202, n. 102989.

Bengtson, S., Conway Morris, S., Cooper, B.J., Jell, P.A., and Runnegar, B., 1990, Early Cambrian fossils from South Australia: Memoirs of the Association of Australasian Palaeontologists, v. 9, 364 p.

Billings, E., 1872, Fossils in Huronian rocks: Canadian Naturalist and Quarterly Journal of Science, v. 6, p. 478.

https://doi.org/10.1017/jpa.2023.81 Published online by Cambridge University Press

Bobrovskiy, I., Hope, J.M., Ivantsov, A., Nettersheim, B.J., Hallmann, C., and Brocks, J.J., 2018, Ancient steroids establish the Ediacaran fossil *Dickinsonia* as one of the earliest animals: Science, v. 361, p. 1246–1249.
Bobrovskiy, I., Hope, J.M., Golubkova, E., and Brocks, J.J., 2020, Food sources for the Ediacara biota communities: Nature Communications v. 11, n. 1261.
Bobrovskiy, I., Nagovitsyn, A., Hope, J.M., Luzhnaya, E., and Brocks, J.J., 2022, Guts, gut contents, and feeding strategies of Ediacaran animals: Current Biology, v. 32, p. 5382–5389.
Bornemann, J.G., 1884, Über die Fortsetzung seiner Untersuchungen cambrischer Archaeocyathus-Formen und verwandter Organismen von der Insel Sardinien: Deutsche Geologische Gesellschaft, v. 36, 702–706.
Botting, J.P., 2012, Reassessment of the problematic Burgess Shale sponge *Takakkawia lineata* Walcott, 1920: Canadian Journal of Earth Sciences, v. 49, p. 1087–1095.
Botting, J.P, and Muir, L.A., 2018, Early sponge evolution: a review and phylogenetic framework: Palaeoworld v. 27, p. 1–29.
Botting, J.P., Muir, L.A., and Lin, J., 2013, Relationships of the Cambrian Protomonaxonida (Porifera): Palaeontologia Electronica, v. 16, n. 16.2.9A, https://doi.org/10.26879/339.
Bouougri, E.H., Porada, H., Weber, K., and Reitner, J., 2011, Sedimentology and palaeoecology of *Ernietta*-bearing Ediacaran deposits in Southern Namibia: implications for infaunal vendobiont communities: Lecture Notes in Earth Sciences, v. 131, https://doi.org/10.1007/978-3-642-10415-2_29.
Bowring, S.A., Grotzinger, J.P., Condon, J.P., Ramezani, J., Newall, M.J., and Allen, P.A., 2007, Geochronologic constraints on the chronostratigraphic framework of the Neoproterozoic Huqf Supergroup, Sultanate of Oman: American Journal of Science, v. 307, p. 1097–1145.
Bowyer, F.T., Zhuravlev, A.Yu., Wood, R., Shields, G.A., Zhou, Y., Curtis, A., Poulton, S.W., Condon, D.J., Yang, C., and Zhu, M., 2022, Calibrating the temporal and spatial dynamics of the Ediacaran–Cambrian radiation of animals: Earth-Science Reviews, v. 225, n. 103913.
Bowyer, F.T., Uahengob, C.-I., Kaputuazab, K., Ndeunyemab, J., Yilales, M., Alexander, R.D., Curtis, A., and Wood, R.A., 2023, Constraining the onset and environmental setting of metazoan biomineralization: the Ediacaran Nama Group of the Tsaus Mountains, Namibia: Earth and Planetary Science Letters, v. 260, n. 11836.
Bromley, R.G., and Ekdale, A.A., 1984, *Chondrites*: a trace fossil indicator of anoxia in sediments: Science, v. 224, p. 872–874.
Brongniart, A.T., 1828, Historie des Végétaux Fossiles ou Recherches Botaniques et Géologiques sur les Végétaux Renfermés dans les Diverses Couches du Globe: Paris, Dufour, G. and d'Ocagne, 136 p.
Buatois, L.A., 2018, *Treptichnus pedum* and the Ediacaran–Cambrian boundary: significance and caveats: Geological Magazine, v. 155, p. 175–180.
Buatois, L.A., and Mángano, M.G., 2012, An early Cambrian shallow-marine ichnofauna from the Puncoviscana Formation of northwest Argentina: the interplay between sophisticated feeding behaviors, matgrounds and sea-level changes: Journal of Paleontology. v. 86, p. 7–18.
Buatois, L.A., and Mángano, M.G., 2016, Ediacaran ecosystems and the dawn of animals: Topics in Geobiology, v. 39, p. 27–72.
Buatois, L.A., Almond, J., Mángano, M.G., Jensen, S., and Germs, G.J.B., 2018, Sediment disturbance by Ediacaran bulldozers and the roots of the Cambrian explosion: Scientific Reports, v. 8, n. 4514.
Budd, G.E., and Jackson, I.S.C., 2015, Ecological innovations in the Cambrian and the origins of the crown group phyla: Philosophical Transactions of the Royal Society B, v. 371, n. 20150287.
Buss, L.W., and Seilacher, A., 1994, The phylum Vendobionta: a sister group of the Eumetazoa?: Paleobiology, v. 20, p. 1–4. https://doi.org/10.1017/S0094837300011088.
Bütschli, O., 1910, Vorlesungen über vergleichende Anatomie. 1. Lieferung. Einleitung; Vergleichende Anatomie der Protozoen; Integument und Skelet der Metazoen: Leipzig, Engelmann, 401 p.
Capa, M., and Hutchings, P., 2021, Annelid diversity: historical overview and future perspectives: Diversity, v. 13, n. 129, https://doi.org/10.3390/d13030129.
Carbone, C.A., Narbonne, G.M, Macdonald, F.A., and Boag, T.H., 2015, New Ediacaran fossils from the uppermost Blueflower Formation, northwest Canada: disentangling biostratigraphy and paleoecology: Journal of Paleontology, v. 89, p. 281–291.
Chai, S., Wu, Y., and Hua, H., 2021, Potential index fossils for the Terminal Stage of the Ediacaran System: Journal of Asian Earth Sciences, v. 218, n. 104885.
Chang, S., Feng, Q., Clausen, S., and Zhang, L., 2017, Sponge spicules from the lower Cambrian in the Yanjiahe Formation, South China: the earliest biomineralizing sponge record: Palaeogeography, Palaeoclimatology, Palaeoecology, v. 474, 36–44.
Chen, H., Parry, L.A., Vinther, J., Zhai, D., Hou, X., and Ma, X., 2020, A Cambrian crown annelid reconciles phylogenomics and the fossil record: Nature, v. 583, p. 249–252.
Chen, M.E., Chen, Y.Y., and Qian, Y., 1981, Some tubular fossils from Sinian–lower Cambrian boundary sequences, Yangtze Gorges: Bulletin of the Tianjin Institute of Geology and Mineral Resources, v. 3, p. 117–124.
Chen, Z., Zhou, C., Xiao, S., Wang, W., Guan, C., Hua, H., and Yuan, X., 2014, New Ediacara fossils preserved in marine limestone and their ecological implications: Scientific Reports, v. 4, n. 4180.
Cloud, P.E., and Nelson, C.A., 1966, Phanerozoic–Cryptozoic and related transitions: new evidence: Science, v. 154, p. 766–770.
Cohen, P.A., Bradley, A., Knoll, A.H., Grotzinger, J.P., Jensen, S., et al., 2009, Tubular compression fossils from the Ediacaran Nama Group, Namibia: Journal of Paleontology, v. 83, p. 110–122.
Conway Morris, S., 1993, Ediacaran-like fossils in Cambrian Burgess Shale-type faunas of North America: Palaeontology, v. 36, p. 593–635.
Crimes, T.P., and Fedonkin, M.A., 1996, Biotic changes in platform communities across the Precambrian–Phanerozoic boundary: Revista Italiana di Paleontologia e Stratigrafia, v. 102, p. 317–332.
Crimes, T.P., and Germs, G.J.B., 1982, Trace fossils from the Nama Group (Precambrian–Cambrian) of Southwest Africa (Namibia): Journal of Paleontology, v. 56, p. 890–907.
Darroch, S.A.F., Sperling, E.A., Boag, T.H., Racicot, R.A., Mason, S.J., et al., 2015, Biotic replacement and mass extinction of the Ediacara biota: Proceedings of the Royal Society B, v. 282, n. 20151003.
Darroch, S.A.F., Boag, T.H., Racicot, R.A., Tweedt, S., Mason, S.J., Erwin, D.H., and Laflamme, M., 2016, A mixed Ediacaran–metazoan assemblage from the Zaris sub-basin, Namibia: Palaeogeography, Palaeoclimatology, Palaeoecology, v. 459, 198–208.
Darroch, S.A.F., Smith, E.F., Laflamme, M., and Erwin, D.H., 2018, Ediacaran extinction and Cambrian explosion: Trends in Ecology and Evolution, v. 33, p. 653–663.
Darroch, S.A.F., Cribb, A.T., Buatois, L.A., Germs, G.J.B., Kenchington, C.G., et al., 2021, The trace fossil record of the Nama Group, Namibia: exploring the terminal Ediacaran roots of the Cambrian explosion: Earth-Science Reviews, v. 212, n. 103435.
Darroch, S.A.F., Gibson, B.M., Syversen, M., Rahman, I.A., Racicot, R.A., Dunn, F.S., Gutarra, S., Schindler, E., Wehrmann, A., and Laflamme, M., 2022, The life and times of *Pteridinium simplex*: Paleobiology, v. 48, p. 527–556.
Debrenne, F., Zhuravlev, A.Yu., and Kruse, P.D., 2012, Part E, Revised, Volume 4, Chapter 18: General features of the Archaeocyatha: Treatise Online, v. 38, https://doi.org/10.17161/to.v0i0.4260.
Dececchi, T.A., Narbonne, G.M., Greentree, C., and Laflamme, M., 2017, Relating Ediacaran fronds: Paleobiology, v. 43, p. 171–180.
Droser, M.L., Tarhan, L.G., and Gehling, J.G., 2017, The rise of animals in a changing environment: global ecological innovation in the late Ediacaran: Annual Review of Earth and Planetary Sciences, v. 45, p. 593–617.
Droser, M.L., Gehling, J.G., Tarhan, L.G., Evans, S.D., Hall, C.M.S., et al., 2019, Piecing together the puzzle of the Ediacara Biota: excavation and reconstruction at the Ediacara National Heritage site Nilpena (South Australia): Palaeogeography, Palaeoclimatology, Palaeoecology, v. 513, p. 132–145.
Dunn, F.S., Kenchington, G.C., Parry, L.A., Clark, J.W., Kendall, R.S., and Wilby, P.R., 2022, A crown-group cnidarian from the Ediacaran of Charnwood Forest, UK: Nature Ecology and Evolution, v. 6. p. 1095–1104.
Ekdale, A.K., and Bromley, R.G., 1982, Trace fossils and ichnofabric in the Kjølby Gaard Marl, uppermost Cretaceous, Denmark: Bulletin of the Geological Society of Denmark, v. 31, p. 107–119.
Elliott, D.A., Vickers-Rich, P., Trusler, P., and Hall, M., 2011, New evidence on the taphonomic context of the Ediacaran *Pteridinium*: Acta Palaeontologica Polonica, v. 56, p. 641–650.
Elliott, D.A., Trusler, P.W., Narbonne, G.M., Vickers-Rich, P., Morton, N., Hall, M., Hoffmann, K.H., and Schneider, G.I.C., 2016, *Ernietta* from the late Ediacaran Nama Group, Namibia: Journal of Paleontology, v. 90, p. 1017–1026.
Emmons, E., 1844, The Taconic System; Based on Observations in New York, Massachusetts, Maine, Vermont and Rhode Island: Albany, Carroll and Cook, 68 p.
Erpenbeck, D., Sutcliffe, P., Cook, S. de C., Dietzel, A., Maldonado, M., van Soest, R.W.M., Hooper, J.N.A., and Wörheide, G., 2012, Horny sponges and their affairs: on the phylogenetic relationships of keratose sponges: Molecular Phylogenetics and Evolution, v. 63, p. 809–816.
Erwin, D.H., Laflamme, M., Tweedt, S.M., Sperling, E.A., Pisani, D., and Peterson, K.J., 2011, The Cambrian conundrum: early divergence and later ecological success in the early history of animals: Science, v. 334, p. 1091–1097.
Evans, S.D., Tu, C., Rizzo, A., Surprenant, R.L., Boan, P.C., McCandless, H., Marshall, N., Xiao, S., and Droser, M.L., 2022, Environmental drivers of the first major animal extinction across the Ediacaran White Sea–Nama transition: Proceedings of the National Academy of Sciences, v. 119, n. e2207475119.

https://doi.org/10.1017/jpa.2023.81 Published online by Cambridge University Press

Fedonkin, M.A., 1976, [Traces of multicellular organisms from the Valdai series]: Izvestia Akademii Nauk SSSR, Seriya Geologicheskaya, v. 4, p. 128–132. [in Russian]
Fedonkin, M.A., 1981, [Vendian White Sea biota (Precambrian non-skeletal faunas of the northern Russian Platform)]: Trudy Geologicheskogo Instituta Akademii Nauk SSSR, v. 342, 99 p. [in Russian]
Fedonkin, M.A., 1983, [Non-skeletal fauna of Podolia (Dniestr Valley)], *in* Velikanov, V.A., Aseeva, E.A., and Fedonkin, M.A., [Vendian of the Ukraine]: Kyiv, Naukova Dumka, p. 128–139. [in Russian]
Fedonkin, M.A., 1985, [Systematic description of Vendian Metazoa], *in* Sokolov, B.S. and Iwanowski, eds., [The Vendian System, Vol. 1 Paleontology]: Moscow, Nauka, p. 70–112. [in Russian]
Fedonkin, M.A., 1992, Vendian faunas and the early evolution of the Metazoa, *in* Lipps, J.H., and Signor, P.W., eds., Origin and Early Evolution of the Metazoa: New York, Plenum Press, p. 87–129.
Fedonkin, M.A., Gehling, J.G., Grey, K., Narbonne, G.M., and Vickers-Rich, P., 2007, The Rise of Animals, Evolution and Diversification of the Animal Kingdom: Baltimore, Johns Hopkins University Press, 326 p.
Fenton, C.L., and Fenton, M.A., 1937, *Archaeonassa*: Cambrian snail trails and burrows: American Midland Naturalist, v. 18, p. 454–458.
Fu, S., 1991, Funktion, Verhalten und Entstellung fucoider und lophoctenider Lebenspuren: Courier Forschungsinstitut Senckenberg, v. 135, p. 1–79.
Gehling, J.G., and Droser, M.L., 2013, How well do fossil assemblages of the Ediacara biota tell time?: Geology, v. 41, p. 447–450.
Gehling, J.G., and Narbonne, G.M., 2007, Spindle-shaped Ediacara fossils from the Mistaken Point assemblage, Avalon Zone, Newfoundland: Canadian Journal of Earth Sciences, v. 44, p. 367–387.
Gehling, J.G., and Runnegar, B., 2022, *Phyllozoon* and *Aulozoon*: key components of a novel Ediacaran death assemblage in Bathtub Gorge, Heysen Range, South Australia: Geological Magazine, v. 159, p. 1134–1147.
Georgieva, M.N., Little, C.T.S., Watson, J.S., Sephton, M.A., Ball, A.D., and Glover, A.G., 2019, Identification of fossil worm tubes from Phanerozoic hydrothermal vents and cold seeps: Journal of Systematic Palaeontology, v. 17, p. 287–329.
Georgieva, M.N., Little, C.T.S., Maslennikov, V.V., Glover, A.G., Ayupova, N.R., and Herrington, R.J., 2021, The history of life at hydrothermal vents: Earth-Science Reviews, v. 217, n. 103602.
Germs, G.J.B., 1968, Discovery of a new fossil in the Nama System, South West Africa: Nature, v. 219, p. 53–54.
Germs, G.J.B., 1972a, The stratigraphy and paleontology of the lower Nama Group, South West Africa: University of Cape Town, Department of Geology, Chamber of Mines Precambrian Research Unit Bulletin, v.12, 250 p.
Germs, G.J.B., 1972b, New shelly fossils from the Nama Group, South West Africa: American Journal of Science, v. 272, p. 752–761.
Germs, G.J.B., 1972c, Trace fossils from the Nama Group, South-West Africa: Journal of Paleontology, v. 46, p. 864–870.
Germs, G.J.B., 1973, A reinterpretation of *Rangea schneiderhoehni* and the discovery of a related new fossil from the Nama Group, South West Africa: Lethaia, v. 6, p. 1–10.
Germs, G.J.B., 1974, The Nama Group in South West Africa and its relationship to the Pan-African geosyncline: Journal of Geology, v. 82, p. 301–317.
Germs, G.J.B., 1983, Implications of a sedimentary facies and depositional environmental analysis of the Nama Group in South West Africa/Namibia: Special Publications of the Geological Society of South Africa, v. 11, p. 89–114.
Germs, G.J.B., 1995, The Neoproterozoic of southwestern Africa, with emphasis on platform stratigraphy and paleontology: Precambrian Research, v. 73, p. 137–151.
Germs, G.J.B., and Gresse, P.G., 1991, The foreland basin of the Damara and Gariep orogens in Namaqualand and southern Namibia: stratigraphic correlations and basin dynamics: South African Journal of Geology, v. 94, p. 159–169.
Getty, P.R., McCarthy, T.D., Hsieh, S., and Bush, A.M., 2016, A new reconstruction of continental *Treptichnus* based on exceptionally preserved material from the Jurassic of Massachusetts: Journal of Paleontology, v. 90, p. 269–278.
Gibson, B.M., Rahman, I.A., Maloney, K.M., Racicot, R.A., Mocke, H., Laflamme, M., and Darroch, S.A.F., 2019, Gregarious suspension feeding in a modular Ediacaran organism: Science Advances, v. 5, n. eaaw0260.
Gibson, G.G., and Teeter, S.A., 2011, Significance of Ediacaran fossils from Stanly County, NC: geological and pedological [*sic*]: Southeastern Section Annual Meeting, Geological Society of America, Abstracts, https://gsa.confex.com/gsa/2011SE/webprogram/Paper184217.html.
Gibson, G.G., Teeter, S.A., and Fedonkin, M.A., 1984, Ediacarian fossils from the Carolina slate belt, Stanly County, North Carolina: Geology, v. 12, p. 387–390.
Glaessner, M.F., 1963, Zur Kenntnis der Nama-Fossilien Südwest-Afrikas: Annalen des Naturhistorischen Museums in Wien, v. 66, p. 113–120.
Glaessner, M.F., 1978, Re-examination of *Archaeichnium*, a fossil from the Nama Group: Annals of the South African Museum, v. 74, p. 335–342.
Glaessner, M.F., 1979a, An echurid worm from the late Precambrian: Lethaia, v. 12, p. 121–124.
Glaessner, M.F., 1979b, Precambrian, *in* Robison, R.A., and Teichert, C., eds., Treatise on Invertebrate Paleontology, Part A, Introduction Fossilization (Taphonomy), Biogeography and Biostratigraphy: Boulder, Colorado, and Lawrence, Kansas, Geological Society of America and University of Kansas, p. A79–A118.
Glaessner, M.F., and Wade, M., 1966, The late Precambrian fossils from Ediacara, South Australia: Palaeontology, v. 9, p. 599–628.
Goffredi, S.K., Tilic, E., Mullin, S.W., Dawson, K.S., Keller, A., et al., 2020, Methanotrophic bacterial symbionts fuel dense populations of deep-sea feather duster worms (Sabellida, Annelida) and extend the spatial influence of methane seepage: Science Advances, v. 6, n. eaay8562.
Grant, R.E., 1836, Animal Kingdom, *in* Todd, R.B., ed., The Cyclopaedia of Anatomy and Physiology, Volume 1: London, Sherwood, Gilbert, and Piper, 183 p.
Grant, S.W.F., 1990, Shell structure and distribution of *Cloudina*, a potential index fossil for the terminal Proterozoic: American Journal of Science, v. 290-A, p. 261–294.
Gravestock, D.I., 1984, Archaeocyatha from lower parts of the lower Cambrian carbonate sequence in South Australia: Association of Australasian Palaeontologists Memoir, v. 2, 139 p.
Grazhdankin, D., 2004, Patterns of distribution in the Ediacaran biotas: facies versus biogeography and evolution: Paleobiology, v. 30., p. 203–221.
Grazhdankin, D., and Seilacher, A., 2002, Underground Vendobionta from Namibia: Palaeontology, v. 45, p. 57–78.
Grazhdankin, D., and Seilacher, A., 2005, A re-examination of the Nama-type Vendian organism *Rangea schneiderhoehni*: Geological Magazine, v. 142, p. 571–582.
Grotzinger, J.P., Bowring, S.A., Saylor, B.Z., and Kaufman, A.J., 1995, Biostratigraphic and geochronologic constraints on early animal evolution: Science, v. 270, p. 598–604.
Grotzinger, J.P., Watters, W.A., and Knoll, A.H., 2000, Calcified metazoans in thrombolite–stromatolite reefs of the terminal Proterozoic Nama Group, Namibia: Paleobiology, v. 26, p. 334–359.
Grotzinger, J.P., Adams, E.W., and Schröder, S., 2005, Microbial-metazoan reefs of the terminal Proterozoic Nama Group (c. 550–543 Ma), Namibia: Geological Magazine, v. 142, p. 499–517.
Groves, L.T., and Squires, R.L., 2023, LouElla Rankin Saul (1927–2021): her remarkable career and numerous significant contributions to Cretaceous and Paleogene molluscan paleontology: The Nautilus, v. 137, p. 63–78.
Gürich, G., 1930a, Die bislang ältesten Spuren von Organismen in Südafrika: Comptes Rendus 15th International Geological Congress South Africa 1929, p. 670–680.
Gürich, G., 1930b, Über den Kuibis-Quartzit in Südwest-afrika: Zeitschrift der Deutschen Geologischen Gesellschaft, v. 82, p. 637.
Gürich, G., 1933, Die Kuibis-Fossilien der Nama-Formation von Südwestafrika: Paläontologische Zeitschrift, v. 15, p. 137–154.
Hagadorn, J.W., and Waggoner, B.M., 2000, Ediacaran fossils from the southwestern Great Basin, United States: Journal of Paleontology, v. 74, p. 349–359.
Hagadorn, J.W., Fedo, C.M., and Waggoner, B.M., 2000, Early Cambrian Ediacara-type fossils from California: Journal of Paleontology, v. 74, p. 731–740.
Hahn, G., and Pflug, H.D., 1985a, Polypenartige Organismen aus dem Jung-Präkambrium (Nama-Gruppe) von Namibia: Geologica et Palaeontologica, v. 19, p. 1–13.
Hahn, G., and Pflug, H.D., 1985b, Die Cloudinidae n. fam., Kalk-Röhren aus dem Vendium und Unter-Kambrium: Senckenbergiana Lethaea, v. 65, p. 413–431.
Hahn, G., and Pflug, H.D., 1988, Zweischalige Organismen aus dem Jung-Präkambrium (Vendium) von Namibia (SW-Afrika): Geologica et Palaeontologica, v. 22, p. 1–19.
Hall, C.M.S., Droser, M.L., Clites, E.C., and Gehling, J.G., 2020, The short-lived but successful tri-radial body plan: a view from the Ediacaran of Australia: Australian Journal of Earth Sciences, v. 67, p. 885–895.
Hall, J.G., Smith, E.F., Tamura, N., Fakra, S.C., and Bosak, T., 2020, Preservation of erniettomorph fossils in clay-rich siliciclastic deposits from the Ediacaran Wood Canyon Formation, Nevada: Interface Focus, v. 10, n. 20200012.
Hall, M., Kaufman, A.J., Vickers-Rich, P., Ivantsov, A., Trusler, P., et al., 2013, Stratigraphy, palaeontology and geochemistry of the late Neoproterozoic Aar Member, southwest Namibia: reflecting environmental controls on Ediacara fossil preservation during the terminal Proterozoic in African Gondwana: Precambrian Research, v. 238, p. 214–232.
Han, Y., and Pickerill, R.K., 1995, Taxonomic review of the ichnogenus *Helminthopsis* Heer 1877 with a statistical analysis of selected ichnospecies: Ichnos: An International Journal of Plant and Animal Traces, v. 4, p. 83–118.

https://doi.org/10.1017/jpa.2023.81 Published online by Cambridge University Press

Haughton, S.H., 1960, An archaeocyathid from the Nama System: Transactions of the Royal Society of South Africa, v. 36, p. 57–59.
Heer, O., 1877, Flora fossilis Helvetiae: Die vorweltliche Hora der Schweiz: Zürich, J. Wurste, 182 p.
Hertweck, G., Wehrmann, A., and Liebezeit, G., 2007, Bioturbation structures of polychaetes in modern shallow marine environments and their analogues to *Chondrites* group traces: Palaeogeography, Palaeoclimatology, Palaeoecology, v. 245, p. 382–389.
Hilário, A., Capa, M., Dahlgren, T.G., Halanych, K.M., Little, C.T.S., Thornhill, D.J., Verna, C., and Glover, A.G., 2011, New perspectives on the ecology and evolution of siboglinid tubeworms: PLoS ONE, v. 6, n. e16309.
Hill, D., 1965, Archaeocyatha from Antarctica and a review of the phylum: Trans-Antarctic Expedition Scientific Reports, v. 10, 151 p.
Hodgin, E.B., Nelson, L.L., Wall, C.J., Barron-Diaz, A.J., Webb, L.C., Schmitz, M.D., Fike, D.A., Hagadorn, J.W., and Smith, E.F., 2021, A link between rift-related volcanism and end-Ediacaran extinction? Integrated chemostratigraphy, biostratigraphy, and U–Pb geochronology from Sonora, Mexico: Geology, v. 49, p. 115–119.
Hofmann, H.J., and Mountjoy, E.W., 2010, Ediacaran body and trace fossils in Miette Group (Windermere Supergroup) near Salient Mountain, British Columbia: Canadian Journal of Earth Sciences, v. 47, p. 1305–1325.
Holmes, J.D., and Budd, G.E., 2022, Reassessing a cryptic history of early trilobite evolution: Communications Biology, v. 5, n. 1177.
Horodyski, R.H., Gehling, J.G., Jensen, S., and Runnegar, B., 1994, Ediacaran fauna and earliest Cambrian trace fossils in a single parasequence set, southern Nevada: Geological Society of America, Cordilleran Section, Abstracts with Programs, v. 26, p. 260.
Hoyal Cuthill, J.F., 2022, Ediacaran survivors in the Cambrian: suspicions, denials and a smoking gun: Geological Magazine, v. 159, p. 1210–1219.
Hoyal Cuthill, J.F, and Han, J. 2018, Cambrian petalonamid *Stromatoveris* phylogenetically links Ediacaran biota to later animals: Palaeontology, v. 61, p. 813–823.
Ivanov, A.V., 1954, New Pogonophora from far eastern seas: Systematic Zoology, v. 3, p. 69–80.
Ivanov, A.V., 1963, Pogonophora: New York, Academic Press, 479 p.
Ivantsov, A.Yu., 2017, Finds of Ediacaran-type fossils in Vendian deposits of the Yudoma Group, eastern Siberia: Doklady Earth Sciences, v. 472, p. 143–146.
Ivantsov, A.Yu., 2018, Vendian macrofossils of the Yudoma Group, southeast of the Siberian Platform: Paleontological Journal, v. 52, p. 1335–1346.
Ivantsov, A.Yu., and Fedonkin, M.A., 2002, Conulariid-like fossil from the Vendian of Russia: a metazoan clade across the Proterozoic/Palaeozoic boundary: Palaeontology, v. 45, p. 1219–1229.
Ivantsov, A.Yu., and Grazhdankin, D.V., 1997, A new representative of the Petalonamae from the upper Vendian of the Arkhangelsk region: Paleontological Journal, v. 31, p. 1–16.
Ivantsov, A.Yu., and Zakrevskava, M.A., 2022, *Dickinsonia costata* of the Winter Mountains: features of morphology and ontogenesis: Precambrian Research, v. 379, n. 106788.
Ivantsov, A.Yu., Narbonne, G.M., Trusler, P.W., Greentree, C., and Vickers-Rich, P., 2016, Elucidating *Ernietta*: new insights from exceptional specimens in the Ediacaran of Namibia: Lethaia, v. 49, p. 540–554.
Ivantsov, A.Yu., Vickers-Rich, P., Zakrevskava, M.A., and Hall, M., 2019, Conical thecae of Precambrian macroorganisms: Paleontological Journal, v. 53, p. 1134–1146.
Jell, P.A., 1980, Earliest known bivalve on Earth—a new early Cambrian genus from South Australia: Alcheringa, v. 4, p. 233–239.
Jenkins, R.J.F., 1985, The enigmatic Ediacaran (late Precambrian) genus *Rangea* and related forms: Paleobiology, v. 11, p. 336–355.
Jenkins, R.J.F., 1995, The problems and potential of using animal fossils and trace fossils in terminal Proterozoic biostratigraphy: Precambrian Research, v. 73, p. 51–69.
Jenkins, R.J.F., and Gehling, J.G., 1978, A review of frond-like fossils of the Ediacara assemblage: Records of the South Australian Museum, v. 17, p. 347–359.
Jenkins, R.J.F., Plummer, P.S., and Moriarty, K.C., 1981, Late Precambrian pseudofossils from the Flinders Ranges, South Australia: Transactions of the Royal Society of South Australia, v. 105, p. 67–83.
Jensen, S., 1997, Trace fossils from the lower Cambrian Mickwitzia sandstone, south-central Sweden: Fossils and Strata, v. 42, 110 p.
Jensen, S., 2003, The Proterozoic and earliest Cambrian trace fossil record: patterns, problems and perspectives: Integrative and Comparative Biology, v. 43, p. 219–228.
Jensen, S., and Runnegar, B., 2005, A complex trace fossil from the Spitskop Member (terminal Ediacaran–?lower Cambrian) of southern Namibia: Geological Magazine, v. 142, p. 561–569.
Jensen, S., Gehling, J.G., and Droser, M.L., 1998, Ediacara-type fossils in Cambrian sediments: Nature, v. 393, p. 567–569.
Jensen, S., Saylor, B.Z., Gehling, J.G., and Germs, G.J.B., 2000, Complex trace fossils from the terminal Proterozoic of Namibia: Geology, v. 28, p. 143–146.
Jensen, S., Högström, A.E.S., Almond, J., Taylor, W.L., Meinhold, G., Høybergt, M., Ebbestad, J.O.R., Agić, H., and Palacois, T., 2018, Scratch circles from the Ediacaran and Cambrian of Arctic Norway and southern Africa, with a review of scratch circle occurrences: Bulletin of Geosciences, v. 93, p. 287–304.
Johnson, E.L., Phillios, G., and Allen, C.M., 2016, Ediacaran–Cambrian basin evolution in the Koonenberry Belt (eastern Australia): implications for the geodynamics of the Delamerian Orogen: Gondwana Research, v. 37, p. 266–284.
Karaseva, N.P., Rimskaya-Korsakova, N.N., Smirnov, R.V., Udalov, A.A., Mokievsky, V.O., Gantsevich, M.M., and Malakhov, V.V., 2022, Distribution of gutless siboglinid worms (Annelida, Siboglinidae) in Russian Arctic seas in relation to gas potential: Diversity, v. 14, n. 1061.
Kaufman, A.J., Hayes, J.H., Knoll, A.H., and Germs, G.J.B., 1991, Isotopic compositions of carbonates and organic carbon from upper Proterozoic successions in Namibia: stratigraphic variation and the effects of diagenesis and metamorphism: Precambrian Research, v. 49, p. 301–327.
Kaźmierczak, J., and Kremer, B., 2022, Archaeocyaths: alternatively explained as consortia of siphonous algae and cyanobacteria-like microbes in shallow Cambrian seas: Palaeoworld, v. 31, p. 218–238.
Keller, B.M., and Fedonkin, M.A., 1977, New organic fossil finds in the Precambrian Valday series along the Syuz'ma River: International Geology Review, v. 19, p. 924–930.
Keller, B.M., Menner, V.V., Stepanov, V.A., and Chumakov, N.M., 1974, [New findings of Metazoa in the Vendomian of the Russian Platform]: Izvestiya Akademii Nauk SSSR, Seriya Geologicheskaya, v. 12, p. 16–21. [in Russian]
Knoll, A.H., 2003, Life on a young planet: the first three billion years of evolution on Earth: Princeton, N.J., Princeton University Press, 277 p.
Książkiewicz, M., 1977, Trace fossils in the flysch of the Polish Carpathians: Palaeontologia Polonica, v. 36, 208 p.
Landing, E., 2012, The great American carbonate bank in eastern Laurentia: its births, deaths, and linkage to paleooceanic oxygenation (early Cambrian–Late Ordovician): American Association of Petroleum Geologists Memoir, v. 98, p. 45–492.
Landing, E., Geyer, G., Jirkov, I.A., and Schiaparelli, S., 2021, Lophotrochozoa in the Cambrian evolutionary radiation and the *Pelagiella* problem: Papers in Palaeontology, v. 7, p. 2227–2244.
Linnaeus, C., 1758, Systema naturæ per regna tria naturæ, secundum classes, ordines, genera, species, cum characteribus, differentiis, synonymis, locis: Holmiae, Laurentii Salvii.
Linnemann, U., Ovtcharova, M., Schaltegger, U., Gärtner, A., Hautmann, M., et al., 2019, New high-resolution age data from the Ediacaran–Cambrian boundary indicate rapid, ecologically driven onset of the Cambrian explosion: Terra Nova, v. 31, p. 49–58.
Little, C.T.S., Maslennikov, V.V, Morris, N.J., and Gubanov, A.P., 1999, Two Palaeozoic hydrothermal vent communities from the southern Ural Mountains, Russia: Palaeontology, v. 42, p. 1043–1078.
Luo, C., Zhao, F., and Zeng, H., 2020, The first report of a vauxiid sponge from the Cambrian Chengjiang Biota: Journal of Paleontology, v. 94, p. 28–33.
Luo, C., Yang, A., Zhuravlev, A.Yu., and Reitner, J., 2021, Vauxiids as descendants of archaeocyaths: a hypothesis: Lethaia, v. 54, p. 700–710.
Luo, H., Tao, Y., and Gao, S., 1994, Early Cambrian trace fossils near Kunming, Yunnan: Acta Palaeontologica Sinica, v. 33, p. 666–685.
Luo, H., Hu, S., Chen, L., Zhang, S., and Tao, Y., 1999, Early Cambrian Chengjiang Fauna from Kunming Region, China: Kunming, Yunnan Science and Technology Press, 129 p.
MacGabhann, B.A., Schiffbauer, J.D., Hagadorn, J.W., Van Roy, P., Lynch, E.P., Morrison, L., and Murray, J., 2019, Resolution of the earliest metazoan record: differential taphonomy of Ediacaran and Paleozoic fossil molds and casts: Palaeogeography, Palaeoclimatology, Palaeoecology, v. 513, p. 146–165.
Mángano, M.G., and Buatois, L.A., 2014, Decoupling of body-plan diversification and ecological structuring during the Ediacaran–Cambrian transition: evolutionary and geobiological feedbacks: Proceedings of the Royal Society B, v. 281, n. 20140038.
Mángano, M.G., and Buatois, L.A., 2020, The rise and early evolution of animals: where do we stand from a trace-fossil perspective?: Interface Focus, v. 10, n. 20190103.
Mángano, M.G., Buatois, L.A., West, R.R., and Maples, C.G., 2002, Ichnology of a Pennsylvanian equatorial tidal flat—the Stull Shale Member at Waverly, eastern Kansas: Kansas Geological Survey Bulletin, v. 245, 133 p.
Maloney, K.M., Boag, T.H., Facciol, A.J., Gibson, B.M., Cribb, A., Koester, B.E., Kenchington, C.G., Racicot, R.A., Darroch, S.A.F., and Laflamme, M., 2020, Paleoenvironmental analysis of *Ernietta*-bearing Ediacaran

https://doi.org/10.1017/jpa.2023.81 Published online by Cambridge University Press

deposits in southern Namibia: Palaeogeography, Palaeoclimatology, Palaeoecology, v. 556, n. 109884.
Männil, R.M., 1966, [On vertical burrows in the Ordovician limestones of Baltic], *in* Hecker, R.F., ed., Organizm i sreda v geologischeskom proshlom: Moscow, Nauka, p. 200–207. [in Russian]
Maples, C.G., and Archer, A.W., 1987, Redescription of Early Pennsylvanian trace-fossil holotypes from the nonmarine Hindostan Whetstone Beds of Indiana: Journal of Paleontology, v. 61, p. 890–897.
Marusin, V.V., and Kuper, K.E., 2020, Complex tunnel systems of early Fortunian macroscopic endobenthos in the Ediacaran–Cambrian transitional strata of the Olenek Uplift (NE Siberian Platform): Precambrian Research v. 340, n. 105627.
McFadden, C.S., Quattrini, A.M., Brugler, M.R., Cowman, P.F., Dueñas, L.F., Kitahara, M.V., Paz-García, D.A., Reimer, J.D., and Rodríguez, E., 2021, Phylogenomics, origin, and diversification of anthozoans (phylum Cnidaria): Systematic Biology, v. 16, p. 635–647.
McMenamin, M.A.S., 1998, The Garden of Ediacara: Discovering the First Complex Life: New York, Columbia University Press, 295 p.
McMenamin, M.A.S., and Weaver, P.G., 2002, Proterozoic–Cambrian paleobiogeography of the Carolina Terrane: Southeastern Geology, v. 41, p. 119–128.
Meinhold, G., Willbold, M., Karius, V., Jensen, S., Agić, H., Ebbestad, J.O.R., Palacios, T., Högström, A.E.S., Høyberget, M., and Taylor, W.L., 2022, Rare earth elements and neodymium and strontium isotopic constraints on provenance switch and post-depositional alteration of fossiliferous Ediacaran and lowermost Cambrian strata from Arctic Norway: Precambrian Research, v. 381, n. 106845.
Meyer, M., 2010, *How plastic is Vendobionta morphology? A geometric morphometric study of two groups of* Pteridinium *from the latest Neoproterozoic* [M.Sc. thesis]: Tampa, University of South Florida, 50 p.
Meyer, M., and Xiao, S., 2010, How synthetic is Vendobionta morphology? A geometric morphometric study of *Pteridinium* from the latest Neoproterozoic: Journal of Earth Science, v. 21, p. 6–8.
Meyer, M., Elliott, D., Wood, A.D., Polys, N.F., Colbert, M., et al., 2014a, Three-dimensional microCT analysis of the Ediacara fossil *Pteridinium simplex* sheds new light on its ecology and phylogenetic affinity: Precambrian Research, v. 249, p. 79–87.
Meyer, M., Elliott, D., Schiffbauer, J.D., Hall, M., Hoffman, K.-H., Schneider, G., Vickers-Rich, P., and Xiao, S., 2014b, Taphonomy of the Ediacaran fossil *Pteridinium simplex* preserved three-dimensionally in mass flow deposits, Nama Group, Namibia: Journal of Paleontology, v. 88, p. 240–252.
Mghazli, K., Lazreq, N., Geyer, G., Landing, E., Boumehdi, M.A., and Youbi, N., 2023, Cambrian microfossils from the High Atlas, Morocco: taxonomic, biostratigraphic, palaeobiogeographic, and depositional significance of the Brèche à *Micmacca* limestone beds: Journal of African Earth Sciences, v. 197, n. 104751.
Miller, S.A., 1889, North American Geology and Paleontology for the Use of Amateurs, Students and Scientists: Cincinnati, Ohio, Western Methodist Book Concern, 664 p.
Mitchell, E.G., Evans, S.D., Chen, Z., and Xiao, S., 2022, A new approach for investigating spatial relationships of ichnofossils: a case study of Ediacaran–Cambrian animal traces: Paleobiology, v. 48, p. 557–575.
Moczydłowska, M., Westall, F., and Foucher, F., 2014, Microstructure and biogeochemistry of the organically preserved Ediacaran metazoan *Sabellidites*: Journal of Paleontology, v. 88, p. 224–239.
Monastersky, R., and Mazzatenta, O.L., 1998, Life grows up: National Geographic Magazine, v. 193, no. 4, p. 100–115.
Myrow, P.M., 1992, Pot and gutter casts from the Chapel Island Formation, southeast Newfoundland: Journal of Sedimentary Petrology, v. 62, p. 992–1007.
Narbonne, G.M., 1998, The Ediacara biota: a terminal Neoproterozoic experiment in the evolution of life: GSA Today, v. 8, no. 2, p. 1–6.
Narbonne, G.M., 2005, The Ediacara biota: Neoproterozoic origin of animals and their ecosystems: Annual Review of Earth and Planetary Sciences, v. 33, p. 421–442.
Narbonne, G.M., and Aitken, J.D., 1990, Ediacaran fossils from the Sekwi Brook area, Mackenzie Mountains, northwestern Canada: Palaeontology, v. 33, p. 945–980.
Narbonne, G.M., Saylor, B.Z., and Grotzinger, J.P., 1997, The youngest Ediacaran fossils from southern Africa: Journal of Paleontology, v. 71, p. 953–967.
Nelson, L.L., Ramezani, J., Almond, J.E., Darroch, S.A.F., Taylor, W.L., Brenner, D.C., Furey, R.P., Turner, M., and Smith, E.F., 2022, Pushing the boundary: a calibrated Ediacaran–Cambrian stratigraphic record from the Nama Group in northwestern Republic of South Africa: Earth and Planetary Science Letters, v. 580, n. 117396.
Nelson, L.L., Crowley, J.L., Smith, E.F., Schwartz, D.M., Hodgin, E.B., and Schmitz, M.D., 2023, Cambrian explosion condensed: high-precision geochronology of the lower Wood Canyon Formation, Nevada: Proceedings of the National Academy of Sciences, v. 120, n. e2301478120.
Okulitch, V.J., 1935, Cyathospongia—a new class of Porifera to include the Archaeocyathinae: Royal Society of Canada, Transactions, series 3, section 4, v. 29, p. 75–106.
Orlowski, S., and Zylinska, A., 1996, Non-arthropod burrows from the middle and late Cambrian of the Holy Cross Mountains, Poland: Acta Palaeontologica Polonica, v. 41, p. 385–409.
Osgood, R.G., 1970, Trace fossils of the Cincinnati area: Palaeontographica Americana, v. 41, p. 281–444.
Palij, V.M., Posti, E., and Fedonkin, M.A., 1979, [Soft-bodied Metazoa and Vendian and early Cambrian trace fossils,] *in* Keller, B.M., and Rozanov, A.Y., eds., [Paleontology of Upper Precambrian and Cambrian deposits of the East European Platform]: Moscow, Nauka, p. 49–82. [in Russian]
Palij, V.M., Posti, E., and Fedonkin, M.A., 1983, Soft-bodied Metazoa and animal trace fossils in the Vendian and early Cambrian, *in* Urbanek, A., and Rozanov, A.Y., eds., Paleontology of Upper Precambrian and Cambrian Palaeontology of the East European Platform: Warsaw, Wydawnictwa Geologiczne, p. 56–94.
Parry, L.A., Boggiani, P.C., Condon, D.J., Garwood, R.J., Leme, J. de M., et al., 2017, Ichnological evidence for meiofaunal bilaterians from the terminal Ediacaran and earliest Cambrian of Brazil: Nature Ecology and Evolution, v. 1, p. 1455–1464.
Penny, A.M., Wood, R., Curtis, A., Bowyer, F., Tostevin, R., and Hoffman, K.-H., 2014, Ediacaran metazoan reefs from the Nama Group, Namibia: Science, v. 344, p. 1504–1506.
Pflug, H.D., 1966, Neue Fossilreste aus den Nama-Schichten in Südwest-Africa: Paläontologische Zeitschrift, v. 40, p. 14–25.
Pflug, H.D., 1970a, Zur Fauna der Nama-Schichten in Südwest-Afrika I, Pteridinia, Bau und systematische Zugehörigkeit: Palaeontographica Abt. A, v. 134, p. 226–262.
Pflug, H.D., 1970b, Zur Fauna der Nama-Schichten in Südwest-Afrika II. Rangeida, Bau und systematische Zugehörigkeit: Palaeontographica Abt. A, v. 135, p. 198–231.
Pflug, H.D., 1972, Zur Fauna der Nama-Schichten in Südwest-Afrika III. Erniettomorpha, Bau und Systematik: Palaeontographica Abt. A, v. 139, p. 134–170.
Pleijel, F., Dahlgren, T.G., and Rouse, G.W., 2009, Progress in systematics: from Siboglinidae to Pogonophora and Vestimentifera and back to Siboglinidae: Comptes Rendus Biologies, v. 332, p. 140–148.
Plese, B., Kenny, N.J., Rossi, M.E., Cárdenas, P., Schuster, A., Taboada, S., Koutsouveli, V., and Riesgo, A., 2021, Mitochondrial evolution in the Demospongiae (Porifera): phylogeny, divergence time, and genome biology: Molecular Phylogenetics and Evolution, v. 155, n. 107011.
Prantl, F., 1946, Dve zahadne zkameneliny (stopy) z vrstev chrustenickych – dB3: Rozpravy Ceske Akademie Ved a Umeni, Tfida II, v. 55, no. 3, p. 1–18.
Qiang, Y., Guo, J., Li, G., Song, Z., Peng, J., Sun, J., Han, J., and Zhang, Z., 2023, *Aldanella attleborensis* (Mollusca) from Cambrian Stage 2 of the Three Gorges Area and its stratigraphic implications: Biology, v. 12, n. 261.
Rayner, D.H., 1957, A problematical structure from the Ingletonian rocks, Yorkshire: Transactions of the Leeds Geological Association, v. 7, p. 34–42.
Reid, L.M., García-Bellido, D.C., Payne, J.L., Runnegar, B., and Gehling, J.G., 2017, Possible evidence of primary succession in a juvenile-dominated Ediacara fossil surface from the Flinders Ranges, South Australia: Palaeogeography, Palaeoclimatology, Palaeoecology, v. 476, p. 68–76.
Resser, C.E., and Howell, B.F., 1938, Lower Cambrian *Olenellus* zone of the Appalachians: Geological Society of America Bulletin, v. 49, p. 195–248.
Richter, R., 1955, Die ältesten Fossilien Süd-Afrikas: Senckenbergiana Lethaea, v. 36, p. 243–289.
Rigby, J.K., 1980, The new middle Cambrian sponge *Vauxia magna* from the Spence Shale of northern Utah and the taxonomic position of the Vauxiidae: Journal of Paleontology, v. 54, p. 234–240.
Rigby, J.K., 1986, Sponges of the Burgess shale (middle Cambrian), British Columbia: Palaeontographica Canadiana, v. 2, 105 p.
Rowland, S.M., 2001, Archaeocyaths—a history of phylogenetic interpretation: Journal of Paleontology, v. 75, p. 1065–1078.
Runnegar, B., 2022, Following the logic behind biological interpretations of the Ediacaran biotas: Geological Magazine, v. 159, 1093–1117.
Runnegar, B., and Fedonkin, M.A., 1992, Proterozoic metazoan body fossils, *in* Schopf, J.W., and Klein, C., eds., The Proterozoic Biosphere, A Multidisciplinary Study: Cambridge, Cambridge University Press, p. 369–388.
Runnegar, B., and Pojeta, J., 1992, The earliest bivalves and their Ordovician descendants: American Malacological Bulletin, v. 9, p. 117–122.
Šamánek, J., Vallon, L.H., Mikuláš, R., and Vachek, M., 2022, A glimpse into ancient food storage: sequestrichnia and associated nucleocave *Chondrites* from Eocene deep-sea deposits: Acta Palaeontologica Polonica, v. 67, p. 767–779.

Savrda, C.E., and Bottjer, D.J., 1987, The exaerobic zone, a new oxygen-deficient marine biofacies: Nature, v. 327, p. 54–56.
Saylor, B.Z., 1996, *Sequence stratigraphic and chemostratigraphic constraints on the evolution of the terminal Proterozoic to Cambrian Nama Basin, Namibia* [Ph.D. thesis]: Cambridge, Massachusetts, Massachusetts Institute of Technology, 358 p.
Saylor, B.Z., 2003, Sequence stratigraphy and carbonate–siliciclastic mixing in a terminal Proterozoic foreland basin, Urusis Formation, Nama Group, Namibia: Journal of Sedimentary Research, v. 73, p. 264–279.
Saylor, B.Z., and Grotzinger, J.P., 1996, Reconstruction of important Proterozoic–Cambrian exposures through the recognition of thrust deformation in the Nama Group of southern Namibia: Communications of the Geological Survey of Namibia, v. 11, p. 1–12.
Saylor, B.Z., Grotzinger, J.P., and Germs, G.J.B., 1995, Sequence stratigraphy and sedimentology of the Neoproterozoic Kuibis and Schwarzrand subgroups (Nama Group), southwestern Namibia: Precambrian Research, v. 73, p. 153–171.
Saylor, B.Z., Kaufman, A.J., Grotzinger, J.P., and Urban, F., 1998, A composite reference section for terminal Proterozoic strata of southern Namibia: Journal of Sedimentary Research, v. 68, p. 1223–1235.
Saylor, B.Z., Poling, J.M., and Huff, W.D., 2005, Stratigraphic and chemical correlation of volcanic ash beds in the terminal Proterozoic Nama Group, Namibia: Geological Magazine, v. 142, p. 519–538.
Schieber, J., and Wilson, R.D., 2021, Burrows without a trace—how meiofaunal bioturbation affects rock fabrics and leaves a record of meiobenthos activity in shales and mudstones: Paläontologische Zeitschrift, v. 95, p. 767–791.
Schiffbauer, J.D., Huntley, J.W., O'Neil, G.R., Darroch, S.A.F., Laflamme, M., and Cai, Y., 2016, The latest Ediacaran wormworld fauna: setting the ecological stage for the Cambrian Explosion: GSA Today, v. 26, p. 4–11.
Schiffbauer, J.D., Selly, T., Jacquet, S.M., Merz, R.A., Nelson, L.L., Strange, M.A., Cai, Y., and Smith, E.F., 2020, Discovery of bilaterian-type through-guts in cloudinomorphs from the terminal Ediacaran Period: Nature Communications, v. 11, n. 205.
Schmitz, M.D., 2012, Radiometric ages used in GTS 2012, *in* Gradstein, F.M., Ogg, J.G., Schmitz, M.D., and Ogg, G.M., eds., The Geologic Timescale 2012: Oxford, Elsevier, p. 1045–1082.
Schmitz, M.D., Singer, B.S., and Rooney, A.D., 2020, Radioisotope geochronology, *in* Gradstein, F.M., Ogg, J.G., Schmitz, M.D., and Ogg, G.M., eds., Geological Time Scale 2020: Amsterdam, Elsevier, p. 193–210.
Schneiderhöhn, H., 1920, Beiträge zur Kenntnis der Erzlagerstätten und der geologischen Verhältnisse des Otaviberglandes, Deutsch-Südwestafrika: Abhandlungen herausgegeben von der Senckenbergischen naturforschenden Gesellschaft, v. 37, p. 221–318.
Seilacher, A., 1955, Spuren und fazies im Unterkambrium, *in* Schindewolf, O.H., and Seilacher, A., eds., Beitrage zur Kenntnis des Kambriums in der Salt Range: Abhandlungen Akademie der Wissenschaften und der Literatur zu Mainz, Mathematisch-Naturwissenschaftliche Klasse, v. 10, p. 373–99.
Seilacher, A., 1992, Vendobionta and Psammocorallia: lost constructions of Precambrian evolution: Journal of the Geological Society, v. 149, p. 607–613.
Seilacher, A., 1997, Fossil Art, An Exhibition of the Geologisches Institut Tuebingen University, Germany: Drumheller, Royal Tyrrell Museum of Palaeontology, 64 p.
Seilacher, A., 2007, The nature of vendobionts: Geological Society London Special Publications, v. 286, p. 387–397.
Seilacher, A., 2008, Fossil Art, an Exhibition of the Geologisches Institut Tuebingen University, Germany: Laasby, CBM-publishing, 102 p.
Seilacher, A., Grazhdankin, D., and Legouta, A., 2003, Ediacara biota: the dawn of animal life in the shadow of giant protists: Paleontological Research, v. 7, p. 43–54.
Selly, T., Schiffbauer, J.D., Jacquet, S.M., Smith, E.F., Nelson, L.L., et al., 2020, A new cloudinid fossil assemblage from the terminal Ediacaran of Nevada, USA: Journal of Systematic Palaeontology, v. 18, p. 357–379.
Serezhnikova, E.A., 2014, Skeletogenesis in problematic late Proterozoic lower Metazoa: Paleontological Journal, v. 48, p. 1457–1472.
Shaler, N.S., and Foerste, A.F., 1888, Preliminary description of North Attleboro fossils: Bulletin of the Museum of Comparative Zoology at Harvard College, v. 16, p. 27–41.
Shi, X., Howard, R.J., Edgecombe, G.D., Hou, X., and Ma, X., 2022, *Tabelliscolex* (Cricocosmiidae: Palaeoscolecidomorpha) from the early Cambrian Chengjiang Biota and the evolution of seriation in Ecdysozoa: Journal of the Geological Society, v. 179, n. jgs2021-060.
Smith, E.F., Nelson, L.L., Strange, M.A., Eyster, A.E., Rowland, S.M., Schrag, D.P., and Macdonald, F.A., 2016, The end of the Ediacaran: two exceptionally preserved body fossil assemblages from Mt. Dunfee, Nevada: Geology, v. 44, p. 911–914.
Smith, E.F., Nelson, L.L., Tweedt, S.M., Zeng, H., and Workman, J.B., 2017, A cosmopolitan late Ediacaran biotic assemblage: new fossils from Nevada and Namibia support a global biostratigraphic link: Proceedings of the Royal Society B, v. 284, n. 20170934.
Smith, E.F., Nelson, L.L., O'Connell, N., Eyster, A., and Lonsdale, M.C., 2022, The Ediacaran–Cambrian transition in the southern Great Basin, United States: Geological Society of America Bulletin, v. 135, p. 1393–1414, https://doi.org/10.1130/B36401.1.
Smith, O.A., 1999, *Terminal Proterozoic Carbonate Platform Development: Stratigraphy and Sedimentology of the Kuibis Subgroup (ca. 550–548 Ma), Northern Nama Basin, Namibia* [M.Sc. thesis]: Cambridge, Massachusetts Institute of Technology, 132 p.
Sokolov, B.S., 1965, Drevnejshie otlozheniya rannego kembriya i sabelliditidy [The oldest early Cambrian deposits and sabelliditids]: Vsesoyuznyj simposium po paleontologii dokembriya i rannego kembriya, v. 25, no. 30, p. 78–92.
Sokolov, B.S., 1967, Drevneyshiye pognofory [The oldest Pogonophora]: Doklady Akademii Nauk SSSR, v. 177, p. 201–204.
Sokolov, B.S., 1976, [The organic world on the path of Phanerozoic differentiation]: Vestinik Akademii Nauk SSSR, v. 1, p. 126–143. [in Russian]
Sokolov, B.S., and Iwanowskii, A.B. (eds.), 1985, The Vendian System. Historic-Geological and Paleontological Basis. 1. Paleontology: Moscow, Nauka, 221 p. [in Russian]
Sprigg, R.C., 1947, Early Cambrian (?) jellyfishes from the Flinders Ranges, South Australia: Transactions of the Royal Society of South Australia, v. 71, p. 212–224.
Sprigg, R.C., 1949, Early Cambrian "jellyfishes" of Ediacara, South Australia and Mount John, Kimberley District, Western Australia: Transactions of the Royal Society of South Australia, v. 73, pp. 72–99.
St. Jean, J., 1973, A new Cambrian trilobite from the Piedmont of North Carolina: American Journal of Science, v. 273A, p. 196–216.
Stankovskiy, A.F., Verichov, Ye.M., Grib, V.P., and Dobeyko, I.P., 1983, Vendian sequence of the southeastern White Sea Region: International Geology Review, v. 25, p. 897–905.
Tarhan, L.G., Droser, M.L., Gehling, J.G., and Dzaugis, M.P., 2015, Taphonomy and morphology of the Ediacara form genus *Aspidella*: Precambrian Research, v. 257, p. 124–136.
Tarhan, L.G., Myrow, P.M., Smith, E.F., Nelson, L.L., and Sadler, P.M., 2020, Infaunal augurs of the Cambrian explosion: an Ediacaran trace fossil assemblage from Nevada, USA: Geobiology, v. 18, p. 486–496.
Tate, R., 1892, The Cambrian fossils of South Australia: Transactions of the Royal Society of South Australia, v. 15, p. 183–189.
Thomas, R.D.K., Runnegar, B., and Matt, K., 2020, *Pelagiella exigua*, an early Cambrian stem gastropod with chaetae: lophotrochozoan heritage and conchiferan novelty: Palaeontology, v. 63, p. 601–627.
Topper, T., Betts, M.J., Dorjnamjaa, D., Li, G., Li, L., Altanshagai, G., Enkhbaatar, B., and Skovsted, C.B., 2022, Locating the BACE of the Cambrian: Bayan Gol in southwestern Mongolia and global correlation of the Ediacaran–Cambrian boundary: Earth-Science Reviews, v. 229, n. 104017.
Trewin, N.H., 1979, Transported graptolites and associated tool marks from Grieston Quarry, Innerleithen, Peeblesshire: Scottish Journal of Geology, v. 15, p. 287–292.
Turk, K., Maloney, K., Laflamme, M., and Darroch, S.A.F., 2021, Priapulid trace fossils from the late Ediacaran of Namibia: Geological Society of America Abstracts with Programs, v. 53, no. 6, https://doi.org/10.1130/abs/2021AM-369978.
Turk, K.A., Maloney, K.M., Laflamme, M., and Darroch, S.A.F., 2022, Paleontology and ichnology of the late Ediacaran Nasep–Huns transition (Nama Group, southern Namibia): Journal of Paleontology, v. 96, p. 753–769.
Turner, E.C., 2021, Possible poriferan body fossils in early Neoproterozoic microbial reefs: Nature, v. 596 , p. 87–91.
Uchman, A., 1999, Ichnology of the Rhenodanubian Flysch (Lower Cretaceous–Eocene) in Austria and Germany: Beringeria, v. 25, p. 61–173.
Uchman, A., 2001, Eocene trace fossils from the Hecho Group of the Pyrenees, northern Spain: Beringeria, v. 28, p. 3–41.
Uchman, A., and Martyshyn, A., 2020, Taxis behaviour of burrowing organisms recorded in an Ediacaran trace fossil from Ukraine: Palaeogeography, Palaeoclimatology, Palaeoecology, v. 538, n. 109441.
Ulrich, E.O., 1904, Fossils and age of the Yakutat Formation. Description of collections made chiefly near Kadiak, Alaska: Harriman Alaska Expedition, 4 (Geology and Paleontology), p. 125–146.
Vaziri, S.H., Majidifard, M.R., and Laflamme, M., 2018, Diverse assemblage of Ediacaran fossils from Central Iran: Scientific Reports, v. 8, n. 5060.
Vaziri, S.H., Majidifard, M.R., Darroch, S.A.F., and Laflamme, M., 2021, Ediacaran diversity and paleoecology from central Iran: Journal of Paleontology, v. 95, p. 236–251.
Vendrasco, M.J., Checa, A.G., and Kouchinsky, A.V., 2011, Shell microstructure of the early bivalve *Pojetaia* and the independent origin of nacre within the Mollusca: Palaeontology, v. 54, p. 825–850.
Verrill, A.E, 1865, Classification of Polyps (Extract condensed from a synopsis of the Polypi of the North Pacific exploring expedition under Captains

Ringgold and Rodgers, U.S.N.): Communications of the Essex Institute, v. 4, p. 145–152.
Vickers-Rich, P., The Nama fauna for southern Africa, *in* Fedonkin, M.A., Gehling, J.G., Grey, K., Narbonne, G.M., and Vickers-Rich, P., eds., 2007, The Rise of Animals, Evolution and Diversification of the Animal Kingdom: Baltimore, Johns Hopkins University Press, p. 69–88.
Vickers-Rich, P., Ivantsov, A.Yu., Trusler, P.W., Narbonne, G.M., Hall, M., et al., 2013, Reconstructing *Rangea*: new discoveries from the Ediacaran of southern Namibia: Journal of Paleontology, v. 87, https://doi.org/10.1666/12-074R.1.
Vinn, O., and Toom, U., 2016, Rare tool marks from the Upper Ordovician of Estonia (Baltica): Neues Jahrbuch für Geologie und Paläontologie–Abhandlungen, v. 281, p. 221–226.
Vrijenhoek, R.C., 2013, On the instability and evolutionary age of deep-sea chemosynthetic communities: Deep-Sea Research I, v. 92, p. 189–200.
Wade, M., 1971, Bilateral Precambrian chondrophores from the Ediacara fauna, South Australia. Royal Society of Victoria Proceedings, v. 84, p. 183–188.
Walcott, C.D., 1911, Cambrian geology and paleontology II: no. 3—middle Cambrian holothurians and medusae: Smithsonian Miscellaneous Collections, v. 57, p. 41–68.
Walcott, C.D., 1920, Middle Cambrian spongiae. Cambrian geology and paleontology IV: Smithsonian Miscellaneous Collections, v. 67, p. 261–364.
Weaver, P.G., and Ganis, R., 2013, Overview of Ediacaran age fossils from the Carolina Terrane: past, present and future research, *in* Hibbard, J., and Pollock, J., eds., One Arc, Two Arcs, Old Arc, New Arc: The Carolina Terrance in Central North Carolina: Salisbury, Carolina Geological Society, p. 63–73.
Weaver, P.G., McMenamin, M.A.S., and Tacker, R.C., 2006, Paleoenvironmental and paleobiogeographic implications of a new Ediacaran body fossil from the Neoproterozoic Carolina Terrane, Stanly County, North Carolina: Precambrian Research, v. 150, p. 123–135.
Webby, B.D., 1984, Precambrian–Cambrian trace fossils from western New South Wales: Australian Journal of Earth Sciences, v. 31, p. 427–437.
Wei, F., Zhao, Y., Chen, A., Hou, X., and Cong, P., 2021, New vauxiid sponges from the Chengjiang Biota and their evolutionary significance: Journal of the Geological Society, v. 178, n. jgs2020-162.
Wetzel, A., and Bromley, R.G., 1996, Re-evaluation of the ichnogenus *Helminthopsis*—a new look at the type material: Palaeontology, v. 39, 1–19.
Wilson, J.P., Grotzinger, J.P., Fischer, W.W., Hand, K.P., Jensen, S., et al., 2012, Deep-water incised valley deposits at the Ediacaran–Cambrian boundary in southern Namibia contain abundant *Treptichnus pedum*: Palaios, v. 27, p. 252–273.
Wood, R.A, Poulton, S.W., Prave, A.R., Hoffmann, K.-H., Clarkson, M.O., et al., 2015, Dynamic redox conditions control late Ediacaran metazoan ecosystems in the Nama Group, Namibia: Precambrian Research, v. 261, 252–271.
Wörheide, G., Dohrmann, M., Erpenbeck, D., Larroux, C., Maldonado, M., Voigt, O., Borchiellinijj, C., and Lavrov, D.V., 2012, Deep phylogeny and evolution of sponges: Advances in Marine Biology, v. 6, p. 1–78.
Xiao, S., Yuan, X., Steiner, M., and Knoll, A.H., 2002, Macroscopic carbonaceous compressions in a terminal Proterozoic shale: a systematic reassessment of the Miaohe biota, South China: Journal of Paleontology, v. 76, p. 347–376.
Xiao, S., Chen, Z., Pang, K., Zhou, C., and Yuan, X., 2021, The Shibantan Lagerstätte: insights into the Proterozoic–Phanerozoic transition: Journal of the Geological Society, v. 178, n. jgs2020-135.
Yang, B., Steiner, M., Schiffbauer, J.D., Selly, T., Wu, X., Zhang, C., and Liu, P., 2020, Ultrastructure of Ediacaran cloudinids suggests diverse taphonomic histories and affinities with non-biomineralized annelids: Scientific Reports, v. 10, n. 535.
Yang, B., Warren, L.V., Steiner, M., Smith, E.F., and Liu, P., 2022, Taxonomic revision of Ediacaran tubular fossils: Cloudina, Sinotubulites *and* Conotubus*: Journal of Paleontology*, v. 96, p. 256–273.
Yang, C., Rooney, A.D., Condon, D.J., Li, X.-H., Grazhdankin, D.V., Bowyer, F.T., Hu, C., Macdonald, F.A., and Zhu, M., 2021, The tempo of Ediacaran evolution: Science Advances, v. 7, n. eabi9643.
Yang, S.P., Song, Z., and Liang, D., 1983, Late Carboniferous–Early Permian flysch trace fossils from Ali, Xizang (Tibet), China: Earth Science: Journal of Wuhan College of Geology, v. 19. p. 93–104.
Yanishevsky, M., 1926, Ob ostatkah trubchatyh chervei iz kembriyskoy siney gliny. [On the remains of the tubular worms from the Cambrian blue clays]: Ezhegodnik Russkogo Paleontologicheskogo Obchestva, v. 4, p. 99–112. [in Russian]
Yochelson, E.L., and Fedonkin, M.A., 1997, The type specimens (middle Cambrian) of the trace fossil *Archaeonassa* Fenton and Fenton: Canadian Journal of Earth Sciences, v. 34, p. 1210–1219.
Zachos, J.C., Flower, B.P., and Paul, H., 1997, Orbitally paced climate oscillations across the Oligocene/Miocene boundary: Nature, v. 388, p. 567–570.
Zhang, G., Parry, L.A., Vinther, J., and Ma, X., 2022, Exceptional soft tissue preservation reveals a cnidarian affinity for a Cambrian phosphatic tubicolous enigma: Proceedings of the Royal Society B, v. 289, n. 20221623.
Zhang, L., Buatois, L.A., and Mángano, M.G., 2022, Potential and problems in evaluating secular changes in the diversity of animal–substrate interactions at ichnospecies rank: Terra Nova, v. 34, p. 433–440.
Zhao, Y., Vinther, J., Li, Y.-J., Wei, F., Hou, X.-G., and Cong, P.-Y., 2021, An early Cambrian mackenziid reveals links to modular Ediacaran macroorganisms: Papers in Palaeontology, v. 8, n. e1412.

Appendix. Descriptions of fossil localities explored for this study.

UCLA 7307. **Aar (Amphitheatre)**. One meter-thick quartz sandstone, ~32 m above base of Kliphoek Member, Dabis Formation, Kuibis Subgroup, Nama Group on Aar farm, 27 km east southeast of Aus, southern Namibia; Schakalskuppe 1:50,000 map sheet (2616DA), 16.532737°E, 26.720682°S; 3–6 August 1993, C.K. Brain, J.G. Gehling, M.A.S. McMenamin, F. Pflüger, B. Runnegar, A. Seilacher; 29–30 August 1996, M.L. Droser, J.G. Gehling, S. Jensen, M.A. Motus, M.R. Saltzman.

Beltanelliformis brunsae Menner in Keller et al., 1974
Aspidella sp.
Namalia villiersiensis Germs, 1968
Pteridinium simplex Gürich, 1933

UCLA 7308. **Aar East**. Type locality of *Ernietta plateauensis* Pflug, 1966. Buchholzbruun Member, Dabis Formation, Kuibis Subgroup, Nama Group on Aar farm, 28 km east southeast of Aus, southern Namibia; Schakalskuppe 1:50,000 map sheet (2616DA), 16.564213°E, 26.726652°S; 4 August 1993, C.K. Brain, J.G. Gehling, M.A.S. McMenamin, F. Pflüger, B. Runnegar.

Pteridinium simplex Gürich, 1933

UCLA 7309. **Armias**. Type section of *Nasepia altae* Germs, 1972. Quartz sandstone float specimens mostly from lowest part of Huns Limestone Member (sensu Saylor et al., 1995), 0–12 m above Nasep Sandstone Member, Urusis Formation, Schwarzrand Subgroup, Nama Group, 1 km west of old dwelling on Arimas farm, about 35 km north northeast of Rosh Pinah, southern Namibia; Uitsig 1:50,000 map sheet (2717CA), 17.019382°E, 27.696984°S; 11–12 August 1993, J.G. Gehling, B. Runnegar; 9–10, 12–13 May 1995, S. Jensen, B. Runnegar, B.Z. Saylor; 22 August 1996, J.E. Almond, M.L. Droser, J.G. Gehling, S. Jensen, B. Runnegar, M.R. Saltzman.

Archaeichnium haughtoni Glaessner, 1963
Arimasia germsi n. gen. n. sp.
Nasepia altae Germs, 1972a
cf. *Calyptrina striata* Sokolov, 1967
Ariichnus vagus n. igen. n. isp.
Helminthopsis isp.
Treptichnus isp.

UCLA 7310. **Helmeringhausen**. Lower part of Mooifontein limestone just above nonconformity with granitic basement, Mooifontein Member, Dabis Formation, Kuibis Subgroup, Nama Group on road D414 to Gibeon, 10 km east northeast of Helmeringhausen, southern Namibia; Helmeringhausen 1:50,000 map sheet (2516DD), 16.901393°E, 25.864823S; 8 August 1993, C.K. Brain, J.G. Gehling, B. Runnegar; 29 May 1995, S. Jensen, B. Runnegar.

https://doi.org/10.1017/jpa.2023.81 Published online by Cambridge University Press

Cloudina hartmannae Germs, 1972b

UCLA 7311. **Kliphoek 1**. Finer-grained beds just above prominent ledge of quartzite near top of Kliphoek Member, Dabis Formation, Kuibis Subgroup, Nama Group on Kliphoek farm, 200 m south of track running east from road P727 about 1 km north of Kliphoek homestead; Geelperdhoek 1:50,000 map sheet (2716BD), 16.796368°E, 27.283205°S; 9 August 1993, C.K. Brain, J.G. Gehling, B. Runnegar.

Beltanelliformis brunsae Menner in Keller et al., 1974

UCLA 7312. **Nooitgedacht**. Thin sandstone with tool-marked base 3.5 m below base of Mooifontein Limestone, Kliphoek Member, Dabis Formation, Kuibis Subgroup, Nama Group on hill 1,354 m on east side of road D727, 0.8 km east southeast of Nooitgedacht ruins; Diamantpoort 1:50,000 map sheet (2716BB), 16.785454°E, 27.250061°S; 12 August 1993, J.G. Gehling, B. Runnegar.

Ernietta plateauensis Pflug, 1966

UCLA 7313. **Klipdrif**. Shale interval immediately below base of Mooifontein limestone, top of Kliphoek Member, Dabis Formation, Kuibis Subgroup, Nama Group, in small quarry on north side of road P437 from Bethanie to Farm Vrede, 6.3 km east of Klipdrif homestead, 4.1 km east of boundary of Klipdrif, and 17.3 km by road from Bethanie; Buchholzbrunn 1:50,000 map sheet (2617CA), 17.029624°E, 26.522701°S; 13 August 1993, J.G. Gehling, B. Runnegar.

Ernietta plateauensis Pflug, 1966

UCLA 7314. **Namaland 1**. Shale interval immediately below base of Mooifontein limestone, top of Kliphoek Member, Dabis Formation, Kuibis Subgroup, Nama Group, in small quarry on east side of road P435, 2.4 km from Goageb–Aus road (B4), southern Namibia; Buchholzbrunn 1:50,000 map sheet (2617CA), 17.095833°E, 26.649938°S; 13 August 1993, J.G. Gehling, B. Runnegar.

Ernietta plateauensis Pflug, 1966

UCLA 7315. **Namaland 2**. Shale interval immediately below base of Mooifontein limestone, top of Kliphoek Member, Dabis Formation, Kuibis Subgroup, Nama Group, in small quarry on west side of road P435, 6.7 km from Bethanie–Goageb road (C14), southern Namibia; Buchholzbrunn 1:50,000 map sheet (2617CA), 17.1420961E, 26.630036°S; 14 August 1993, J.G. Gehling, B. Runnegar.

Pteridinium sp.
Ernietta plateauensis Pflug, 1966
Palaeopaschichus sp.
Pseudorhizostomites? sp.

UCLA 7317. **Buchholzbrunn**. Shale interval immediately below base of Mooifontein limestone, top of Buchholzbrunn Member, Dabis Formation, Kuibis Subgroup, Nama Group at base of channel in road metal quarry on Buchholzbrunn farm, about 1.5 km south of old B4 road, 12 km northwest of Goageb, southern Namibia; Buchholzbrunn 1:50,000 map sheet (2617CA), 17.120122°E, 26.692510°S; 29 April 1995, S. Jensen, B. Runnegar.

Ernietta plateauensis Pflug, 1966

UCLA 7318. **Driedoornvlakte**. Carbonate bioherm in Kuibis Subgroup on Driedoornvlakte farm, about 45 km northeast of Büllsport and about 100 km north of Maltahöhe, southern Namibia (stop 2.3 of IGCP excursion); TBD 1:50,000 map sheet (2316DC), 16.664167°E, 23.860489°S; 2 May 1995, B. Runnegar.

Cloudina hartmannae Germs, 1972b

UCLA 7319. **Donker Gange**. Fossiliferous limestone in Omkyk Member, Kuibis Subgroup, Nama Group, canyon section ~100 m south of the Zebra River, Donker Gange farm, about 80 km west northwest of Maltahöhe, southern Namibia (stop 4.2 of IGCP excursion); Donker Gange 1:50,000 map sheet (2416CA), 16.178702°E, 24.533310°S; 4 May 1995, B. Runnegar; 8 September 1996, M.L. Droser, J.G. Gehling, S. Jensen, M.A. Motus, B. Runnegar, M.R. Saltzman.

Cloudina hartmannae Germs, 1972b
Namacalathus hermanastes Grotzinger, Watters, and Knoll, 2000

UCLA 7320. **Kyffhauser**. Thin beds of sandstone (all float), Neiderhagen Member, Nudaus Formation, Schwarzrand Subgroup, Nama Group, on north side of road D850, 4.0 km west of D855 turnoff, Kyffhauser farm, about 70 km northwest of Maltahöhe, southern Namibia; Harughas 1:50,000 map sheet (2416AD), 16.357980°E, 24.485664°S; 5 May 1995; D. Erwin, S. Jensen, B. Runnegar, and M. Walter; 9 September 1996, M.L. Droser, J.G. Gehling, S. Jensen, M.A. Motus, B. Runnegar, M.R. Saltzman.

Pteridinium sp.
Archaeichnium haughtoni Glaessner, 1963
cf. *Calyptrina striata* Sokolov, 1967

UCLA 7321. **Kliphoek 2**. Thin-bedded siltstones of Nudaus Formation, Schwartzrand Subgroup, Nama Group in slope section south of D727 road, about 2 km south of Kliphoek homestead, Kliphoek farm, southern Namibia (stop 6.1b of IGCP excursion, at 27 m [6.1b.A] and 68 m [6.1b.B)] above exposed base); Geelperdhoek 1:50,000 map sheet (2716BD), 16.766205°E, 27.308895°S; 6 May 1995, B. Runnegar.

Vendotaenia sp.

UCLA 7322. **Swartkloofberg 1**. Thin sandstones, Nasep Member, Urusis Formation, Schwarzrand Subgroup, Nama Group on dip slope immediately north of Swartkloofberg homestead, Swartkloofberg farm, southern Namibia; Rekvlakte 1:50,000 map sheet (2716BC), 16.523883°E, 27.485491°S; 7 May 1995, A.J. Kaufman, G. Narbonne, B. Runnegar; 25 August 1996, J.E. Almond, M.L. Droser, J.G. Gehling, S. Jensen, M.A. Motus, M.R. Saltzman.

Pteridinium sp.
trace fossils

UCLA 7323. **Swartkloofberg 2**. Pinnacle reef that grew from Huns carbonate platform and was embedded in shales of the highstand Felschuhhorn Member, Urusis Formation near Niras trig station (69; 1,121.4 m), Swartkloofberg farm, Rekvlakte 1:50,000

https://doi.org/10.1017/jpa.2023.81 Published online by Cambridge University Press

map sheet (2716BC), southern Namibia; 16.564731°E, 27.451876°S; 7 May 1995, B. Runnegar; 26 August 1996, M.L. Droser, J.G. Gehling, S. Jensen, and B. Runnegar.

Cloudina hartmannae Germs, 1972b

UCLA 7324. **Sonntagsbrunn**. Thin event beds in siltstones of the Kreyrivier Member, Nomtsas Formation, Schwarzrand Subgroup, Nama Group on east and west sides of hill 850 m on east side of road D463, about 1.5 km south of Koedoeslaagte homestead, west of the Fish River Canyon, southern Namibia; Koedoeslaagte 1:50,000 map sheet (2717DA), 17.509523°E, 27.368114°S; 12 May 1995, S. Jensen, B. Runnegar, B.E. Saylor; 20–21 August 1996, J.E. Almond, M.L. Droser, S. Jensen, M.A. Motus, M.R. Saltzman.

Treptichnus pedum (Seilacher, 1955)

UCLA 7325. **Holoog River**. Thin-bedded sandstone in base of Huns Limestone Member (sensu Saylor et al., 1995), Urusis Formation, Schwarzrand Subgroup, Nama Group, both sides of unnumbered road, 0.7 km from turnoff from road M28 (C12) to the Augurabis Steenboks Naturpark, 1.7 km north of the Gaap (Holoog) River, southern Namibia; Holoog 1:50,000 map sheet (2717BD), 16.564731°E, 27.451876°S; 11 May 1995, S. Jensen, B. Runnegar, B.Z. Saylor; 19 August 1996, J.E. Almond, M.L. Droser, J.G. Gehling, S. Jensen , M.A. Motus, B. Runnegar.

Archaeichnium haughtoni Glaessner, 1963
cf. *Calyptrina striata* Sokolov, 1967
cf. *Sekwitubulus annulatus* Carbone et al., 2015
cf. *Sinotubulites baimatuoensis* Chen, Chen, and Qian, 1981

UCLA 7326. **Arimas B**. Float quartz sandstones and other material from siliciclastic interval 37–43 m above base of Huns Member (sensu Saylor et al., 1995), Urusis Formation, Schwarzrand Subgroup, Nama Group about 1 km west of abandoned dwelling on Arimas farm, about 35 km north northeast of Rosh Pinah, southern Namibia; Uitsig 1:50,000 map sheet (2717CA), 17.022857°E, 27.695409°S; 9–10, 12–13 May 1995, S. Jensen, B. Runnegar, B.Z. Saylor; 22 August 1996, J.E. Almond, M.L. Droser, J.G. Gehling, S. Jensen, B. Runnegar, M.R. Saltzman.

Archaeichnium haughtoni Glaessner, 1963
Nasepia altae Germs, 1972
cf. *Sekwitubulus annulatus* Carbone et al., 2015
Archaeonassa isp.
Ariichnus vagus n. igen. n. isp.
Gordia isp.
Helminthopsis isp.
tool marks attributed to *Pteridinium*

UCLA 7370. **Holoog South**. Limestone in base of Huns Member, Urusis Formation, Schwarzrand Subgroup, Nama Group, east side of road M28 (C12), 1.1 km south of Gaap (Holoog) River, southern Namibia; Holoog 1:50,000 map sheet (2717BD), 17.943201°E, 27.414291°S; 19 August 1996, J.D. Almond, J.G. Gehling, B. Runnegar; 20 August 1996, J.E. Almond, M.L. Droser, J.G. Gehling, S. Jensen, B. Runnegar, M.R. Saltzman.

Olenichnus sp.

UCLA 7371. **Arimas C**. Siliciclastic interval in upper part of Huns Member, ~160 m above base, Urusis Formation, Schwarzrand Subgroup, Nama Group about 1 km west of abandoned homestead on Arimas farm, about 35 km north northeast of Rosh Pinah, southern Namibia; Uitsig 1:50,000 map sheet (2717CA), 17°00′00″E, 27°41′45″S; 22 August 1996, J.E. Almond, M.L. Droser, J.G. Gehling, S. Jensen, B. Runnegar, M.R. Saltzman.

Treptichnus isp.

UCLA 7372. **Dundas A**. Shales beneath the Pteridinium bed (Fossil Bed A of Narbonne et al., 1997), about 65 m stratigraphically from top of Dundas hill (1,169 m) on Swartpunt farm, west of road C13, about 50 km north of Rosh Pinah, southern Namibia; Rekvlakte 1:50,000 map sheet (2716BC); 16.696509°E, 27.476517°S; 23 August 1996, B. Runnegar.

tool marks attributed to *Pteridinium*

UCLA 7373. **Dundas B**. *Pteridinium* bed (Fossil Bed A of Narbonne et al., 1997), about 65 m stratigraphically from top of Dundas (1,169 m) on Swartpunt farm, west of road C13, about 50 km north of Rosh Pinah, southern Namibia; Rekvlakte 1:50,000 map sheet (2716BC); 16.696509°E, 27.476517°S; 23 August 1996, M.L. Droser, J.G. Gehling, B. Runnegar.

Pteridinium carolinaensis (St. Jean, 1973)
Swartpuntia germsi Narbonne, Saylor, and Grotzinger, 1997

UCLA 7374. **Dundas C**. *Swartpuntia* bed (Fossil Bed B of Narbonne et al., 1997), about 45 m stratigraphically from top of Dundas (1,169 m) on Swartpunt farm, west of road C13, about 50 km north of Rosh Pinah, southern Namibia; Rekvlakte 1:50,000 map sheet (2716BC); 16.696509°E, 27.476517°S; 24 August 1996, B. Runnegar.

Swartpuntia germsi Narbonne, Saylor, and Grotzinger, 1997

UCLA 7375. **Dundas D**. *Streptichnus* bed, thin sandstone interbedded with thin carbonates, Spitskop Member, Urusis Formation, Schwarzrand Subgroup, Nama Group about 12 m stratigraphically from top of Dundas (1,169 m) on Swartpunt farm, west of road C13, about 50 km north of Rosh Pinah, southern Namibia; Rekvlakte 1:50,000 map sheet (2716BC); 16.696509°E, 27.476517°S; 23 August 1996, S. Jensen and B. Runnegar.

Streptichnus narbonnei Jensen and Runnegar, 2005

UCLA 7376. **Swartkloofberg 3**. Thin carbonate at top of the Huns Member, Urusis Formation, Schwarzrand Subgoup, Nama Group on north side of pinnacle reef near Niras, Swartkloofberg farm, Rekvlakte 1:50,000 map sheet (2716BC), southern Namibia; 16.564731°E, 27.451876°S; 25–26 August 1996, M.L. Droser, J.G. Gehling, S. Jensen, M.A. Motus, B. Runnegar.

Swartpuntia germsi Narbonne, Saylor, and Grotzinger, 1997

UCLA 7377. **Swartkloofberg 4**. Calcareous shales, Feldschuhhorn Member, Urusis Formation, Schwarzrand Subgoup, Nama Group on south side of pinnacle reef near Niras,

https://doi.org/10.1017/jpa.2023.81 Published online by Cambridge University Press

Swartkloofberg farm, Rekvlakte 1:50,000 map sheet (2716BC), southern Namibia; 16.564731°E, 27.451876°S; 26 August 1996, M.L. Droser, J.G. Gehling, S. Jensen, M.A. Motus, B. Runnegar.

Pteridinium carolinaensis (St. Jean, 1973)
Swartpuntia germsi Narbonne, Saylor, and Grotzinger, 1997
cf. *Sinotubulites baimatuoensis* Chen, Chen, and Qian, 1981
tool marks attributed to *Pteridinium*

UCLA 7378. **Twyfel**. Sandstone and shale of upper Kliphoek Member, Kubis Formation, Schwarzrand Subgroup, Nama Group on Twyfel farm south of road D425 where it turns abruptly east, about 1 km from house belonging to owners of Wegkruip, southern Namibia; Sandkop 1:50,000 map sheet (2616BC), 16.733175°E, 26.259967°S; 31 August 1996, S. Jensen and B. Runnegar.

Ernietta plateauensis Pflug, 1966
Gordia isp.
Helminthopsis isp.

UCLA 7379. **Wegkruip**. Float from silty interval at top of Kliphoek Member, Kubis Formation, Schwarzrand Subgroup, Nama Group on Wegkruip farm south of road D425 where it turns abruptly east, about 1 km from house belonging to owners of Wegkruip, southern Namibia; Sandkop 1:50,000 map sheet (2616BC), 16.733721°E, 26.276168°S; 1 September 1996, M.L. Droser, J.G. Gehling, S. Jensen, M.A. Motus, B. Runnegar, M.R. Saltzman.

Ernietta plateauensis Pflug, 1966

UCLA 7380. **Aar 3 (northern boundary)**. Sandstone in Kliphoek Member, Dabis Formation, Kuibis Subgroup, Nama Group near track from Plateau homestead to Aar homestead at boundary between Plateau and Aar farms, 27 km east southeast of Aus, southern Namibia; Schakalskuppe 1:50,000 map sheet (2616DA), 16.528941°E, 26.682818°S; 30 August 1996, S. Jensen, M.A. Motus.

Pteridinium simplex Gürich, 1933

UCLA 7381. **Zuurberg**. Lonestones in siltstones of Aar Member just below Mooifontein Limestone, Dabis Formation, Kuibis Subgroup, Nama Group in small quarry on north side of road D425, exactly 10 km west of its intersection with road C14, north of Bethanien, southern Namibia; Tumaub 1:50,000 map sheet (2616BB), 16.947402°E, 26.243034°S; 30 August 1996; S. Jensen and B. Runnegar.

Ernietta plateauensis Pflug, 1966

UCLA 7382. **Mamba**. Sandstone of Urikos Member? below second carbonate (Hoogland Member), Zaris Formation, Kuibis Subgroup, Nama Group on prominent ridge south of Mamba homestead, Mamba/Bergplaas farms, about 70 km east of Maltahöhe, southern Namibia; Uitkoms 1:50,000 map sheet (2416CD), 16.407120°E, 24.957826°S; 4 September 1996, M.L. Droser, J.G. Gehling, S. Jensen, M.A. Motus, B. Runnegar.

Aspidella sp.
Cloudina sp.
trace fossils

UCLA 7383. **Zaris**. Sandstone of Urikos Member? below second carbonate (Hoogland Member), Zaris Formation, Kuibis Subgroup, Nama Group on prominent ridge southeast of Zaris homestead, Zaris farm, about 70 km east of Maltahöhe, southern Namibia; Uitkoms 1:50,000 map sheet (2416CD), 16.381886° E, 24.957982°S; 4 September 1996, S. Jensen.

cf. *Sekwitubulus annulatus* Carbone et al., 2015
cf. *Sinotubulites baimatuoensis* Chen, Chen, and Qian, 1981

UCLA 7384A-C. **Zaris Pass**. Sandstone of Urikos Member? below second carbonate (Hoogland Member), Zaris Formation, Kuibis Subgroup, Nama Group in quarry on south side of road C19 and on boundary between Zaris and Mamba/Bergplaas farms, about 70 km east of Maltahöhe, southern Namibia; Uitkoms 1:50,000 map sheet (2416CD), 16.430187°E, 24.924517° S; 4 September 1996, M.L. Droser, J.G. Gehling, S. Jensen, M.A. Motus, B. Runnegar; 5 September 1996, S. Jensen, M.A. Motus, B. Runnegar.

cf. *Sinotubulites baimatuoensis* Chen, Chen, and Qian, 1981

Some other classical Ediacaran fossil localities in Namibia

Kuibis (Guibes). Type locality of *Rangea schneiderhoehni* Gürich, 1930a; float from Kliphoek Member, Dabis Formation, Kuibis Subgroup, Nama Group, probably on slope to southwest of trigonometric station 18 (1,438 m), Klein Kubis Sud Farm, about 40 km west northwest of Goageb, southern Namibia; Guibes 1:50,000 map sheet (2616DB), 16.875803°E, 26.681243°S; 1914, H. Schneiderhöhn (Schneiderhöhn, 1920).

Rangea schneiderhoehni Gürich, 1930a
Pteridinium simplex Gürich, 1933

SAFM K4812-3. **Gründoorn (Gründorn 57)**. Float from Nakop Member, upper Kuibis or lower Schwarzrand Subgroup, Nama Group, in a small gully cut in the low Nama escarpment on Gründorn 57 farm, about 60 km east of Karasburg, southern Namibia; Kokerboom 1:50,000 map sheet (2819AB), near 19.295356°E, 28.094153°S; 1927, H.F. Frommurze, S.H. Haughton (Haughton, 1960).

Archaeichnium haughtoni Glaessner, 1963
Paramedusium africanum Gürich, 1933

SMSWA 45731. **Kosos**. From black limestone "Uit Schwarzkalk," Mooifontein Member, Kuibis Subgroup, Nama Group on Kosis Farm, about 20 km north of Helmeringhausen, southern Namibia; Kosos 1:50,000 map sheet (2516DB), near 16.799850°E, 25.633408°S (Spitskop 1,752 m); before 1966 (when the specimen was cast at UCLA by LouElla Saul), J. Erasmus.

Pteridinium carolinaensis? (St. Jean, 1973)

Buchholzbrunn. Kliphoek Member, Dabis Formation, Kuibis Subgroup, Nama Group on Buchholzbrunn, Buchholzbrunn farm, 12 km northwest of Goageb, southern Namibia; Buchholzbrunn 1:50,000 map sheet (2617CA), near 17.121828°E, 26.697830°S (Buchholzbrunn railway stop; before 1968, G.J.B. Germs.

Namalia villiersiensis Germs, 1968

SAFM K4367. **Chamis**. Float from lower quartzite, Nudaus Formation, Schwarzrand Subgroup, Nama Group, on Chamis Sud farm, 28 km southeast of Helmeringhausen, southern

https://doi.org/10.1017/jpa.2023.81 Published online by Cambridge University Press

Namibia; Tumaub 1:50,000 map sheet (2616BB), near 16.984762°E, 26.050855°S; 1968, G.J.B. Germs.

Rangea schneiderhoehni Gürich, 1930a

Vrede. Float from Kliphoek Member, Dabis Formation, Kuibis Subgroup, Nama Group, on Vrede farm, 50 km west of Bethanien via road D437, southern Namibia; Sandkop 1:50,000 map sheet (2616BC), near 16.712653°E, 26.475912°S (Vrede homestead); 1968, G.J.B. Germs.

Namalia villiersiensis Germs, 1968
Rangea schneiderhoehni Gürich, 1930a

Kolke. Nasep Quartzite Member, Urusis Formation, Schwarzrand Subgroup, Nama Group on Kolke Farm, about 20 km north of Helmeringhausen, southern Namibia; Kolke 1:50,000 map sheet (2716DB), near 16.860209°E, 27.634541°S (Kolke settlement); before 1972, G.J.B. Germs.

Nasepia altae Germs, 1972a

Accepted: 3 October 2023

https://doi.org/10.1017/jpa.2023.81 Published online by Cambridge University Press